MOLECULAR DETERMINANTS OF RESPONSE TO ANTIANGIOGENIC THERAPIES IN PRECLINICAL MODELS OF HEAD AND NECK SQUAMOUS CELL CARCINOMA

by

Rekha Gyanchandani

Master of Science, University of Mumbai, 2005

Submitted to the Graduate Faculty of

the Department of Pharmacology & Chemical Biology in partial fulfillment

of the requirements for the degree of

Doctor of Philosophy

University of Pittsburgh

2013

UNIVERSITY OF PITTSBURGH

DEPARTMENT OF PHARMACOLOGY & CHEMICAL BIOLOGY

This dissertation was presented

by

Rekha Gyanchandani

It was defended on

April 12th, 2013

and approved by

Seungwon Kim, MD, Dept. of Pharmacology & Chemical Biology

Lin Zhang, PhD, Dept. of Pharmacology & Chemical Biology

Jennifer Grandis, MD, Dept. of Pharmacology & Chemical Biology

Zhou Wang, PhD, Dept. of Pharmacology & Chemical Biology

Satdarshan (Paul) Singh Monga, MD, Dept. of Pathology

Dissertation Director: Seungwon Kim, MD, Dept. of Pharmacology & Chemical Biology

ABSTRACT

MOLECULAR DETERMINANTS OF RESPONSE TO ANTIANGIOGENIC THERAPIES IN PRECLINICAL MODELS OF HEAD AND NECK SQUAMOUS CELL CARCINOMA

Rekha Gyanchandani, PhD

University of Pittsburgh, 2013

BACKGROUND

Head and neck squamous cell carcinoma (HNSCC) is the eighth leading cancer by incidence worldwide. In the past 5 decades there have been significant advances in surgery and chemoradiotherapy, but very little improvement in survival rates. Hence, there is a pressing need to develop new therapeutic strategies in HNSCC. Antiangiogenic therapy represents a promising strategy in at least a subset of patients. Currently, there are no reliable predictive and resistance biomarkers to identify those patients most likely to benefit. Studies using relevant preclinical models that identify mechanisms of resistance to antiangiogenic agents will help meet these challenges.

PRINCIPLE FINDINGS

In this dissertation, we established preclinical models of intrinsic and acquired resistance to anti-VEGF antibody bevacizumab and identified potential biomarkers of drug response.

To characterize mechanisms of intrinsic resistance, we evaluated the angiogenic profile

of HNSCC cells from sensitive and resistant models using antibody array. We showed that resistant cells expressed higher levels of proangiogenic factors including interleukin-8 (IL-8). We identified PI3K and IL-1α signaling as the molecular basis for overexpression of IL-8. Downregulation of IL-8 resulted in sensitization of resistant tumors to bevacizumab. Overexpression of IL-8 in sensitive tumors conferred resistance to bevacizumab. Serum analysis of HNSCC patients treated with a bevacizumab-containing regime indicated high baseline IL-8 levels in a subset of patients refractory to treatment but not in responders.

In a novel xenograft model of acquired resistance, human-specific microarray analysis revealed upregulation of angiogenesis-related genes including fibroblast growth factor-2 (FGF2), fibroblast growth factor receptor-3 (FGFR3), phospholipase C gamma-2 (PLCg2), frizzled receptor-4 (FZD4), chemokine [C-X3-C motif] ligand-1 (CX3CL1), and chemokine [C-C motif] ligand-5 (CCL5). Upstream genes PLCg2, FZD4, CX3CL1, and CCL5 regulated increased expression of FGF2 via increased extracellular signal-regulated kinase (ERK) signaling. Co-targeting VEGF and FGFR sensitized resistant tumors to bevacizumab.

CONCLUSIONS AND SIGNIFICANCE

Our work has identified two distinct molecular mechanisms of resistance to bevacizumab in preclinical HNSCC models. IL-8 signaling mediated intrinsic resistance while upregulation of FGF signaling in response to anti-VEGF therapy contributed to acquired resistance. Above findings provide a mechanistic rationale for co-targeting these pathways in future clinical trials to enhance therapeutic efficacy.

Keywords: Angiogenesis, Acquired resistance, Bevacizumab, Biomarker, FGF, HNSCC, Intrinsic resistance, IL-8.

TABLE OF CONTENTS

LIST OF TABLES

LIST OF FIGURES

PREFACE

I wish to acknowledge several individuals who have immensely contributed to my journey through graduate school. I owe my deepest gratitude to my advisor, Dr. Seungwon Kim for his unfailing support, guidance and patience throughout my research. Our intellectual interactions always motivated me to work hard on every small and big endeavor during my graduate training. I would like to express my heartfelt thanks to Dr. Jennifer Grandis for her valuable advice and insightful discussions that greatly contributed to my research. My special thanks to all the lab members who were always ready to help with a smile.

I would like to extend my sincere thanks to all the members of my dissertation committee for their thoughtful suggestions and important feedback that shaped my research through its early years: Dr. Lin Zhang (chairperson), Dr. Jennifer Grandis, Dr. Zhou Wang and Dr. Satdarshan (Paul) Singh Monga. I wish to express my special thanks to Dr. Patrick Pagano, program director and Patricia Smith, graduate program coordinator, for their unending support and assistance through every major milestone in the pharmacology program.

I would like to thank Dr. Jeffrey Myers for kindly providing the HNSCC cell lines. I would also like to thank the University of Pittsburgh Cancer Institute (UPCI) Lentiviral Core Facility and Dr. Robert Sobol for generating IL-8 and IL-1α shRNA lentiviral particles (Cancer Center Support Grant, P30CA047904). I would like to thank Dr. Jacques Nor (University of Michigan) for sharing expertise with collagen capillary-formation assays. I would like to thank Dr. Daisuke Sano and Dr. Marcus Ortega Alves (University of Texas MD Anderson Cancer Center) for help with CD31/TUNEL immunofluorescence staining. I would like to thank Jonah Klein for help with shRNA experiments. I would like to thank Dr.

Seungwon Kim, Beth Knapick, Eun Hong for help with animal experiments, and Dr. Sufi Thomas for teaching murine blood extraction techniques. I would like to thank Kelly Quesnelle for helpful discussions on preclinical model generation. I would like to thank Sanders Oh for help with transwell migration assays. I would like to thank Sarah Wheeler for help with reagents and experiment troubleshooting.

My biggest thanks go to my family for their constant support and encouragement. Above all, I wish to thank my husband, Robin and my son, Ronak for their unconditional love and sacrifice during my doctoral study. I dedicate this dissertation to them.

My research was funded, in part, by the following awards to S. Kim:

1. NIH Mentored Clinical Scientist Development Award - K08DE019201-01
2. American College of Surgeons/ Triological Society Career Development Award
3. UPMC Endowed Assistant Professorship in Otolaryngology

Parts of this thesis have appeared on the following publications:

1. **R. Gyanchandani**, D. Sano, M. V. Ortega Alves, J. D. Klein, B. A. Knapick, S. Oh, J. N. Myers, S. Kim. Interleukin-8 as a modulator of response to bevacizumab in preclinical models of head and neck squamous cell carcinoma. *Oral Oncology*. 2013 (In Press).
2. **R. Gyanchandani**, S. Kim. Predictive Biomarkers to Anti-VEGF Therapy: Progress toward an Elusive Goal. *Clinical Cancer Research*. 2013 Feb 15;19(4):755-7.
3. A. Argiris, A. P. Kotsakis, T. Hoang, F. P. Worden, P. Savvides, M. K. Gibson, **R. Gyanchandani**, G. R. Jr Blumenschein, H. X. Chen, J. R. Grandis, P. M. Harari, M. S. Kies, S. Kim. Cetuximab and bevacizumab: preclinical data and phase II trial in recurrent or metastatic squamous cell carcinoma of the head and neck. *Annals of Oncology*. 2013 Jan;24(1):220-5.

1.0 INTRODUCTION

1.1 HEAD AND NECK SQUAMOUS CELL CARCINOMA (HNSCC)

Head and neck cancers include cancers of the oral cavity, pharynx, larynx, and other mucosal surfaces of the upper aerodigestive tract. The most common type of head and neck cancer is the squamous cell carcinoma (HNSCC), originating from the mucosal lining (epithelium) of these regions. HNSCC is the eighth most common malignancy and a major cause of cancer morbidity and mortality worldwide [1]. Globally, an estimated $650,000$ new cases are reported annually. In the United States, approximately $40,000$ new cases are diagnosed in both the sexes each year. Currently, the average five-year survival rate for this disease is 62%. This rate is highly dependent on the stage at diagnosis; with early stage diagnoses having an 82% five-year survival rate and advanced stages having only a 35% survival rate [2]. Approximately two-thirds of HNSCC patients present with advanced stage disease. Initial presentation with distant metastasis occurs in about 16% of all patients. However, recurrence of disease either in local or distant sites occurs in close to 47% of patients. These patients have a dismal prognosis with a median survival of only 6-9 months.

The major etiological factors for HNSCC include tobacco use and alcohol consumption. The substances present in tobacco such as nicotine and polycyclic hydrocarbons have been shown to exert direct carcinogenic effects [3]. In fact, mutations in the tumor suppressor gene, *TP53*, have been shown to correlate with substantial exposure to alcohol and tobacco [4]. HNSCC is also increased by tobacco chewing as seen in certain parts of Asia where chewing of betel quid is prevalent [5]. In addition, viruses such as Epstein-Barr virus (EBV) and HPV have been linked with head and neck cancer. EBV is associated with nasopharyngeal

carcinoma (NPC) [6, 7]. However, HPV is mostly associated with oropharyngeal carcinoma specifically those of the lingual and palatine tonsils [8]. The increasing trend of HPV-linked oropharyngeal carcinoma is predominant in patients under the age of forty-five due to the practice of oral sex, and the increasing number of sexual partners [9].

Head and neck tumorigenesis is a multistep process driven by specific genetic alterations caused by continuous exposure to carcinogens. These molecular changes involve the activation of oncogenes as well as the inactivation of tumor suppressor genes [10,11]. This results in oncogenic transformation and concomitant phenotypic changes in the tumor cells that allow them to survive and proliferate forming a clinically detectable tumor mass. Some of these important phenotypic changes include evasion of apoptosis, tissue invasion and metastasis, as well as acquiring the ability to induce angiogenesis.

1.2 ANGIOGENESIS AND HNSCC

Angiogenesis, the sprouting of new blood vessels from a pre-existing network, is of critical importance during tumor formation and also in a number of normal physiologic processes including embryonic development [12], wound healing [13] and reproduction [14]. Like normal tissues, tumors require an adequate supply of oxygen and nutrients for their growth and survival. Initially, solid tumors arise as avascular masses that can derive metabolites from pre-existing vasculature by simple passive diffusion. But, in order to grow beyond the size of 2 to 3mm in diameter, tumors require inducing their own blood supply [15]. Available evidence suggests that the so called "angiogenic switch" (induction of tumor vasculature) is triggered in response to an imbalance between the relative amounts of molecules that stimulate (proangiogenic) and inhibit (antiangiogenic) angiogenesis [16, 17].

Like all solid tumors, HNSCC relies upon angiogenesis in order to continue to proliferate and metastasize [18, 19]. Normal keratinocytes and HNSCC cells are known to produce a variety of angiogenic factors including IL-8, vascular endothelial growth factor (VEGF), pla-

cental growth factor (PlGF) and FGF. IL-8 expression has been shown to be associated with tumor cells in HNSCC samples using immunohistochemistry [20]. In addition, in the closely related bronchogenic carcinomas, IL-8 has been the primary mediator of angiogenesis found in fresh tumor homogenates [21]. VEGF on the other hand, is considered as the prototypical proangiogenic factor whose biological activity is primarily associated with endothelial cells [22]. These proangiogenic proteins can bind to their corresponding receptors located on the surface of endothelial cells and activate signaling cascades that lead to endothelial cell proliferation, directional migration and vessel formation. There can also be an indirect induction of angiogenesis by interaction of tumor cells with their surrounding stroma. HNSCC cells have been shown to attract monocytes and activate them to secrete angiogenic factors [23]. Also, macrophages are known to produce cytokines that stimulate the tumor cells (via paracrine signaling) to produce increased levels of IL-8 and VEGF.

1.2.1 Vascular Endothelial Growth Factor (VEGF)

An extensive body of evidence indicates that blockage of proangiogenic factor signaling can result in inhibition of tumor growth [24–29]. Among the validated antiangiogenic strategies, perturbation of VEGF signaling has gained primary focus. VEGF-A or commonly VEGF is the most important member of the VEGF family of growth factors consisting of VEGF-A, PlGF, VEGF-B, VEGF-C and VEGF-D. Multiple isoforms of human VEGF-A are generated by alternative exon splicing of a single gene [30]. VEGF121, VEGF165, VEGF189 and VEGF206 are the major VEGF-A isoforms, with less frequent splice variants VEGF145, VEGF183 [31].

VEGF-A mediates its cellular responses by binding to tyrosine kinase receptors (the VEGFRs) on the surface of endothelial cells, resulting in receptor dimerization and activation through transphosphorylation (Figure 1.1) [32]. The VEGFRs have an extracellular region consisting of seven immunoglobulin-like domains, a single transmembrane spanning region, and an intracellular kinase domain. VEGF-A binds to VEGFR-1 (Flt-1) and VEGFR-2 (KDR/Flk-1). VEGFR-2 appears to be the principal receptor of VEGF-A supporting its

proliferative functions [31, 33]. Tyr1175 (Y1175) and Tyr1214 (Y1214) are the two major autophosphorylation sites in VEGFR-2. PLC-g binds to Y1175, leading to the phosphorylation and activation of this protein. Y1214 appears to be required to trigger the sequential activation of Cdc42 and p38 MAPK. Many proteins are activated by VEGFR-2 through an unknown mechanism, including FAK, PI3K and Src.The activation of downstream signal transduction molecules leads to several different endothelial cell functions such as migration, vascular permeability, survival and proliferation. VEGF-C and VEGF-D, but not VEGF-A, are ligands for a third receptor (VEGFR-3), which mediate lymphangiogenesis.

1.2.2 Role of VEGF in HNSCC

VEGF-A is widely expressed in most human cancers [34–36] including head and neck cancers and higher levels of expression have been associated with increased tumor vascularity [37], metastasis [38] and poor prognosis [39]. The study by Sauter et. al. provided the first direct evidence of a correlation between VEGF expression and increased microvessel density in HNSCC compared to normal tissues [37]. In another study involving 29 specimens from human nasopharyngeal carcinoma, a significant relationship between microvessel density and high VEGF expression was determined, suggesting the importance of VEGF-dependent angiogenesis in the occurrence of lymph node metastasis [38]. Further, the study by Mineta et. al. showed that high VEGF expressors were associated with the progression of lymph node spread, which correlated with poor disease-free survival [39].

Expression of VEGF is regulated by a variety of stimuli such as hypoxia, growth factors, and p53 mutation, etc. Rapid tumor cell growth creates intracellular hypoxia, which initiates a series of cell signaling events that promote angiogenesis. VEGF is transcriptionally regulated by hypoxia-inducible factor (HIF-1α), which is in turn negatively regulated by the von Hippel-Lindau (VHL) tumor suppressor protein during normoxia [40, 41]. Apart from the hypoxia triggered up-regulation of VEGF, a number of growth factors including epidermal growth factor (EGF), insulin-like growth factor-1 (IGF-1), and platelet-derived growth factor (PDGF), up-regulate *VEGF* mRNA expression, suggesting that paracrine or

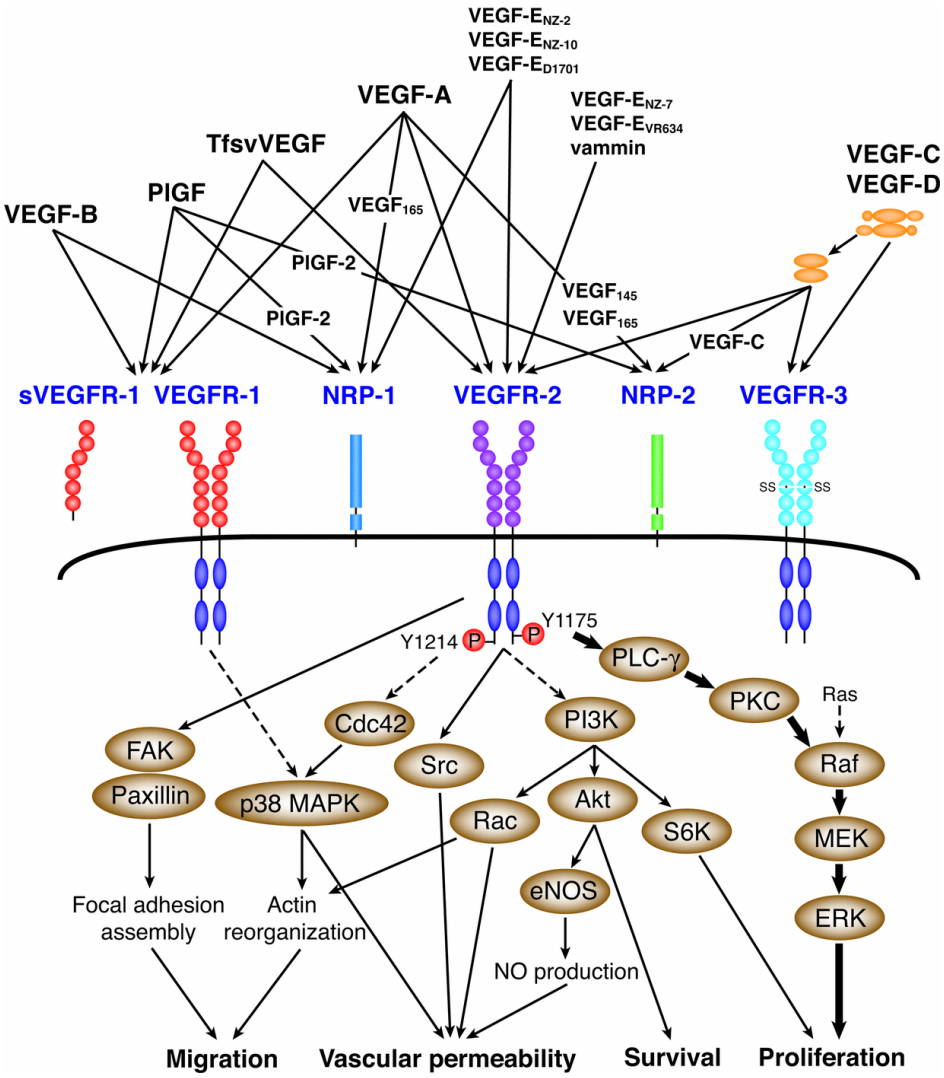

Figure 1.1: Binding specificity of various vascular endothelial growth factor (VEGF) family members and VEGFR signaling. The VEGF family consists of seven ligands derived from distinct genes (VEGF-A, -B, -C, -D and -E, placenta growth factor [PlGF] -1 and -2). In addition, specific family members, such as VEGF-A, may be expressed as isoforms due to mRNA alternative splicing. VEGF family members and isoforms have specific binding affinities to VEGF receptor (VEGFR) -1, VEGFR-2 and VEGFR-3 tyrosine kinase receptors as shown. In addition, neuropilin (NRP) -1 and NRP-2 are co-receptors for specific isoforms of VEGF family members and increase binding affinity of these ligands to their respective receptors. The activation of downstream signal transduction molecules leads to several different endothelial cell functions such as migration, vascular permeability, survival and proliferation [32].

autocrine release of such factors can contribute in regulating VEGF release in the microenvironment [42]. In addition, wild type p53 down-regulates VEGF, whereas the p53 mutants have no effect on the VEGF promoter activity [43]. A study by Riedel et. al. revealed that the number of p53 mutations was significantly higher in the VEGF-positive HNSCC than the VEGF-negative HNSCC, indicating the important role of p53 in the regulation of VEGF-dependent angiogenesis in HNSCC [44].

1.2.3 VEGF-targeted Therapeutics in HNSCC

Several therapeutic strategies have been developed to inhibit VEGF-induced angiogenesis (Figure 1.2) [45]. They involve neutralization of the biological activity of VEGF protein using monoclonal antibodies such as bevacizumab (Avastin, Genentech, Inc.) (Figure 1.3A) [46,47] or inhibition of the tyrosine kinases stimulated by VEGF using small molecules (tyrosine kinase inhibitors or TKIs) such as sunitinib (Sutent, Pfizer, Inc.) (Figure 1.3B) [48] and sorafenib (Nexavar, Onyx/Bayer) (Figure 1.3C) [49]. Currently, these agents have been FDA-approved for the treatment of metastatic neoplasms such as colon, lung, and renal cancers (Table 1.1). However, in head and neck cancers, they are still under active clinical investigation [50].

1.2.3.1 Monoclonal Antibodies Bevacizumab is a fully humanized monoclonal antibody against VEGF. It is the first and by far the most successful antiangiogenic drug that has been FDA approved for use in metastatic colorectal cancer, non-small cell lung cancer, and renal cell carcinoma [51]. Bevacizumab is also approved for use as second-line agent in glioblastoma multiforme.

Preclinical studies have reported that bevacizumab can enhance the therapeutic efficacy of established therapy for HNSCC such as chemotherapy, radiation therapy, and epidermal growth factor receptor (EGFR) directed therapy including cetuximab [52–54]. Although bevacizumab is currently being evaluated in phase III clinical trials (NCT00588770), results from phase II clinical trials indicate that bevacizumab shows little activity as single agent

in HNSCC. The single-agent response rate is less than 10%, and even in patients who do respond, the duration of response is typically less than 3 months [55, 56]. VEGF has been shown to be a downstream target of EGFR signaling cascade and VEGF up-regulation through EGFR activation has been correlated with resistance to EGFR-targeting agents [57]. Using this rationale, a phase I/II study of bevacizumab in combination with elotinib was conducted by Vokes et. al. involving 51 patients with recurrent or metastatic (R/M) HNSCC [55]. An overall response rate of about 15% was seen, which was significantly higher than that with either agent alone. However, median survival was similar to that with chemotherapy alone with less toxicity. Two (4%) of the patients had complete response, five (10%) had partial response, twenty-six (56%) had stable disease and fifteen (30%) had progressive disease. Interim analysis of an on-going phase II study of pemetrexed and bevacizumab in patients with R/M HNSCC at the University of Pittsburgh [56], showed that two (18%) of the patients had complete response, three (27%) had partial response, six (54%) had stable disease and none (0%) had progressive disease.

1.2.3.2 Small Molecule Inhibitors Sunitinib, an oral multikinase inhibitor, which is approved for metastatic renal cell carcinoma and gastrointestinal stromal tumors, targets VEGFRs, PDGFR, RET and c-KIT kinases. A Phase II study conducted to evaluate the tolerability and efficacy of sunitinib in metastatic and/or recurrent HNSCC patients, also concluded that sunitinib had low single agent activity [58]. Sorafenib, another multikinase inhibitor targeting VEGFRs, PDGFR-β and Raf-1, has shown anti-cancer activity in pre-clinical studies [59] and is approved for unresectable hepatocellular carcinoma and renal cell carcinoma. Phase II trials in R/M HNSCC patients with single agent sorafenib showed stable disease in ten (38%) patients and a median overall survival of 8 months [60].

1.2.4 Resistance to VEGF-targeted Therapeutics in HNSCC

Clinical trials with VEGF-targeted agents in HNSCC and several other cancers indicate that the therapeutic efficacy of these drugs is limited to date. Majority of the patients demonstrate an initial clinical response to the treatment but eventually exhibit progressive disease (*acquired resistance*). In addition, some patients show pre-existing indifference to angiogene-

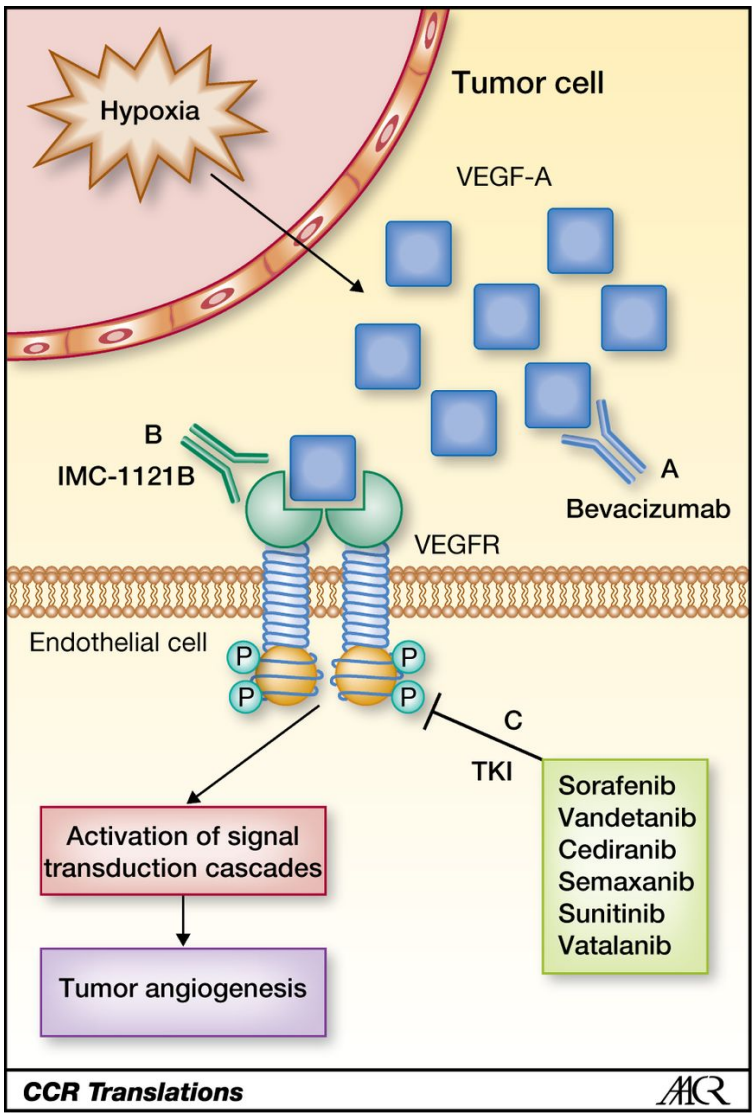

Figure 1.2: Current clinical agents targeting VEGF pathway and their mechanisms of inhibition. A, bevacizumab is a humanized monoclonal antibody directed at VEGF. B, IMC-1121B is a humanized monoclonal antibody targeting the VEGFR-2, thereby inhibiting ligand binding and activation of the receptor. C, TKIs are orally available agents that compete with ATP in the intracellular tyrosine kinase domain of the receptor. [45, 61].

	DRUG	CATEGORY	DESCRIPTION	APPROVED INDICATIONS
1	Bevacizumab/ Avastin	Humanized Monoclonal Antibody	Binds biologically active form of VEGF	• Metastatic Renal Cell Cancer (RCC) • Metastatic Colorectal Cancer (CRC) • Recurrent or Metastatic Non-Small Cell Lung Cancer (NSCLC)
2	Sorafenib/ Nexavar	Small molecule TKI	Inhibits VEGFR-1, VEGFR-2, VEGFR-3, PDGFR-β, & Raf-1.	• Advanced Renal Cell Carcinoma • Advanced Hepatocellular Carcinoma (HCC)
3	Sunitinib/ Sutent	Small molecule TKI	Inhibits VEGFR-1, VEGFR-2, VEGFR-3, PDGFR-β, & RET.	• Advanced Renal Cell Carcinoma • Gastrointestinal Stromal Tumor (GIST)

Table 1.1: FDA approved antiangiogenic drugs.

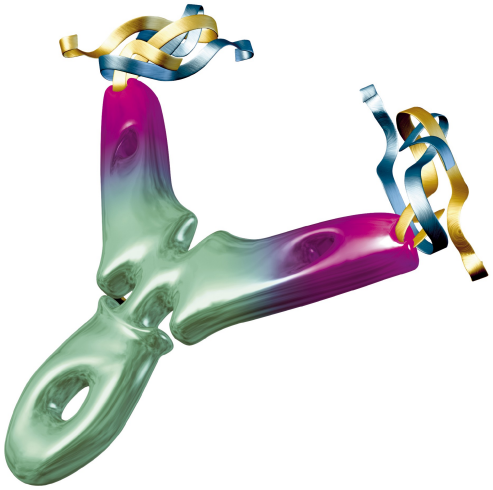

(A)

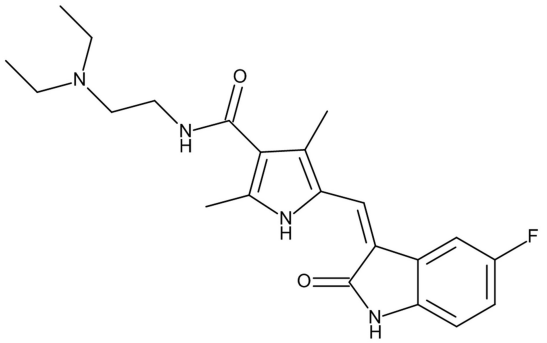

(B)

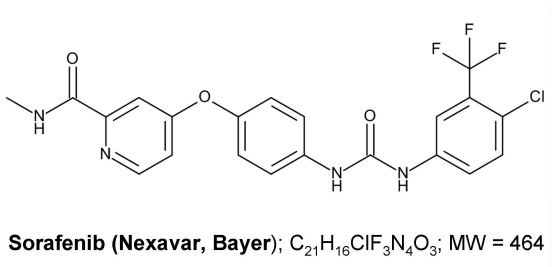

(C)

Figure 1.3: Structures of VEGF inhibitors. (A) Bevacizumab, (B) Sunitinib, (C) Sorafenib.

sis inhibition (*intrinsic resistance*), such that tumor progression continues unabated. These incomplete drug responses are likely due to the complexity of signaling networks that the tumor cells can exploit in the setting of VEGF blockade. Currently, there are no reports that elucidate the molecular mechanisms of resistance to anti-VEGF therapy in HNSCC. However, some potential mechanisms have been proposed in other cancers to account for the resistance of tumors to antiangiogenic therapy that are briefly discussed below [33, 62–66].

1.2.4.1 Intrinsic Resistance to VEGF-targeted Therapeutics Although VEGF is the predominant angiogenic factor in human tumors, there is a pre-existing multiplicity of redundant growth factors produced by both tumor cells as well as the stroma that can compensate for the suppression of VEGF-mediated angiogenesis.

A recent study by Huang et. al. showed that IL-8 expression was elevated in human renal cell carcinoma (RCC) tumors with intrinsic resistance to sunitinib therapy [67]. Further, neutralization of IL-8 activity in RCC xenograft models resensitized tumors to sunitinib treatment. In murine tumor models, infiltrating myeloid cells produced proangiogenic factors including Bv8 and tumor cells secreted HGF, which mediated intrinsic resistance to anti-VEGF antibody and sunitinib respectively [68, 69].

1.2.4.2 Acquired Resistance to VEGF-targeted Therapeutics Unlike intrinsic resistance, tumors can activate and/or upregulate other angiogenic factors in response to anti-VEGF inhibitors. By acquiring alternative ways to sustain growth and survival, tumors can adapt to the effects of angiogenic inhibitors thereby displaying acquired resistance. Antiangiogenic therapies reduce and normalize tumor vasculature but increase intratumor hypoxia [70]. This can result in HIF-1α-mediated expression of several genes involved in angiogenesis.

In a xenograft murine model of human Wilms' tumor, vascular remodeling was seen in tumors that recurred during chronic suppression of angiogenesis [71]. In addition, remodeled vessels were marked by increased expression of ephrinB2 and platelet-derived growth factor-

B (PDGF-β). In a xenograft model of pancreatic-islet tumors, Casanovas et. al. showed that treatment with an anti-VEGFR2 monoclonal antibody was associated with a decrease in microvessel density after ten days of therapy [72]. However, an angiogenic revascularization was observed at four weeks that was associated with an increased expression of other proangiogenic factors including members of the FGF family. In addition, antiangiogenic therapy showed in antitumor effects in mouse models but concomitantly resulted in increased local invasion and distant metastasis [73]. In a separate study, levels of plasmatic PlGF have been shown to be increased following anti-VEGF therapy and seem to be implicated in acquired resistance [74]. In a preclinical study, antibody to PlGF resensitized xenografts to anti-VEGFR2 therapy by preventing infiltration of angiogenic macrophages [75]. Up-regulated stromal EGFR and FGFR have been described in bevacizumab-resistant NSCLC xenografts [76]. Higher expression of proinflammatory factors resulted in increased aggressiveness of bevacizumab-resistant pancreatic tumors [77]. In a mouse model of endometrial cancer, bevacizumab treatment over a 5-week period retards tumor growth in mice but is accompanied by up-regulation of certain proto-oncogenes including c-Jun [78]. A recent study in glioma xenografts models of acquired sunitinib resistance presented with activation of prosurvival pathways including upregulation of PLCg-1 signaling [79].

1.3 RATIONALE, HYPOTHESIS AND SPECIFIC AIMS

Preclinical and clinical studies in HNSCC have revealed bevacizumab to be a promising drug for antiangiogenic therapy in at least a subset of patients. Currently, there are no reliable biomarkers to identify those patients most likely to benefit. Therapeutic efficacy of this drug can be further improved if the molecular determinants of resistance to bevacizumab are known. As discussed above, studies from other cancers indicate that tumors can rely on multiple escape mechanisms using a variety of angiogenic proteins secreted by both tumor cells and stromal cells. These molecular mechanisms of resistance are completely unknown in HNSCC. Also, among the several potential mechanisms known from other cancers, selection of one critical mediator of resistance for cotargeting with VEGF remains a daunting task. To

address these issues, it is necessary to carry out studies that will address the mechanisms of resistance to anti-VEGF therapy in HNSCC. Further, preclinical models that test combinatorial therapies along with VEGF inhibitors will be integral in selection of a suitable cotarget.

We therefore propose to establish HNSCC xenograft models of bevacizumab resistance to mimic the resistance seen in the clinical setting. **We hypothesize that altered signaling through angiogenic factors other than VEGF (such as IL-8, IL-1α, and FGF), contribute to anti-VEGF therapy resistance in HNSCC**. We will explore this hypothesis using preclinical models in the three specific aims outlined below. Completion of these studies will elucidate mechanisms of anti-VEGF therapy resistance in HNSCC thus facilitating the design of more effective anti-cancer treatments by employing novel combination therapies.

1. **To establish and characterize preclinical HNSCC models of intrinsic and acquired models of resistance to VEGF-targeted agents.**

   These studies will test the hypothesis that HNSCC cell lines display differential sensitivity to anti-VEGF agents in vivo, and that these cell lines can serve as the basis for models of intrinsic resistance to anti-VEGF therapy. We further hypothesize that chronic treatment of the sensitive cell lines with anti-VEGF therapy will result in evasive resistance, resulting in the establishment of models of acquired resistance to anti-VEGF therapy.

2. **To identify signaling molecules that contribute to anti-VEGF refractoriness in the preclinical HNSCC models.**

   These studies will test the hypothesis that altered signaling through angiogenic factors other than VEGF (such as IL-8, IL-1α and FGF) provides a mechanism of escape from VEGF blockade in the preclinical HNSCC models that are established in aim 1.

3. **To develop novel co-targeting strategies for overcoming anti-VEGF resistance in the preclinical HNSCC models.**

These studies will test the hypothesis that co-targeting molecules responsible for escape of VEGF blockade (such as IL-8, IL-1α and FGF) in conjunction with VEGF will improve therapeutic efficacy of anti-VEGF agents in preclinical HNSCC models.

2.0 HNSCC XENOGRAFT MODELS OF INTRINSIC RESISTANCE TO BEVACIZUMAB

2.1 INTRODUCTION

Promising results from preclinical studies in HNSCC, have reported that bevacizumab can enhance the therapeutic efficacy of established treatment modalities such as chemotherapy, radiation therapy, and epidermal growth factor receptor (EGFR) targeted therapy including cetuximab [52–54]. Clinical data also suggests that targeting the vasculature in a subset of patients will represent an effective therapeutic strategy [55, 56, 80–82]. However, currently there are no validated biomarkers that can be used reliably to determine which patients will respond to bevacizumab therapy. The identification of such biomarkers will enable design of novel combinatorial approaches to specifically target the subgroup of patients who are expected to be resistant to this antiangiogenic agent. A fundamental understanding of the molecular mechanisms of resistance is therefore a necessary prerequisite to help meet these goals.

Here, we investigated the mechanisms of intrinsic resistance to bevacizumab in preclinical HNSCC models. A panel of head and neck cancer cell lines were screened *in vivo* for their differential response to bevacizumab treatment. The HNSCC cell lines that displayed low sensitivity to bevacizumab served as a model of intrinsic resistance and the cell lines that showed high sensitivity to bevacizumab were used as a non-isogenic model for comparison. In order to characterize the escape mechanisms underlying intrinsic resistance and identify potential biomarkers of drug response, we evaluated the angiogenic profile of HNSCC cells from sensitive and resistant cell lines using antibody array. We further examined the differentially expressed proteins both *in vitro* and *in vivo* for their involvement in conferring

intrinsic resistance, using loss- and gain-of-function approaches.

2.2 MATERIALS AND METHODS

2.2.1 Cells and Reagents

Human umbilical vein endothelial cells (HUVECs) were purchased from Lonza Inc. (San Jose, CA) and were maintained in EBM2 media supplemented with growth factors. Tu138 and HN5 cells were maintained in DMEM/F12 with 10% FBS. FaDu cells were maintained in DMEM with 10% FBS, 1% non-essential amino acids and 1% sodium pyruvate. SCC61 cells were maintained in DMEM with 20% FBS, 1% non-essential amino acids, 1% sodium pyruvate and 0.4ug/ml hydrocortisone. All four previously characterized cell lines were validated by genotyping using short tandem repeat analysis [83]. Bevacizumab (Avastin, Genentech Inc., South San Francisco, CA) was purchased from the University of Pittsburgh Pharmacy with stock concentration of 25mg/ml and diluted as recommended in the instructions. NVP-BEZ235 was purchased from Selleck Chemicals (Houston, TX). Recombinant hVEGF, hIL-8 and hEGF were purchased from R&D Systems (Minneapolis, MN).

2.2.2 Animal studies

Five- to six-week-old female athymic nude-Foxn1nu mice were purchased from Harlan Laboratories (Indianapolis, IN) and were maintained under guidelines provided by the University of Pittsburgh Institutional Animal Care and Use Committee (IACUC). For the differential sensitivity screen, tumor cells (3×10^6 cells/mouse) were suspended in complete medium and subcutaneously implanted into the dorsal flank of mice. After formation of palpable tumors within 2 weeks of inoculation, the mice were randomized to receive either vehicle (control) or bevacizumab (4mg/kg) and administered biweekly via intraperitoneal injection for a period of 29 days. Tumor volumes were assessed using caliper measurements as $3.14/6 \times \text{length} \times \text{width}^2$. Mean tumor values were compared using students' t-test. P-value < 0.05 was considered significant.

For the combination treatment experiments, Fadu-shIL8, SCC61-shIL8 and Tu138-IL8 overexpressing cells along with the respective control cells were used to generate xenografts and tumor growth was assessed in the absence or presence of bevacizumab (4mg/kg). Ten mice were subcutaneously implanted with FaDu-control or -shIL8 cell lines (3×10^6 cells/mouse) while 20 mice were subcutaneously implanted with SCC61-control or -shIL8 cell lines (2×10^6 cells/mouse). For Tu138-control or -IL8 overexpressing cell lines (3×10^6 cells/mouse) ten mice each were used. All *in vivo* studies were carried out for a period of 29 days, except for the Tu138 IL8 overexpression study, which was ended at day 18 due to tumor ulceration.

2.2.3 Antibody array

Nineteen angiogenesis-related proteins were measured in tumor cell-conditioned medium using antibody array (Panomics/ Affymetrix Inc., Santa Clara, CA) according to the manufacturer's instructions. The growth factors that we examined were as follows: TIMP-1, TIMP-2, IP-10, IL-12, IFN-g, TGF-α, TNF-α, FGF-a, FGF-b, PlGF, IL-8, IL-6, IL-1α, IL-1β, VEGF, Leptin, HGF, G-CSF and Ang. Biotin-conjugated antibodies spotted on every membrane served as positive controls. For conditioned media, Tu138 and SCC61 cell lines were plated at a density of 1×10^6 cells/10cm dish. Culture medium was replaced with serum-free medium and collected after 48 hours.

2.2.4 ELISA

HNSCC cell lines were plated at a density of 1×10^5 cells per 6-well plate. Cell culture supernatant was collected after 24 hours and centrifuged at 1200rpm for 5 min. IL-8, IL-1α, VEGF, FGF-a and TNF-α were measured from the supernatant using individual ELISA kits (R&D Systems, Inc. Minneapolis, MN) according to the manufacturer's protocol.

IL-8 was also measured in patient sera using ELISA. Baseline (pretreatment) serum samples from thirty-two patients were run in duplicates and the mean value was used for analysis.

2.2.5 Cell Proliferation

HUVECs were plated in 48-well plates (in triplicates) at a density of 3×10^4 cells/well. The following day complete EBM-2 was replaced with medium (4% FBS containing EBM-2) alone or medium containing VEGF, IL-8, or bevacizumab. Complete EBM-2 medium was used as a positive control. Standard MTT [3-(4,5-Dimethylthiazol-2-yl)-2,5-diphenyltetrazolium bromide] assay was performed at the start of the experiment and after 24 hrs to obtain day zero and day one reading for different treatment groups. 200μl of MTT solution was added to each well, and the plates were incubated at 37 °C for 2 hr in a 5% CO_2 incubator. To dissolve the formazan crystals, 150μl of Dimethyl sulfoxide (DMSO) was added to each well and mixed by pipetting. The optical density (OD) of each well was measured at 570nm with an enzyme-linked immunosorbent assay (ELISA) microtiter plate reader, model 3550 (Bio-Rad Laboratories, Hercules, CA).

2.2.6 Transwell migration

5×10^3 HUVECs were plated in the upper chamber of 8-micron transwell filters (BD Biosciences, Bedford, MA) with serum-free EBM-2 medium in duplicate. In the lower chamber of transwell filters, 250μl of medium (4% FBS containing EBM-2) alone or medium containing VEGF, IL-8, or bevacizumab was added and the cells were allowed to migrate for 24 hrs in 5% CO_2 at 37 °C. At the end of the assay, the filter side of the upper chamber was cleansed with a cotton swab and stained with Fisher Hema 3 system (Fisher Scientific, Pittsburgh, PA) and then rinsed in water. The number of cells that migrated across the filters was counted under 200× magnification.

2.2.7 Capillary-tube formation

1×10^5 HUVECs were plated on 24-well plates precoated with type I collagen gels (3mg/ml) (PureCol, Advanced BioMatrix, Inc., San Diego, CA) in medium alone (1% FBS containing EBM-2) or medium containing VEGF, IL-8, or bevacizumab. Complete EBM-2 medium was used as a positive control. After 24 hrs of incubation, plates were examined for capillary tube formation by microscopy and photographed. Each assay was done in triplicate and

each experiment was repeated four times. Quantitative analysis of capillary tube formation was performed by counting the number of tubes (defined as multicellular cord-like structures between two multicellular nodes) in two-dimensional brightfield microscope images.

2.2.8 Western

HUVECs were plated at a density of 1.5×10^6 cells /10cm dish. The following day complete EBM-2 was replaced with serum-free EBM-2 medium alone or medium containing VEGF, IL-8, or bevacizumab. After 24 hrs of incubation, whole cell lysates were prepared using 25mM Tris-HCl (pH 7.6), 150mM NaCl, 0.5% Sodium dodecylsulphate, 0.1% SDS and protease inhibitor cocktail set (Roche). Protein content was quantified using Bradford assay.

40μg of total protein was separated by 8% SDS-PAGE and blotted onto PVDF membranes (Amersham Biosciences). The membranes were blocked for 1 hr using 5% milk in PBS containing 0.1% Tween-20 and then incubated with 1:1000 diluted rabbit anti-pAKT (Ser473) antibody (Cell Signaling Technology, Inc. Danvers, MA) at 40 °C overnight. Secondary antibody incubations were carried out using 1:2000 diluted goat anti-rabbit IgG (H+L)-HRP conjugate antibody (Bio-Rad Laboratories, Hercules, CA). Reactive bands were detected by chemiluminiscence using ECL plus western blotting detection kit (Amersham Biosciences) and analyzed by densitometry using ImageJ (NIH, Bethesda, Maryland, USA). The membranes were also probed with 1:1000 diluted rabbit anti-AKT and anti-β-Actin polyclonal antibody (Cell Signaling Technology, Inc. Danvers, MA) and 1:2000 diluted goat anti- rabbit IgG (H+L)-HRP conjugate antibody (Bio-Rad Laboratories, Hercules, CA) as a control for equal gel loading. Similarly, immunoblots were performed for SCC61 cells treated with DMSO, EGF or NVP-BEZ235 using the following antibodies; EGFR, pEGFR (Tyr992) (Cell Signaling Technology Inc., Danvers, MA) and IL-8 (Abcam, Cambridge, MA).

2.2.9 Plasmids

Lentiviral shRNA was used to knockdown IL-8 expression in bevacizumab-resistant (FaDu and SCC61) cells. Lentiviral particles were provided by Dr. Robert W. Sobol (University of Pittsburgh Cancer Institute (UPCI) Lentiviral Core Facility). HNSCC cells were incubated

with lentivirus particles and polybrene 8μg/mL for 16 hours and then washed with media. Cells were selected with 0.5μg/ml puromycin for two weeks before confirmation of knockdown using ELISA. Five different oligonucleotide sequences of IL-8 shRNA were tested for optimal knockdown of protein and the following sequences were selected.

CCGGCAAGAGAATATCCGAACTTTACTCGAGTAAAGTTCGGATATTCTCTTGTTTTTG
CCGGCAAGGAGTGCTAAAGAACTTACTCGAGTAAGTTCTTTAGCACTCCTTGTTTTTG

For overexpressing IL-8, bevacizumab-sensitive Tu138 cells were transfected with pSELECT-PURO-MCS or pSELECT-PURO-IL-8 expression plasmids (InvivoGen, San Diego, California) followed by selection with puromycin (1.5μg/ml) and ELISA to validate increased expression of IL-8 protein.

2.2.10 Immunohistochemistry and Immunofluorescence

Frozen tumor sections (8-10 mm) from each group were mounted on positively charged Superfrost slides (Fischer Scientific, Houston, TX). The slides were washed in Tris Buffer Saline/ Tween 20 and incubated in endogenous peroxidase and protein blocking solution Rodent block (BioCare, Concord, CA). The samples were then incubated with rat anti-mouse CD31 antibody (BD Biosciences Pharmingen, San Jose, CA). After washing, the slides were incubated in rat Probe followed by Rat polymer (Biocare Rat on Mouse Kit). The slides were then incubated in chromogen DAB Quanto (Thermo Scientific/Lab Vision, Kalamazoo, MI). Slides were stained in Mayer's Hematoxilin and coversliped with Permount.

Frozen tumor sections were fixed and blocked as above, excluding the endogenous peroxidase step. The slides were incubated with rat anti-mouse CD31 monoclonal antibody, washed with PBS, blocked with protein block and incubated with Texas Red-X goat anti-rat IgG antibody (Invitrogen, Grand Island, NY). To stain for terminal deoxynucleotidyl transferase-mediated dUTP nick end labeling (TUNEL), a commercially available Apoptosis Detection kit (Promega, Madison, WI) was used. Slides were washed with PBS and mounted using Vectashield Mounting Medium with DAPI (Vector laboratories, Burlingame,

CA). Immunofluorescence microscopy was carried out using an Olympus IX81-DSU Spinning Disk Confocal Microscope. Images were captured using a Hamamatsu ORCA II ER camera (Hamamatsu Corp.) and 3i Slidebook 5.0 software.

For quantification of CD31 expression, vessels completely stained with anti-CD31 antibodies were counted in random $0.04 - \text{mm}^2$ fields at using a $20\times$ objective. Quantification of CD31/TUNEL staining was done as the average percentage of apoptotic endothelial cells in 10 random $0.01 - \text{mm}^2$ fields using a $40\times$ objective.

2.2.11 Statistical Analysis

Data are expressed as mean ± S.E.M. Student's t test was used for all statistical analyses except for the serum IL-8 study where P-values were derived from a two-tailed probability generated using Mann Whitney test. Significance tests were performed with a two-sided significance level of 0.05.

2.3 RESULTS

2.3.1 Differential sensitivity of HNSCC xenografts to bevacizumab

We first sought to investigate the efficacy of bevacizumab in different preclinical HNSCC models. Tu138 (Figure 2.1A) and HN5 (Figure 2.1B) tumors were sensitive to bevacizumab resulting in 88% and 75% growth inhibition compared to the respective vehicle controls. FaDu (Figure 2.1C) tumors showed an intermediate response with 58% growth inhibition while SCC61 (Figure 2.1D) tumors exhibited the least response (non-significant 41% growth inhibition). Overall, HNSCC xenografts displayed a differential response to bevacizumab where Tu138 tumors were most sensitive and SCC61 tumors were least sensitive. Given this finding, we initially focused our efforts on identifying the mechanisms of resistance to anti-VEGF treatment by comparing the Tu138 and SCC61 xenograft models.

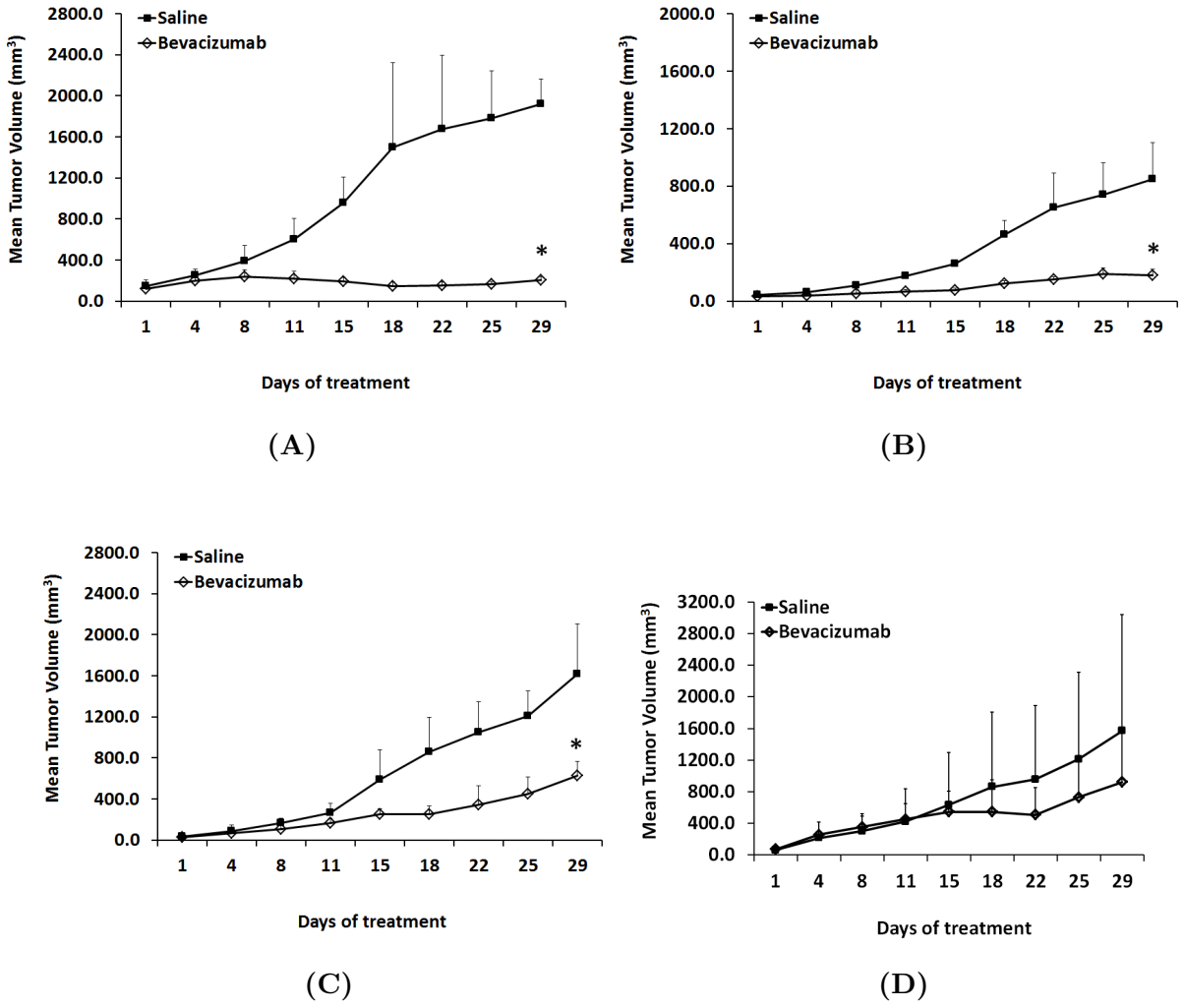

Figure 2.1: Differential sensitivity of HNSCC xenografts to bevacizumab. Athymic nude mice (n=8) were subcutaneously implanted with HNSCC cell lines including Tu138 (A), HN5 (B), FaDu (C) & SCC61 (D). After tumor formation, mice were grouped and given saline or bevacizumab. Tumor volumes were assessed using caliper measurements and compared using student's t-test. P-value < 0.05 was considered significant ($\star$). Tu138, 88% inhibition, $P = 0.0007$; HN5, 75% inhibition, $P = 0.014$; Fadu, 58% inhibition, $P = 0.023$; & SCC61, 41% inhibition, $P = 0.2613$.

2.3.2 Resistant HNSCC cells secrete higher levels of several angiogenic factors including IL-8

We assayed for differences in secreted angiogenic factors between the bevacizumab-sensitive (Tu138) and -resistant (SCC61) HNSCC cell lines by performing antibody array using conditioned media. We found higher expression of both pro- and antiangiogenic factors in the resistant cells compared to the sensitive cells (Figure 2.2A). The differentially expressed proangiogenic factors were IL-8 (264-fold), IL-1α (36-fold), VEGF (20-fold), FGF-a (12-fold) and TNF-α (6-fold) as validated by ELISA (Figure 2.2B-F). Among these cytokines, IL-8 was the most differentially expressed protein with 264-fold higher expression in the resistant cells. We then compared IL-8 expression across our panel of HNSCC cell lines and observed an inverse correlation between IL-8 levels and the *in vivo* sensitivity of these cell lines to bevacizumab (Figure 2.2G). These results suggest that IL-8 levels might predict response to bevacizumab and that IL-8 might be involved in bevacizumab-associated intrinsic resistance in our HNSCC xenograft models.

Since we observed a significantly higher expression of VEGF (20-fold) in the resistant cells compared to the sensitive cells, we also measured plasma human VEGF levels from the respective xenograft models to further confirm that the intrinsic resistance was not due to incomplete inhibition of VEGF in the bevacizumab-treated tumors (Figure 2.3).

We also examined the differentially expressed proangiogenic factors in HNSCC tumors compared to normal tissues from 3 independent gene expression datasets [84–86] using the oncomine resource (www.oncomine.org) (Figure 2.4). In these datasets, gene expression is represented as log2 median-centered intensity and results are expressed as mean fold changes (tumor versus normal). The P-values were determined using student's t-test. Among the cytokines analyzed, IL-8 was the most significantly overexpressed gene in HNSCC tumors compared to normal control tissues.

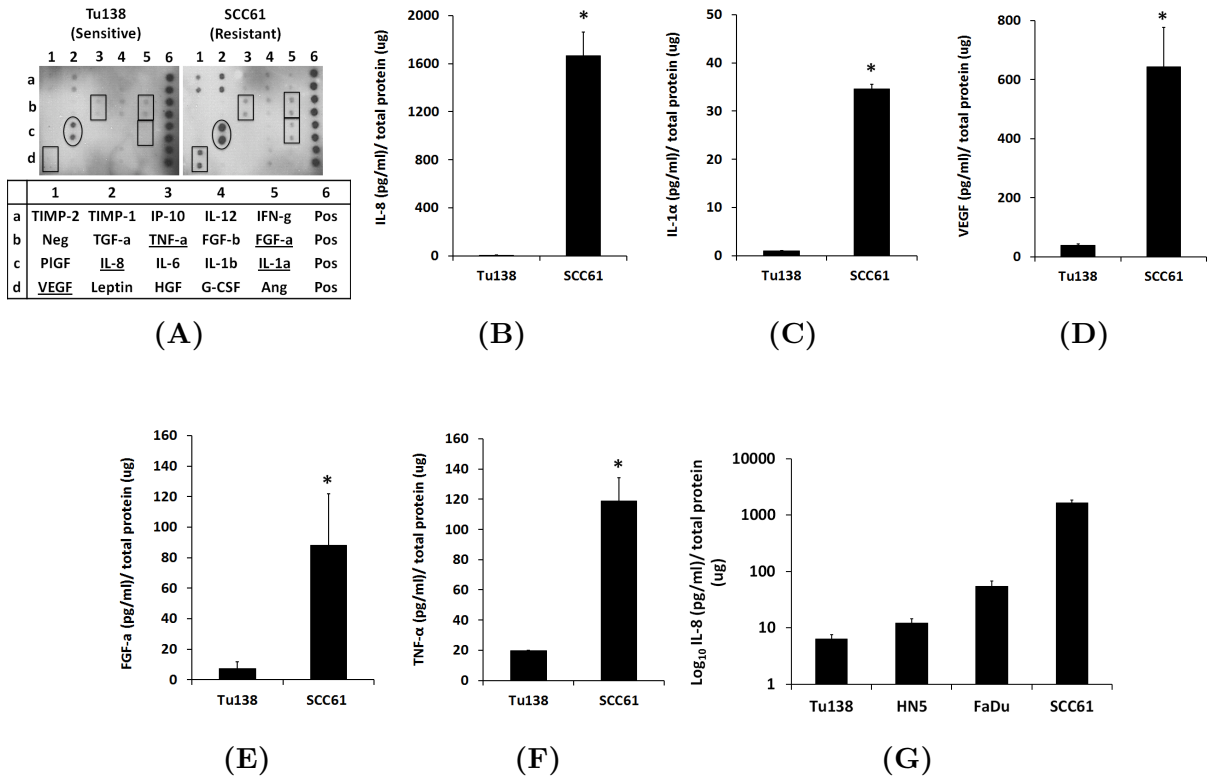

Figure 2.2: Resistant HNSCC cells secrete higher levels of several angiogenic factors including IL-8. (A), *in vitro* angiogenic profile of bevacizumab-sensitive (Tu138) and -resistant (SCC61) HNSCC cell lines was examined using antibody array. Conditioned medium was collected after 48 hours and incubated with Panomics angiogenesis antibody array membranes. The growth factors that were analyzed are indicated in the bottom panel; pos, positive controls, neg, negative controls. (B)-(F), Quantitative analysis of proangiogenic proteins (IL-8; P=0.0003, IL-1α; $P = 0.0092$, VEGF; $P = 0.0021$, FGF-a; $P = 0.0073$, and TNF-α; $P = 0.0004$) was carried out in the supernatant from sensitive and resistant cells using ELISA. (G), Comparative analysis of secreted IL-8 levels in the panel of HNSCC cell lines by ELISA.

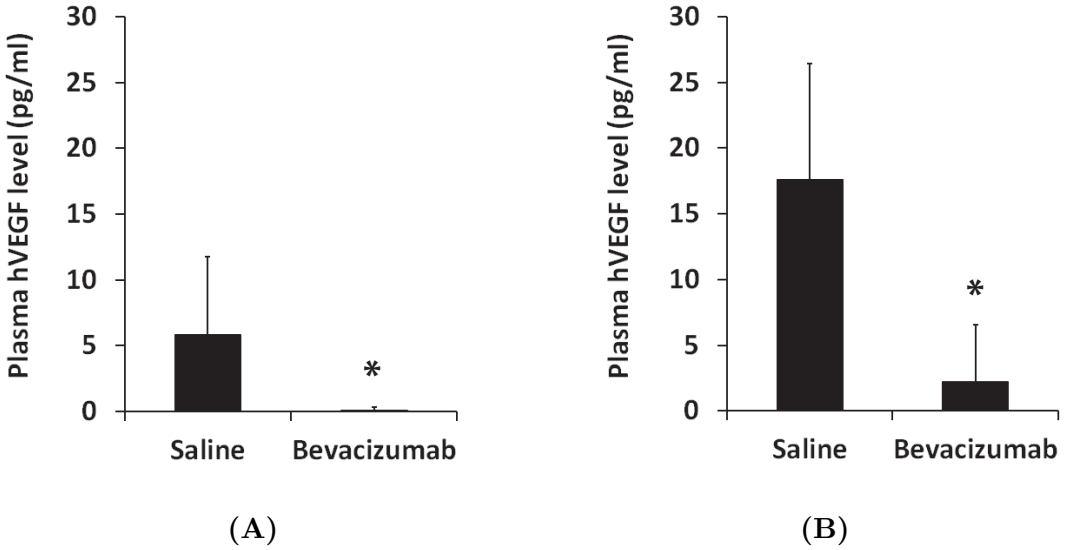

Figure 2.3: Inhibition of VEGF in bevacizumab-treated sensitive and resistant tumors. Human VEGF levels were measured in plasma from mice bearing sensitive and resistant tumors that were treated with saline or bevacizumab (4mg/kg). Bevacizumab treatment resulted in a significant reduction in VEGF plasma levels in both sensitive/Tu138 (A) tumors (98% inhibition; $P = 0.0383$) and resistant/SCC61 (B) tumors (87% inhibition; $P = 0.0270$).

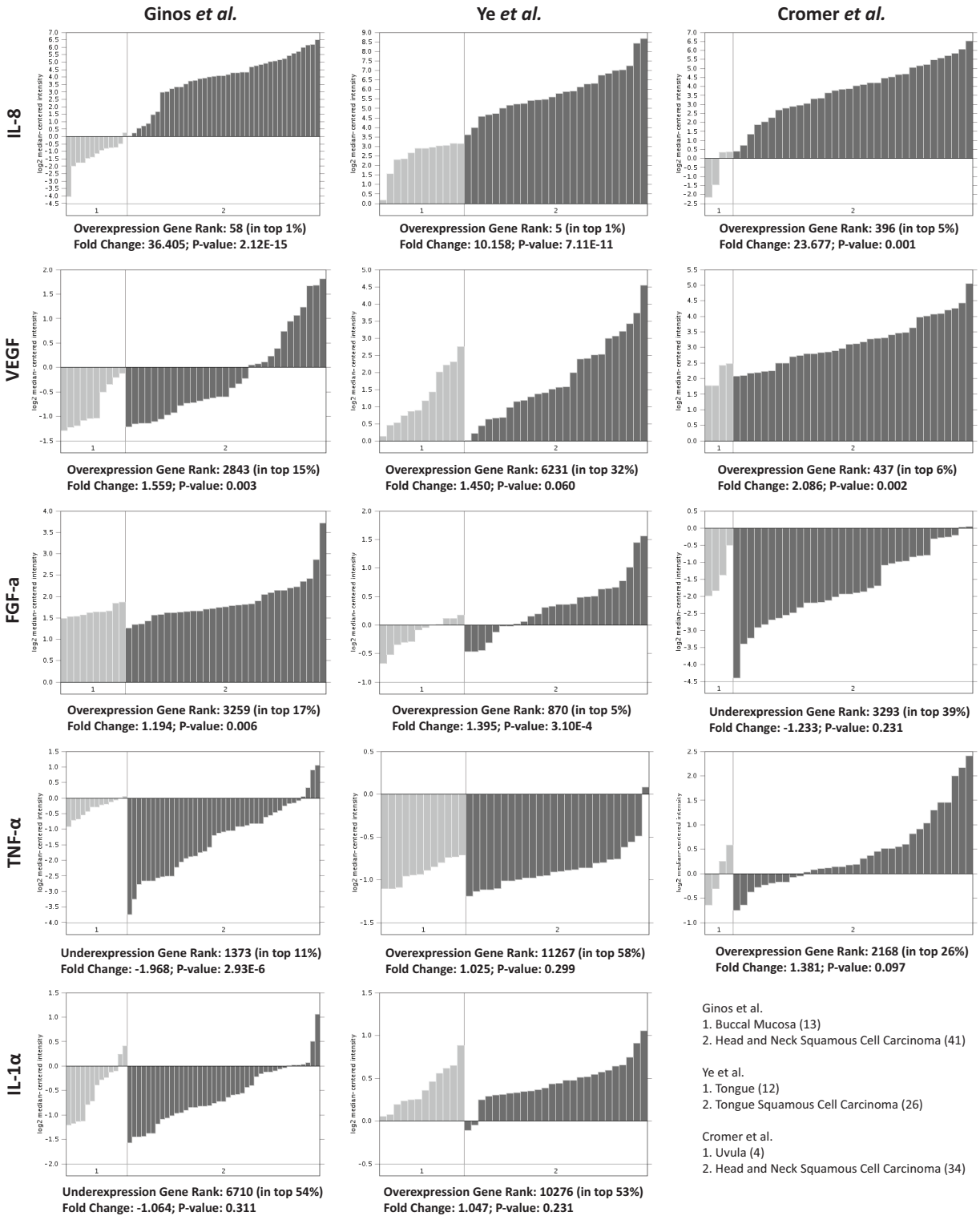

Figure 2.4: Expression of proangiogenic factors in HNSCC tumors compared to normal tissues from publically available microarray datasets in Oncomine.

2.3.3 IL-8 mediates rescue of *in vitro* angiogenesis in bevacizumab-treated endothelial cells

To test our hypothesis that IL-8 contributes to resistance to bevacizumab, we examined the ability of IL-8 to support endothelial cell proliferation, migration and capillary-tube formation in the presence of VEGF and bevacizumab.

We did not observe any significant difference in the rate of proliferation between bevacizumab-inhibited HUVECs in the presence and absence of IL-8 stimulation using the MTT assay (Figure 2.5A).

In a transwell migration assay, bevacizumab caused a 25% reduction in the number of migrated cells in VEGF-stimulated HUVECs (Figure 2.5B). Interestingly, addition of IL-8 to bevacizumab-treated HUVECs fully restored cell migration. Consistently, VEGF induced capillary-tube formation in HUVECs and this effect was abrogated by bevacizumab (Figure 2.5C-D). However, the addition of IL-8 to bevacizumab-treated HUVECs resulted in a significant recovery of capillary-tube formation. These results indicate that IL-8 could compensate for VEGF in setting of bevacizumab-mediated inhibition of *in vitro* angiogenesis. In conjunction with the rescue effect of IL-8, we were interested to see if IL-8 modulated *in vitro* angiogenesis phenotype-associated proteins that are common to VEGF and IL-8 downstream signaling cascades, such as Akt (Figure 2.6A-B). Bevacizumab caused a significant reduction in pAkt levels in VEGF-stimulated HUVECs. However, IL-8 restored the phosphorylation of Akt thereby overcoming the effect VEGF inhibition. These data suggest that the rescue effects of IL-8 to promote *in vitro* angiogenesis and restore pAkt in endothelial cells could in part be contributing to resistance to anti-VEGF therapy.

2.3.4 Downregulation of IL-8 in resistant xenografts leads to bevacizumab-sensitivity

In vitro studies on the compensatory function of IL-8 in endothelial cells provided a rationale to simultaneously target VEGF and IL-8 in bevacizumab-resistant tumors. To perform this loss-of-function analysis, we downregulated IL-8 expression in the resistant cell lines

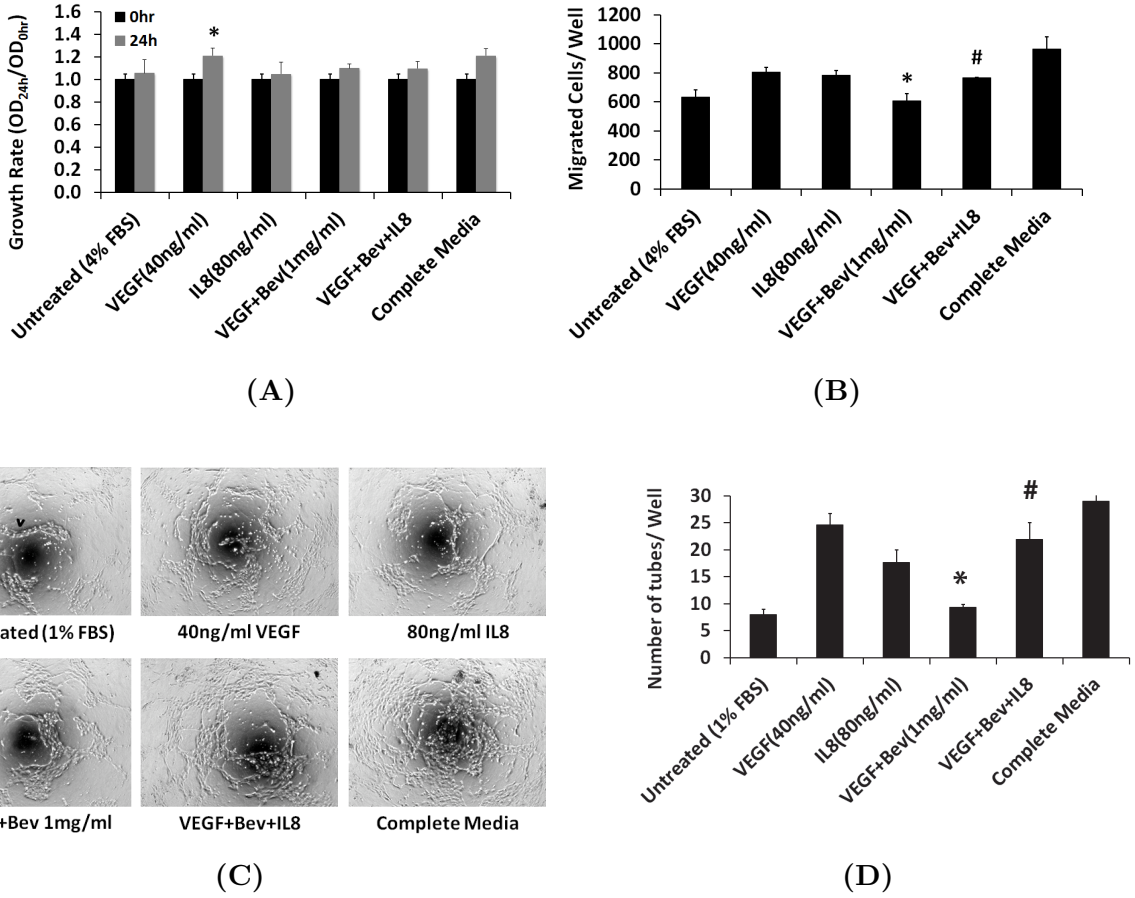

Figure 2.5: IL-8 mediates rescue of *in vitro* angiogenesis in bevacizumab-treated endothelial cells. (A), HUVECs were treated with medium (4% FBS containing EBM-2) alone or medium containing VEGF, IL-8, or bevacizumab. MTT assay was performed at the start of the experiment and after 24 hrs. (B), HUVECs were plated onto transwell filters in different treatment media. After 24 hrs, transwell filters were stained and number of migrated cells was assessed. Bevacizumab significantly reduced the number of migrated cells compared to VEGF alone ($\star$; $P = 0.0010$) while addition of IL-8 restored migration (#; P=0.0077). (C), HUVECs were plated in 24-well plates precoated with type I collagen gels in different treatment media. After 24 hrs of incubation, plates were examined for capillary-tube formation by microscopy. (D), Quantitative analysis of capillary-tube formation was performed by counting the number of tubes. Bevacizumab markedly reduced the number of tubes compared to VEGF alone ($\star$; $P = 0.0011$) while addition of IL-8 significantly recovered tubule formation (#; $P = 0.0142$).

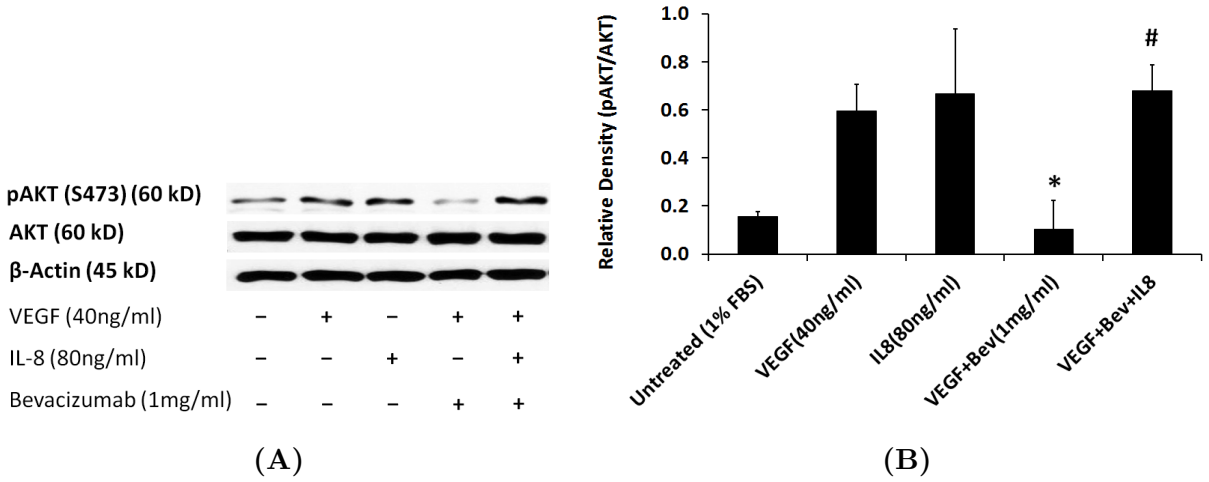

Figure 2.6: IL-8 mediates rescue of *in vitro* angiogenesis phenotype-associated proteins in bevacizumab-treated endothelial cells. (A), IL-8 mediated restoration of pAKT protein levels in HUVECs by western blotting. (B), Bars represent average densitometric values of pAKT normalized to total AKT from three independent experiments.

(FaDu and SCC61) using an shRNA approach. These resistant cell lines were transduced with control shRNA or IL-8 shRNA expressing lentivirus and marked reduction in IL-8 levels were confirmed using ELISA (Figure 2.7A-B). The transduced cells were then used to produce xenografts in nude mice and tumor growth was assessed in the absence or presence of bevacizumab. For the HNSCC cell line FaDu, neither treatment with bevacizumab nor downregulation of IL-8 resulted in statistically significant decrease in tumor growth, confirming the resistant nature of these xenografts (Figure 2.7C). However, downregulation of IL-8 conferred sensitivity to bevacizumab as evidenced by almost complete inhibition of tumor growth. For the HNSCC cell line SCC61, treatment with bevacizumab and the downregulation of IL-8 both resulted in modest but statistically significant decrease in tumor growth (Figure 2.7D). However, similar to FaDu, the greatest degree of inhibition was seen with bevacizumab treatment in setting of IL-8 downregulation.

Using immunohistochemical and immunofluorescence analysis, we further analyzed MVD and endothelial cell apoptosis in these xenografts to confirm whether the combination treat-

ment reversed the angiogenic escape in resistant tumors. Both, treatment with bevacizumab and downregulation of IL-8, reduced MVD and increased endothelial cell apoptosis in the FaDu xenografts (Figure 2.8A-C) as well as the SCC61 xenografts (Figure 2.8A-C). However, the largest difference was seen with combined inhibition. Collectively, the above data show that IL-8 contributed to bevacizumab resistance in our HNSCC tumor models by circumventing inhibition of VEGF-mediated angiogenesis.

2.3.5 Upregulation of IL-8 in sensitive xenografts leads to bevacizumab-resistance

To further substantiate our findings on the role of IL-8 in mediating bevacizumab resistance and to provide counter evidence, we employed a gain-of-function approach to upregulate IL-8 expression in the sensitive tumors and examine emergence of resistance. HNSCC cell line Tu138 was transfected with control or IL-8 expressing vector followed by confirmation of the overexpression using ELISA (Figure 2.10A). Nude mice were subcutaneously implanted with control or IL-8 overexpressing cell lines. Mice were grouped and treated with saline or bevacizumab. As expected, the control xenografts showed significant sensitivity to bevacizumab. However, the IL-8 overexpressing xenografts became refractory to bevacizumab and these xenografts grew at rates similar to saline-treated control xenografts regardless of whether they were treated with saline or bevacizumab (Figure 2.10A-B). CD31 staining in these xenografts revealed significantly higher MVD in bevacizumab-treated IL-8 overexpressing xenografts compared to the control xenografts (Figure 2.11A-B).

2.3.6 Serum IL-8 levels in HNSCC patients treated with cetuximab and bevacizumab suggest correlation with clinical response

As our data identified IL-8 as a mediator of bevacizumab resistance in preclinical HNSCC xenograft models, we next assessed IL-8 levels in sera from HNSCC patients who received bevacizumab as a part of their treatment regimen and correlated these levels with clinical outcome (Figure 2.12). Serum samples were obtained from patients enrolled in a phase II clinical trial of bevacizumab plus cetuximab [80]. In this trial, 43 patients with recurrent or metastatic HNSCC received bevacizumab (15mg/kg IV every 21 days) and cetuximab (200mg/m^2 IV once per week after a loading dose of 400mg/m^2) until progress of their

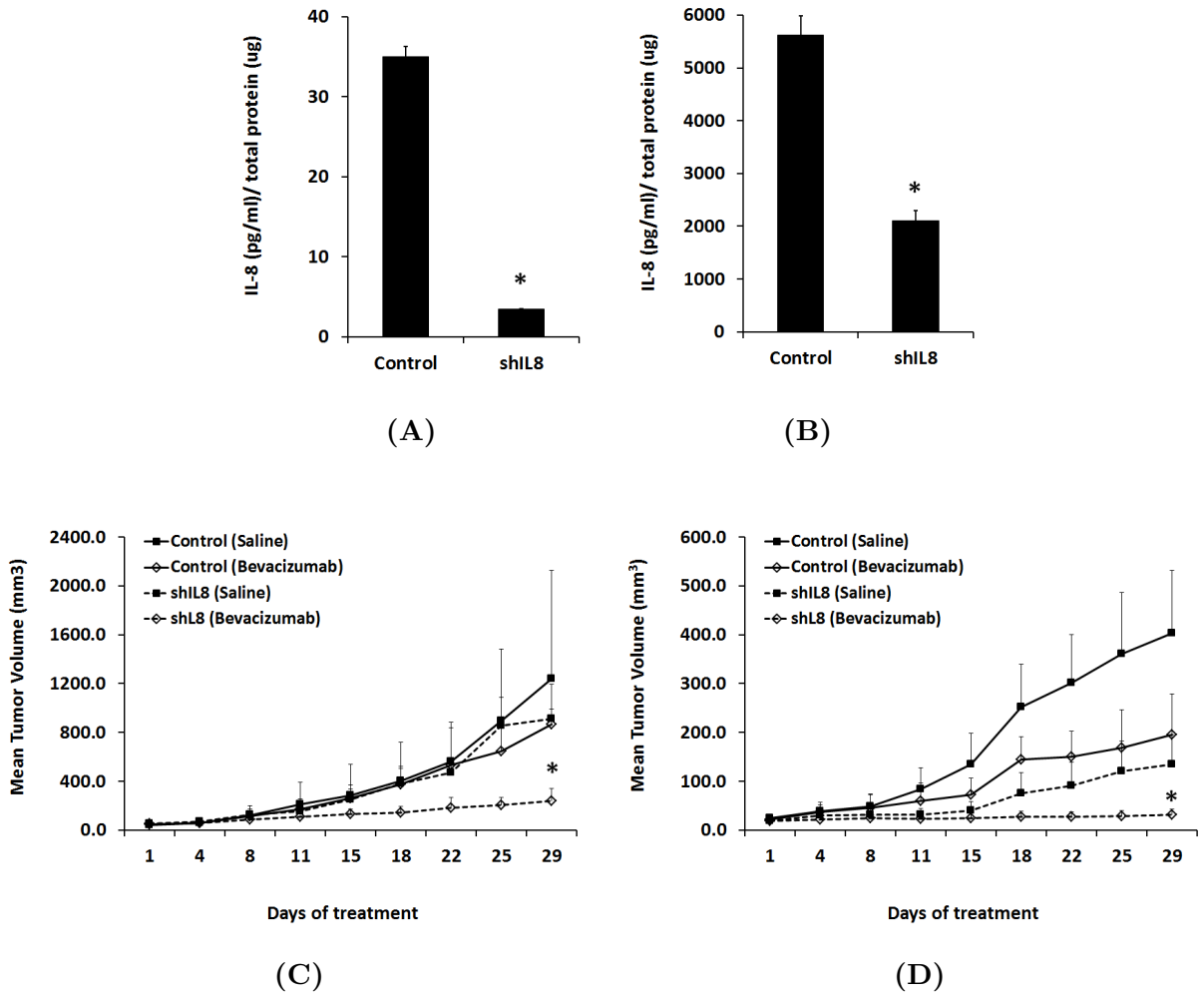

Figure 2.7: Combined knockdown of VEGF and IL-8 significantly inhibits tumor growth in resistant xenografts. (A-B), Knockdown of IL-8 gene in FaDu (A) and SCC61 (B) cells lines. HNSCC cells were infected by control shRNA or IL-8 shRNA lentivirus and cell culture supernatant was subsequently collected for ELISA. (C), Nude mice ($n = 10$) were subcutaneously implanted with FaDu-control or shIL8 cell lines. After tumor formation, mice were grouped and given saline or bevacizumab. Mean tumor volumes were compared using student's t-test. Asterisks indicate significant difference ($p < 0.05$) when comparing bevacizumab alone versus bevacizumab treated shIL8 xenografts ($\star$; $P = 0.0165$). (D), Similarly, nude mice ($n = 20$) were subcutaneously implanted with SCC61-control or shIL8 cell lines and mean tumor volumes in treated groups were compared ($\star$; P=0.0025).

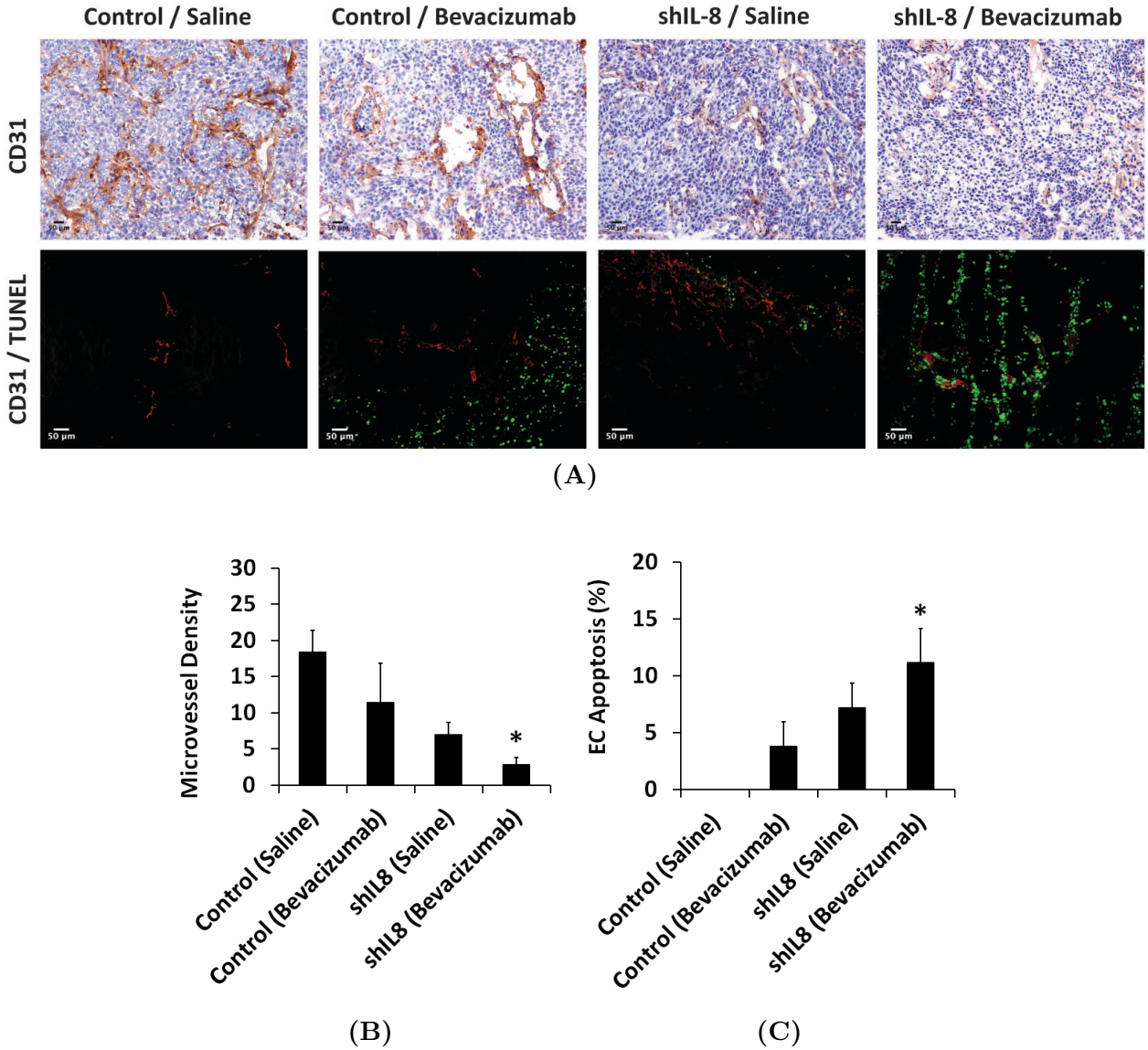

Figure 2.8: Combined knockdown of VEGF and IL-8 disrupts vasculature in resistant FaDu xenografts. (A-C), Microvessel density and endothelial cell apoptosis was assessed in the FaDu xenografts treated with bevacizumab and/or shIL8 by staining for CD31 (red) and or co-staining for TUNEL (green). Combination treatment reduced microvessel density ($P = 0.0439$) and increased endothelial cell apoptosis ($P = 0.0310$) in FaDu tumors compared to bevacizumab alone.

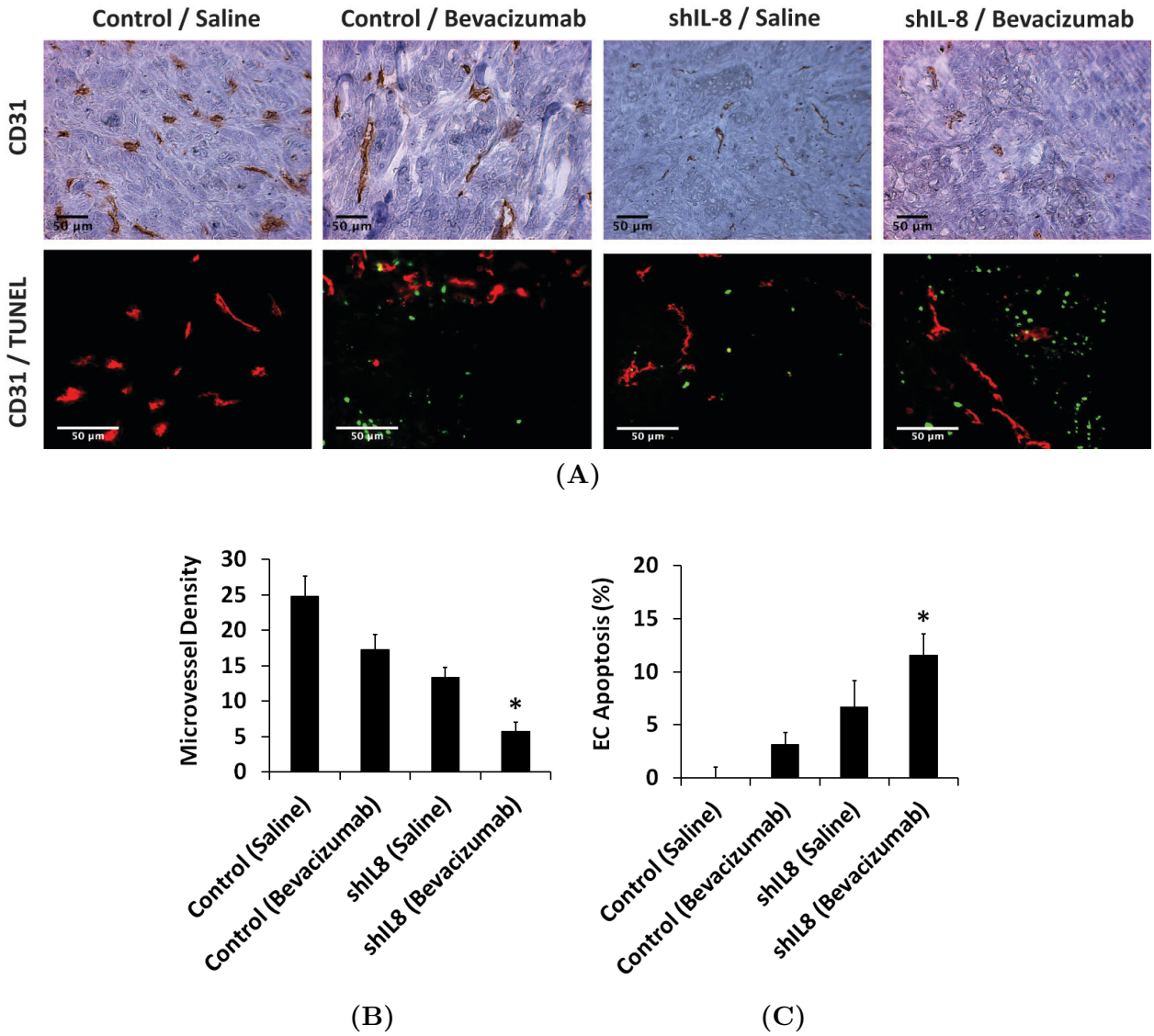

Figure 2.9: Combined knockdown of VEGF and IL-8 disrupts vasculature in resistant SCC61 xenografts. (A-C), Microvessel density and endothelial cell apoptosis was assessed in the SCC61 xenografts treated with bevacizumab and/or shIL8 by staining for CD31 (red) and or co-staining for TUNEL (green). Combination treatment reduced microvessel density ($P = 0.0001$) and increased endothelial cell apoptosis ($P = 0.0012$) in SCC61 tumors compared to bevacizumab alone.

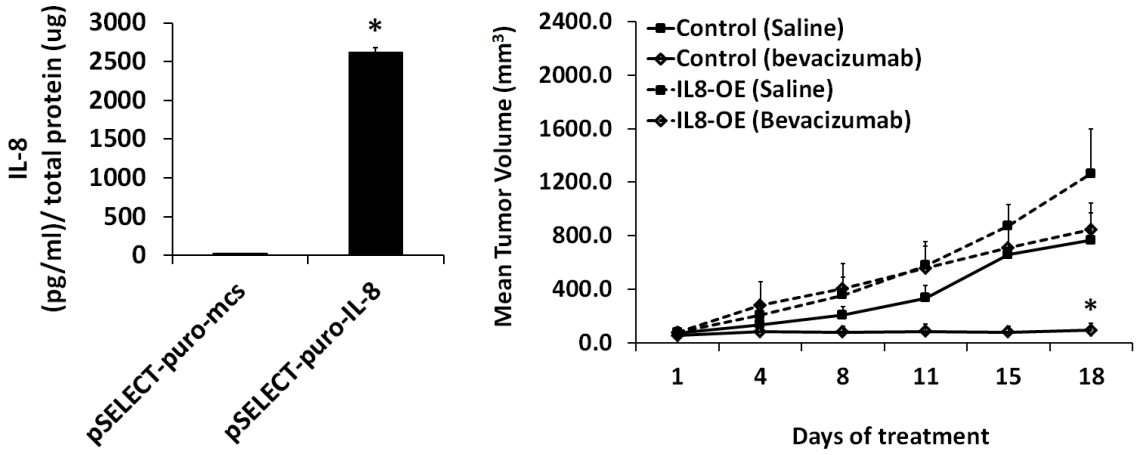

(A) **(B)**

Figure 2.10: Upregulation of IL-8 in sensitive xenografts leads to bevacizumab-resistance. (A), Tu138 cells were transfected with control or IL-8 expressing vector followed by confirmation of the overexpression using ELISA ($\star$; $P < 0.0001$). (B), Nude mice (n=10) were subcutaneously implanted with control or IL-8 overexpressing cell lines. After tumor formation, mice were grouped and given saline or bevacizumab. IL-8 overexpressing xenografts became refractory to bevacizumab resulting in a dramatic increase in tumor growth compared to the control xenografts treated with bevacizumab ($\star$; $P = 0.0011$).

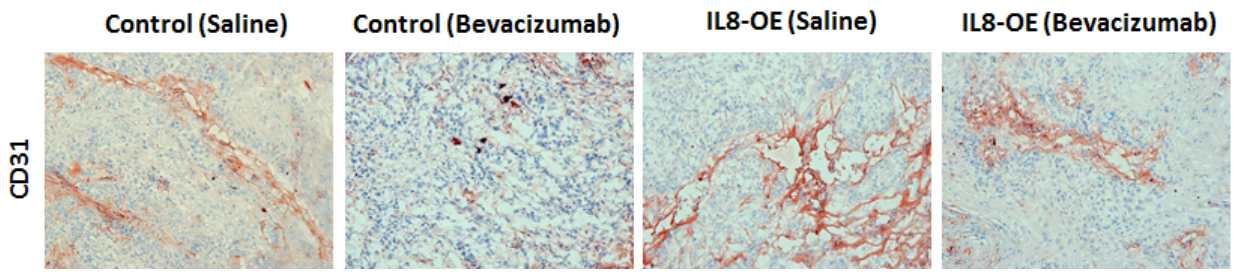

(A)

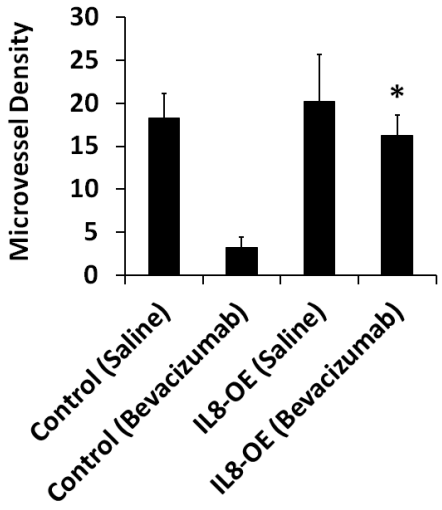

(B)

Figure 2.11: Upregulation of IL-8 leads to increased vasculature in sensitive xenografts. (A), CD31 staining in IL-8 overexpressing and control Tu138 xenografts using immunohistochemistry. (B), MVD analysis indicated increased number of vessels in bevacizumab-treated IL-8 overexpressing xenografts compared to bevacizumab-treated control xenografts ($\star$; $P < 0.0001$).

disease. Baseline serum samples were available from 32 patients. Serum level of IL-8 was noted to be 40% higher at baseline in patients with no response (progressive disease or stable disease) compared to those with partial response (PD/SD= 54.4 pg/ml, PR= 33.0 pg/ml). However, this difference in serum IL-8 levels was not statistically significant (P = 0.2315). Although we observe an encouraging trend in serum IL-8 levels and clinical response to bevacizumab, this analysis is limited by small number of patients in partial response group (n = 4). Hence, validation in a larger cohort of patients is warranted.

2.3.7 Constitutively activated PI3K signaling transactivates IL8 production in resistant cells

It has been reported that bevacizumab-resistant SCC61 cells contain a PI3K activating mutation (E542K) in Exon 9 [87]. We next examined if activated PI3K affected IL-8 production levels in the resistant cells (Figure 2.13). SCC61 cells were treated with DMSO control or NVP-BEZ235 (dual PI3K/mTOR inhibitor) for 24 hrs followed by western blot analysis to determine IL-8 levels. Treatment with NVP-BEZ235 resulted in a dose-dependent decrease in IL-8 levels. These results suggest that constitutive activation of PI3K signaling in the resistant cells regulates increased production of IL-8 in the resistant cells.

2.3.8 IL-1α positively regulates IL-8 & VEGF in resistant cells

In addition to PI3K signaling contributing to increased IL-8 levels, we also examined other mechanisms of IL-8 regulation in the resistant cells. Studies have shown that IL-1α promotes nuclear factor-kappaB and AP-1-induced IL-8 expression, cell survival, and proliferation in head and neck squamous cell carcinomas [88]. To confirm these findings in our HNSCC models, we downregulated IL-1α in SCC61 cells using shRNA approach (Figure 2.14A). We then measured IL-8 (Figure 2.14B) and VEGF (Figure 2.14C) levels in the IL-1α knockdown cells using ELISA. We observed a significant decrease in IL-8 and VEGF expression in IL-1α knockdown cells compared to the vector control. Also, previous experiments have shown that the resistant cells express increased levels of IL-1α along with IL-8 and several other proangiogenic proteins (Figure 2.2C). Collectively, these data suggest that increased expression of IL-1α in the resistant cells contributes to increased IL-8 production, which me-

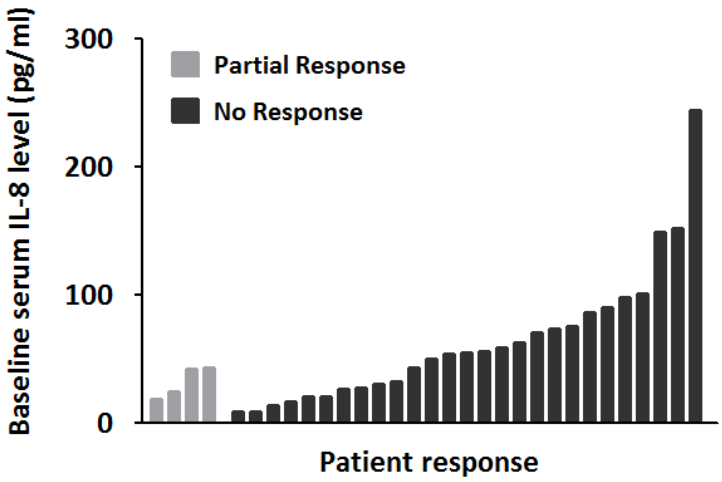

Figure 2.12: IL-8 levels in sera of HNSCC patients treated with cetuximab and bevacizumab. IL-8 expression levels were examined in sera from 32 patients with recurrent or metastastic HNSCC who were treated with bevacizumab and cetuximab. Within this cohort, there were 28 non-responders (those with progressive disease or stable disease) and 4 partial responders. Serum IL-8 was higher at baseline in patients with no response compared to those with partial response, although not statistically significant ($P = 0.2315$). Data are expressed as means ± SEM. P-values are derived from a two-tailed probability generated from a Mann-Whitney test.

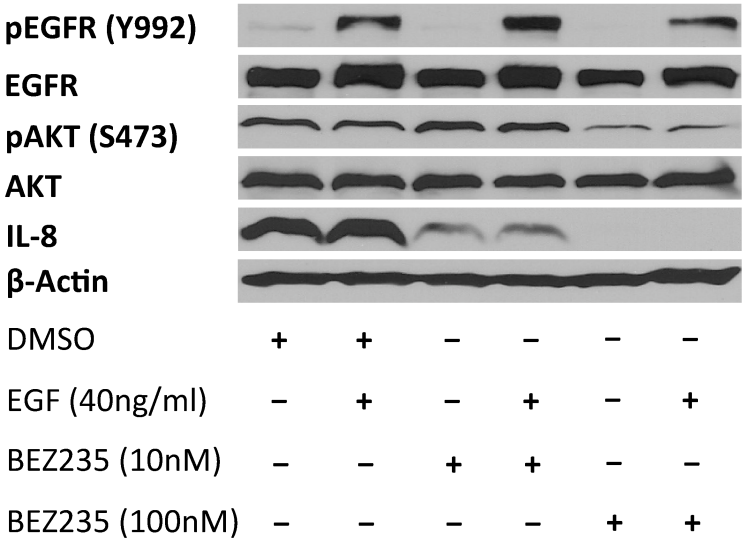

Figure 2.13: Constitutively activated PI3K signaling transactivates IL8 production in resistant cells. SCC61 cells were treated with DMSO control or NVP-BEZ235 (dual PI3K/mTOR inhibitor) for 24 hrs followed by western blot analysis to determine IL-8 levels. Treatment with NVP-BEZ235 resulted in a dose-dependent decrease in IL-8 levels.

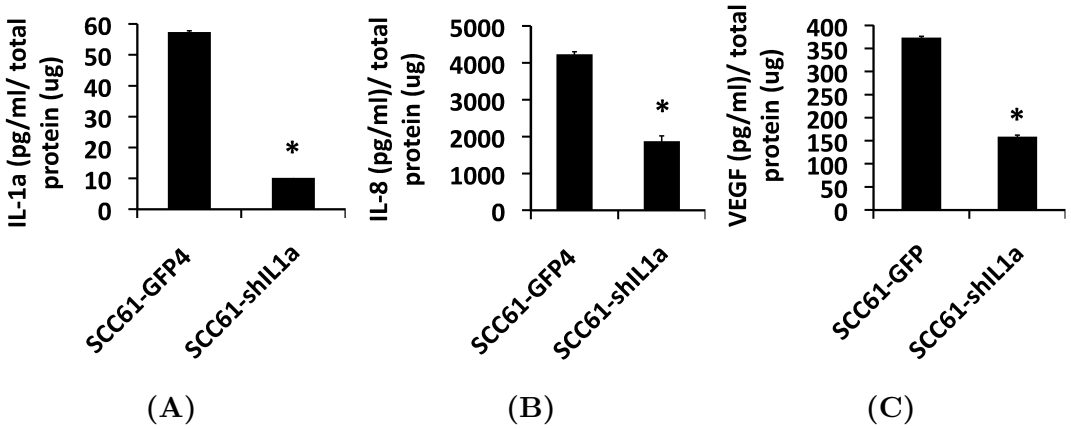

Figure 2.14: IL-1α positively regulates IL-8 & VEGF in resistant cells. (A), Downregulation IL-1α in SCC61 cells using shRNA approach. (B-C), IL-8 (B) and VEGF (C) expression in IL-1α downregulated cells using ELISA. Mean values of proteins levels were compared using student's t-test. P-value < 0.05 was considered significant ($\star$). IL-1α, $P = 0.0051$; IL-8, $P = 0.0091$; VEGF, $P = 0.0091$.

diates bevacizumab resistance. Hence, increased IL-1α signaling could be another potential mechanism of resistance to anti-VEGF therapy in HNSCC.

2.4 CONCLUSIONS AND DISCUSSION

In this study, we investigated the *in vivo* efficacy of bevacizumab in several HNSCC xenograft models and found high expression of IL-8 in the bevacizumab-resistant tumors. IL-8, also known as CXCL-8 is a potent proinflammatory cytokine that belongs to the CXC chemokine family of proteins. In addition to its inflammatory role, IL-8 is known to play an important role in angiogenesis, tumor growth and metastasis [89,90]. Here, we showed that modulation of IL-8 expression in HNSCC xenografts directly controlled the sensitivity of these xenografts to the antitumor and antiangiogenic effects of bevacizumab. We also identified PI3K and IL1-α signaling as the molecular basis for overexpression of IL-8 in the resistant tumors.

It has been previously reported that SCC61 cells (bevacizumab-resistant) contain a PI3K

activating mutation (E542K) in Exon 9 [87]. Our studies showed that treatment with NVP-BEZ235 (dual PI3K/mTOR inhibitor) resulted in a dose-dependent decrease in IL-8 levels. These data suggest that constitutive activation of PI3K signaling in the resistant cells could serve as an escape mechanism to anti-VEGF therapy by regulating increased production of IL-8.

In addition to PI3K signaling, we also demonstrated IL-1α as a mechanism IL-8 regulation in the resistant cells. Studies have shown that IL-1α promotes nuclear factor-kappa B and Activator Protein-1 induced IL-8 expression, cell survival, and proliferation in head and neck squamous cell carcinomas [88]. We validated these findings in our HNSCC models, by downregulating IL-1α in SCC61 cells using shRNA approach and observed a significant decrease in IL-8 and VEGF expression. Also, in our antibody array analysis, we have shown that the resistant cells express increased levels of IL-1α along with IL-8 and several other proangiogenic proteins. These findings suggest that increased expression of IL-1α in the resistant cells contributes to increased IL-8 production, which mediates bevacizumab resistance. Hence, IL-1α signaling could be another potential mechanism of resistance to anti-VEGF therapy in HNSCC.

The exact mechanism by which IL-8 obviates the need for VEGF during tumor angiogenesis is unclear. However, one possible explanation is that IL-8 is able to act directly on endothelial cells and activate endothelial pathways that ultimately result in resistance to anti-VEGF therapy. It is well established that endothelial cells express CXCR1 and CXCR2, the cognate receptors for IL-8, and that IL-8 is a proangiogenic molecule [91,92]. Conversely, administration of inhibitors of the IL-8 pathway to animals bearing tumor xenografts results in decreased MVD [93,94]. In our *in vitro* studies, we showed that IL-8 functionally replaced VEGF in mediating migration and capillary-tube formation in endothelial cells in presence of bevacizumab. Furthermore, addition of IL-8 to bevacizumab-treated endothelial cells restored the activation levels of signaling molecules that are common to both VEGF and IL-8 pathways such as Akt. Our *in vivo* studies further validated these findings where combined targeting of VEGF and IL-8 lead to significantly reduced MVD and increased endothelial

cell apoptosis compared to inhibition of either protein alone.

The exact effects of IL-8 on the tumor endothelium that lead to resistance to anti-VEGF therapy have yet to be defined clearly. However, a potential mechanism can be proposed based on a study by Petreaca et. al. [95]. This study showed that IL-8 is able to induce the transactivation of VEGFR2 in endothelial cells. Furthermore, this interaction was found to be due to direct interaction between VEGFR2 and CXCR1/ CXCR2, and was independent of extracellular VEGF. In our studies with murine endothelial cells we have found a similar induction of pVEGFR2 levels with IL-8.

It is also possible that IL-8 may act on other elements of the tumor microenvironment, which then act on the endothelial cells to produce resistance to anti-VEGF therapy. Possible candidates from the tumor microenvironment that may act in this intermediary role include stromal cells such as fibroblasts and tumor infiltrating myeloid derived cells. Although IL-8 was first identified by chemotatic property on neutrophils, it also has chemotactic effects on fibroblasts [96]. Cascone et. al. [76] has shown in a recent study that stromal upregulation of EGFR and FGFR may be involved in resistance to bevacizumab therapy in preclinical lung cancer models. Similarly, Shojaei et. al. [97] has shown that murine xenografts resistant to anti-VEGF agents express cytokines such as granulocyte colony stimulating factor (G-CSF), which induces the infiltration of the tumor xenografts by CD11b+Gr1+ myeloid cells. These myeloid cells produce Bv8, a secreted protein with angiogenic properties, which then promote angiogenesis in the absence of VEGF [98, 99]. Although we have not assessed our model for differences in tumor-infiltrating myeloid cells or lymphocytes, the proinflammatory properties of IL-8 suggest that its influence on the tumor microenvironment may be a major factor leading to resistance.

We also examined the IL-8 expression levels in sera from HNSCC patients before treatment with VEGF-targeting monoclonal antibodies. High IL-8 levels were observed exclusively in a subset of patients in the non-responder group but not in the partial responders. Although there were no significant differences in median values of IL-8 between the two pa-

tient groups, the observed trends are encouraging and consistent with previous reports that indicate an inverse correlation of IL-8 levels with progression free survival and increased progression risk [100, 101]. The recent preclinical study by Huang et. al. [67] also showed that IL-8 expression was elevated in human RCC tumors refractory to tyrosine kinase inhibitor sunitinib. In the light of these preclinical and clinical findings, we foresee IL-8 to be an important player in governing sensitivity to antiangiogenic therapy in HNSCC. Hence, future clinical trials with angioangiogenic agents that assess IL-8 levels in patients will further validate the use of IL-8 as a relevant biomarker of treatment response or resistance.

Lastly, there are limitations to this study that should be acknowledged. The study was performed using human xenografts in a murine model and bevacizumab. It is known that bevacizumab binds poorly to murine VEGF and therefore, the role of murine VEGF in our model of resistance is unclear [102]. Secondly, it should be noted that the patients on our clinical trial did not receive single-agent therapy with bevacizumab but rather received both bevacizumab and cetuximab. IL-8 has been implicated as a predictive biomarker in cetuximab therapy [103] and irinotecan plus bevacizumab-based therapy [104] in colorectal cancer. As such, serum IL-8 data from our study may reflect treatment effects of both cetuximab and bevacizumab. Furthermore, the difference in the serum levels of IL-8 between patients with progressive disease/ stable disease and those with partial response did not reach statistical significance.

In summary, this study reveals IL-8 as one of the contributors of bevacizumab resistance in HNSCC tumor models. Several IL-8 agents are currently in clinical development primarily for the treatment of inflammatory diseases and these agents have shown antitumor and antiangiogenic activity in preclinical models [105,106]. Our data suggests that the concurrent use of anti-VEGF drugs such as bevacizumab and IL-8 targeting agents may help overcome resistance and improve therapeutic efficacy of antiangiogenic therapy in HNSCC.

3.0 HNSCC XENOGRAFT MODELS OF ACQUIRED RESISTANCE TO BEVACIZUMAB

3.1 INTRODUCTION

Preclinical and clinical studies from several cancers indicate that the therapeutic benefits of bevacizumab are transitory and are followed by disease progression within a few months of treatment [107–111]. Similar responses are seen in HNSCC [55, 56, 81], where bevacizumab is being evaluated in phase III clinical trials (NCT00588770). Available evidence suggests that tumors can adapt to the effects of these angiogenic inhibitors by acquiring alternative ways to sustain growth and survival. Studies using relevant preclinical models that identify these alternative-signaling pathways, which mediate angiogenic rescue in the bevacizumab-resistant tumors will help develop reliable resistance biomarkers.

Here, we investigated the mechanisms of acquired resistance to bevacizumab in preclinical HNSCC models. HNSCC cell line, Tu138 that exhibited high *in vivo* sensitivity to bevacizumab (from the differential sensitivity screen in Section 2.3.1) was used to generate and validate preclinical models of acquired resistance. In order to establish the xenograft model, we used an incremental drug dosing regime, which eliminated the sensitive tumor cells and sequentially selected for the resistant clones. After prolonged therapy, we observed a significant difference in the tumor growth between the chronically treated Tu138 xenografts (less sensitive) and the isogenic parental (more sensitive) xenografts. To identify molecular changes initiated by tumor cells, we performed human-specific microarray analysis on the isogenic pair of bevacizumab-sensitive and -resistant tumors. We further examined the differentially expressed proteins *in vivo* for their involvement in conferring acquired resistance, using a combinatorial approach.

3.2 MATERIALS AND METHODS

3.2.1 Cell lines and reagents

Tu138 cells and the bevacizumab-resistant isogenic clones TuR3 were maintained in DMEM/F12 medium supplemented with 10% FBS. Both cell lines were validated by genotyping using short tandem repeat analysis [83]. Bevacizumab was purchased from the University of Pittsburgh Pharmacy. PD173074 was purchased from Selleck Chemicals (Houston, TX).

3.2.2 Animal studies

3.2.2.1 Model of acquired resistance To generate the preclinical model, we inoculated Tu138 cells (3×10^6 cells/ mouse) in athymic nude mice ($n = 10$). After formation of subcutaneous tumors ($\sim$ 2 weeks), these mice were randomized to receive vehicle or bevacizumab and treated biweekly by intraperitoneal injection. Tumors were also measured biweekly and mean tumor volumes were computed as previously described in Section 2.2.2. Bevacizumab was administered at a moderate dose of 4mg/kg followed by incrementing the dose by 4mg/kg with every subsequent increase in tumor volume. Drug concentration was increased upto the maximum-tolerated dose in patients (20mg/kg). Mice were sacrificed if the tumors exceeded 20mm in diameter. Resistant tumors were excised and small tumor fragments ($\sim$ 1mm in diameter) were reimplanted into new mice ($n = 2$) to propagate the model. Mice were treated with saline or bevacizumab (increasing concentrations, 8mg/kg-20mg/kg) for a period of two months.

3.2.2.2 Validation experiments Resistant tumor-derived cells were expanded *in vitro* for reinoculation and validation in a second *in vivo* study with a short-term treatment regime (4 weeks). Resistant cells from tumors TuR1, TuR2 and TuR3 were inoculated in mice (n=6). Two weeks after tumor cell inoculation, the mice were randomized to receive vehicle or bevacizumab (4mg/kg).

Small fragments from the resistant tumor (TuR3) were implanted to generate xenografts ($n = 4$) for validation in a separate *in vivo* study. Parental Tu138 cells were also inoculated

in mice ($n = 4$) as a positive control for sensitivity to bevacizumab. After two weeks, the mice were treated with vehicle or bevacizumab (4mg/kg).

In another *in vivo* study, small fragments from a bevacizumab-naıve parental Tu138 tumor were implanted in mice ($n = 10$) to create xenografts. Mice were treated with saline or bevacizumab (4mg/kg).

3.2.2.3 Combination experiments For the combination treatment study, small fragments from the resistant tumor were implanted in mice ($n = 12$). Mice were randomized into four treatment groups receiving saline, bevacizumab, PD173074 or a combination of bevacizumab and PD173074. Bevacizumab and PD173074 were administered intraperitoneally at 8mg/kg (biweekly) and 25mg/kg (daily) respectively. Tumors were measured daily and tumor growth was assessed for two weeks.

3.2.3 Immunohistochemistry and immunofluorescence

Frozen tumor sections ($8 - 10$ mm) from each group were mounted on positively charged Superfrost slides (Fischer Scientific, Houston, TX). The slides were washed in Tris Buffer Saline/ Tween 20 and incubated in endogenous peroxidase and protein blocking solution Rodent block (BioCare, Concord, CA). The samples were then incubated with rat anti-mouse CD31 antibody (BD Biosciences Pharmingen, San Jose, CA). After washing, the slides were incubated in rat Probe followed by Rat polymer (Biocare Rat on Mouse Kit). The slides were then incubated in chromogen DAB Quanto (Thermo Scientific/Lab Vision, Kalamazoo, MI). Slides were stained in Mayers Hematoxilin and coversliped with Permount.

Frozen tumor sections were fixed and blocked as above, excluding the endogenous peroxidase step. The slides were incubated with rat anti-mouse CD31 monoclonal antibody, washed with PBS, blocked with protein block and incubated with Texas Red-X goat anti-rat IgG antibody (Invitrogen, Grand Island, NY). To stain for terminal deoxynucleotidyl transferase-mediated dUTP nick end labeling (TUNEL), a commercially available Apoptosis Detection kit (Promega, Madison, WI) was used. Slides were washed with PBS and

mounted using Vectashield Mounting Medium with DAPI (Vector laboratories, Burlingame, CA). Immunofluorescence microscopy was carried out using an Olympus IX81-DSU Spinning Disk Confocal Microscope. Images were captured using a Hamamatsu ORCA II ER camera (Hamamatsu Corp.) and 3i Slidebook 5.0 software.

For quantification of CD31 expression, vessels completely stained with anti-CD31 antibodies were counted in random 0.04-mm^2 fields at using a 20× objective. Quantification of CD31/TUNEL staining was done as the average percentage of apoptotic endothelial cells in 10 random 0.01-mm^2 fields using a 40× objective.

3.2.4 Microarray

Total RNA was extracted from frozen tumors using TRIzol reagent (Invitrogen/Life Technologies Grand Island, NY) and purified using the RNeasy Kit (Qiagen, Germantown, MD). RNA amplification and biotin labeling was done using Illumina Total Prep RNA Amplification Kit (Ambion Inc.). Biotinylated cRNA was hybridized to human HT-12 v4 BeadChips (Illumina Inc., San Diego, CA) and scanned using an Illumina BeadChip Array Reader.

Efficiency analysis was used to determine the optimal methods for data normalization, transformation, and feature selection that produced the most internally consistent gene set. Raw data were normalized using a log2 and z-transformation and differentially expressed genes were identified using J5 test [112]. Gene expression changes were considered to be statistically significant for genes bearing a J5 score higher than the threshold value 8.0. A pathway level impact analysis [113], was performed to provide both statistical and biological significance in suggesting the potential pathways affected by the observed changes in gene expression. The results are summarized as impact scores and p-values. Differentially expressed genes between bevacizumab-sensitive and -resistant tumors were also subjected to the functional interaction network analysis using Ingenuity Pathways Analysis (IPA) software.

3.2.5 Real-time RT-PCR

Real-time RT-PCR was performed using taqMan one-step RT-PCR master mix kit and taqman gene expression assay kits (Applied Biosystems/ Life Technologies Grand Island, NY) on a 7900HT Real-Time PCR system (Applied Biosystems/ Life Technologies Grand Island, NY). Samples were prepared in triplicates in a 20μl reaction volume containing 200ng input RNA. RT-negative controls were run on each plate to ensure no amplification in the absence of input RNA. Standard cycling conditions were programmed as: 95 °C for 12 minutes, 40 cycles of: 95 °C for 15 seconds, 60 °C for 1 minute. β-Actin was used as endogenous control. Following gene-specific Taqman gene expression assay kits were used; FGF2: Hs00266645_m1, FGFR3: Hs00179829_m1, and PLCg2: Hs00182192_m1.

3.2.6 Western

Parental Tu138 cells and bevacizumab-resistant clones TuR3 were plated in 10cm dishes. The following day complete medium was replaced with serum free medium. After 24 hrs, cells were treated with MEK inhibitor U0126 for 6 hrs and whole cell lysates were prepared and resolved on 10% SDS-page gels. Following transfer onto nitrocellulose membranes, antibody staining was done using: pERK (Thr202/Tyr204), ERK, FGF2 and β-Actin (Cell Signaling Technology Inc., Danvers, MA). Reactive bands were detected by chemiluminiscence using ECL plus western blotting detection kit (Amersham Biosciences, Piscataway, NJ). Similarly, immunoblots were performed using untreated cells and siRNA transfected cells using the following antibodies; FGF1, FGFR1, FGFR3, pPLCg1 (Tyr783), PLCg1, pPLCg2 (Tyr759), PLCg2, pSrc (Tyr416), Src, pAKT (S473), AKT, CCL5 (Cell Signaling Technology Inc., Danvers, MA) FGFR2, FGFR4, FZD4, and CX3CL1 (Abcam, Cambridge, MA).

3.2.7 ELISA

Parental Tu138 cells and bevacizumab-resistant clones TuR3 were plated at a density of 5×10^6 cells/ 10cm dish. Cell culture supernatant was collected after 24 hours and centrifuged at 1200rpm for 5 min. CCL5 was measured in cell culture supernatants from siRNA transfected cells using ELISA kit (R&D Systems, Inc., Minneapolis, MN) as per the manufacturer's

instructions.

3.2.8 siRNA Transfection

Parental Tu138 cells and bevacizumab-resistant clones TuR3 were transfected with siRNA targeting FZD4, PLCg2, CX3CL1, CCL5 and negative control siRNA (non-targeting) using Opti-MEM media, lipofectamine-2000 (Invitrogen/ Life Technologies Grand Island, NY). After 4 hrs, the media was replaced with complete medium and cells were incubated at 37 °C for 1hr. Following incubation, transfected cells were replated in 6-cm plates for western blot analysis after 48hrs of transfection. Following gene-specific siRNA were used; FZD4: s15840, PLCg2: s10634, CX3CL1: s12629, and CCL5: s12575.

3.2.9 Statistical Analysis

Data are expressed as mean ± S.E.M. Student's t test was used for all statistical analyses. Significance tests were performed with a two-sided significance level of 0.05.

3.3 RESULTS

3.3.1 Generation of HNSCC xenograft model of acquired resistance

In order to establish xenograft model of acquired resistance to bevacizumab, we inoculated mice with HNSCC cell line Tu138, which has been previously shown to be highly sensitive to bevacizumab *in vivo* (Section 2.3.1). After generation of subcutaneous tumors, these mice were randomized to receive vehicle or bevacizumab at an initial dose of 4mg/kg followed by incrementing the dose by 4mg/kg with every subsequent increase in tumor volume. Drug concentration was increased upto the maximum-tolerated dose in patients (20mg/kg). Such an escalating dosing regime eliminated the sensitive tumor cells and sequentially selected for the resistant clones. Three out of five xenograft tumors showed resistance quite early in the treatment cycle with growth rates comparable to the saline control (Figure 3.1A). Mean tumor volumes for the resistant xenografts TuR1, TuR2 and TuR3 were 2351.2mm^3,

1329.4mm^3 and 1194.0mm^3 respectively.

The resistant xenografts were then excised and small tumor fragments ($\sim$ 1mm in diameter) were reimplanted into new mice ($n = 2$) to propagate the model (Figure 3.1B-D).

In order to propagate the resistance model, the reimplanted tumors were subjected to a second phase of treatment where the resistant tumor-bearing mice were treated with saline or bevacizumab (increasing concentrations, 8mg/kg-20mg/kg) for a period of two months. We observed a slow emergence of resistance in bevacizumab-treated tumor TuR1 with mean tumor volumes equivalent to the respective saline control (Figure 3.1B). Bevacizumab-treated tumor TuR2 remained fairly sensitive throughout the treatment suggesting that it failed to retain the initial resistance under the incremental drug selection pressure (Figure 3.1C). Interestingly, we observed a steep increase in tumor growth in the bevacizumab-treated tumor TuR3 beyond day 36 (Figure 3.1D). Mean tumor volumes at the end of the treatment were 2571.1mm^3 as compared to 1326.7mm^3 in tumor TuR1. Hence, we selected tumor TuR3 to validate the acquisition of resistance.

In the validation study, we inoculated parental Tu138 cells as a positive control for sensitivity to bevacizumab and implanted small tumor fragments from the resistant tumor (TuR3) instead of using *in vitro* expanded cells to generate xenografts (Figure 3.2A). The parental tumors were sensitive to bevacizumab, as expected, resulting in 88% growth inhibition. In contrast, in the resistant tumors there was no significant reduction in tumor growth.

We then confirmed that the resistant phenotype was not an artifact of reimplanting the resistant tumors as fragments in contrast to the parental tumors, which were generated by inoculating cells (Figure 3.2B). Small tumor fragments from a parental tumor that was not subjected to bevacizumab were implanted in mice to create xenografts. The mice were treated with saline or bevacizumab and we observed that the parental tumors retained sensitivity to bevacizumab.

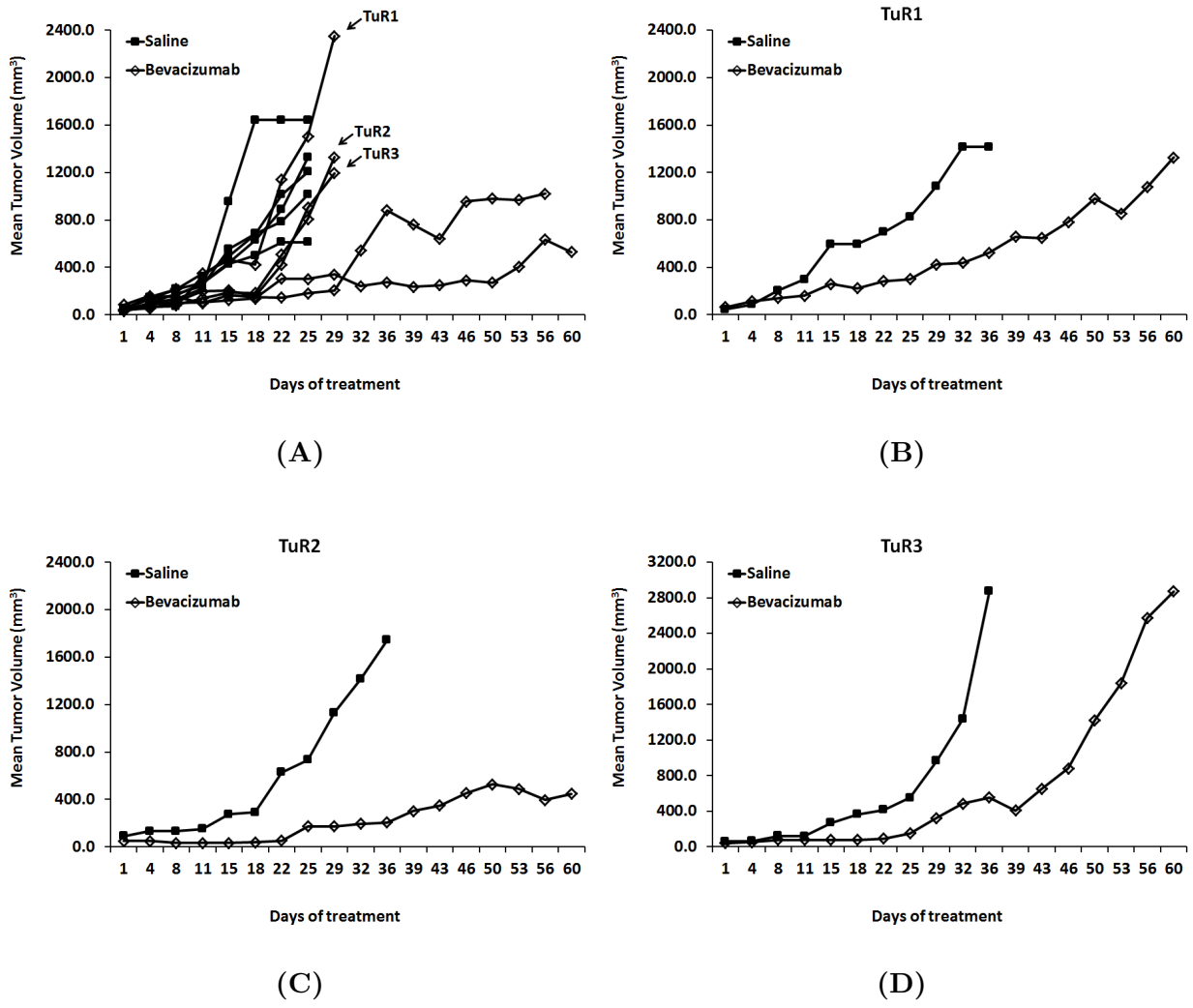

Figure 3.1: Generation of HNSCC xenograft model of acquired resistance to bevacizumab. (A), Growth curve of Tu138 xenografts ($n = 5$ per group) treated with saline or bevacizumab at an initial dose of 4mg/kg followed by incrementing the dose by 4mg/kg with every subsequent increase in tumor volume. 3/5 xenograft tumors (TuR1, TuR2 and TuR3) showed resistance with growth rates comparable to the saline control. (B-D), Resistant xenografts were excised and small tumor fragments (∼1mm in diameter) were reimplanted into new mice ($n = 2$) to propagate the model. The reimplanted tumors were subjected to a second phase of treatment with saline or bevacizumab (increasing concentrations, 8mg/kg-20mg/kg). Emergence of resistance was observed in bevacizumab-treated tumor TuR1 and TuR3 while TuR2 remained fairly sensitive.

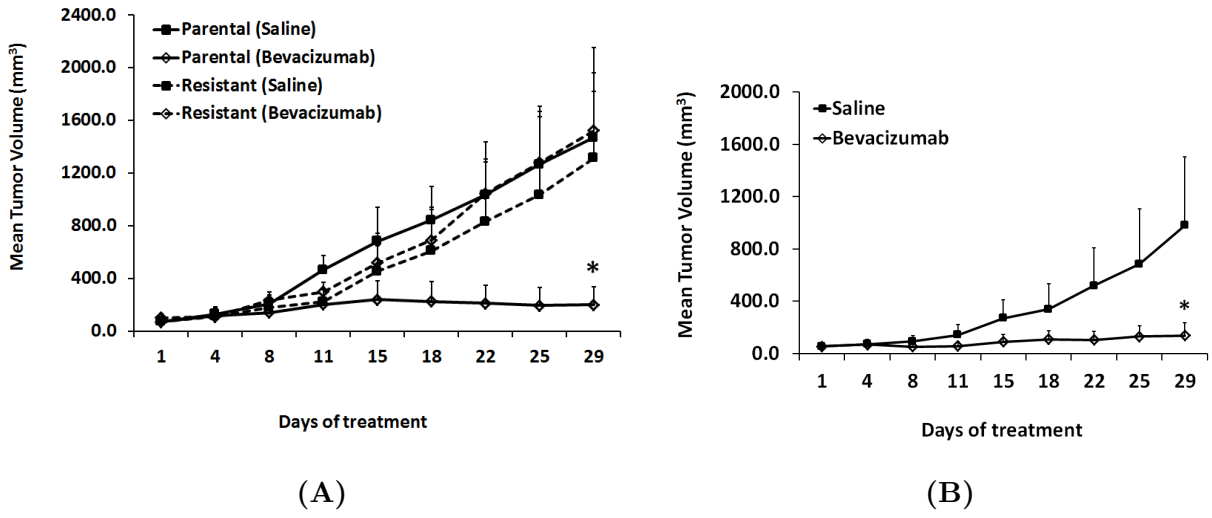

Figure 3.2: Validation of bevacizumab resistance in HNSCC xenograft model. (A), Acquired resistance in reimplanted TuR3 resistant tumors was confirmed by treating xenografts with saline or bevacizumab ($n = 4$ per group). Parental Tu138 tumors were sensitive to bevacizumab resulting in 88% growth inhibition. In contrast, the resistant tumors showed no significant reduction in tumor growth. (B), Parental tumors generated by implanting small fragments from a bevacizumab-naıve parental tumor, which were treated with saline or bevacizumab ($n = 5$ per group), retained sensitivity to bevacizumab.

3.3.2 Bevacizumab-resistant tumors exhibit sustained angiogenesis and reduced apoptosis

To characterize the preclinical model of acquired resistance, we assessed MVD and apoptosis in the bevacizumab-sensitive and -resistant xenografts (from the validation study). Frozen tumor sections were stained with CD31 using immunohistochemistry (Figure 3.3A, 3.3B). Resistant tumors treated with bevacizumab (bevacizumab-resistant) showed significantly higher MVD compared to parental tumors treated with bevacizumab (bevacizumab-sensitive). Further, dual immunofluorescence staining for $TUNEL^{+}$/ $CD31^{+}$ cells was done to analyze the percentage apoptotic endothelial cells (Figure 3.3A, 3.3C). Bevacizumab-sensitive tumors showed a significant increase in endothelial cell-specific apoptosis (6.2%) compared to bevacizumab-resistant tumors with only 1.8% apoptotic cells. These results suggest that the bevacizumab-resistant phenotype is associated with revascularization and reduced cell death.

3.3.3 Bevacizumab-resistant tumors upregulate angiogenesis genes in response to chronic anti-VEGF therapy

To identify molecular changes initiated by the tumor cells to mediate bevacizumab resistance, we performed whole genome microarray analysis. Bevacizumab-sensitive and -resistant isogenic tumor models were compared for differences in gene expression using HumanHT-12 v4 BeadChips (Illumina Inc.). Efficiency analysis was used to determine the best statistical method and the differentially expressed genes were identified using J5 test. We found 150 genes upregulated and 31 genes downregulated in the resistant tumors (Figure 3.4A, Table A1).

Using Ingenuity Pathway Analysis (IPA) tool, we identified disease, disorder, molecular and cellular functions enriched among genes differentially expressed in bevacizumab-resistant tumors (Tables 3.1 & 3.2). Table 3.3 and 3.4 list top 10 upregulated and downregulated genes in resistant tumors. Among the angiogenesis-related genes, we found upregulation of FGF2, FGFR3, PLCg2, FZD4, CX3CL1, and CCL5 in the resistant tumors (Table 3.5). We also analyzed functional interaction network involving differential expressed genes and

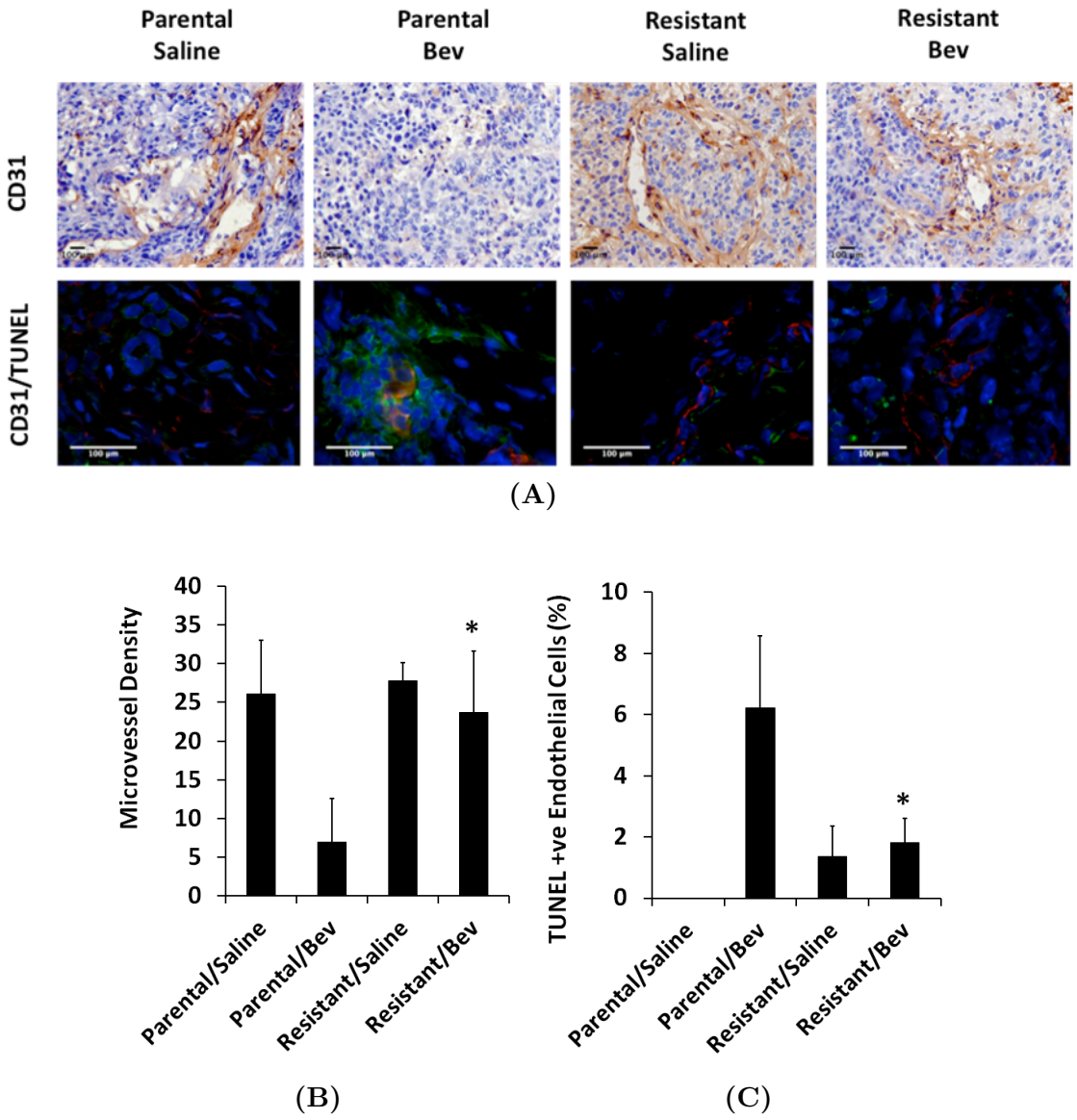

Figure 3.3: Resistant tumors exhibit sustained angiogenesis and reduced endothelial cell apoptosis. (A), CD31 staining (brown) in parental and resistant tumor sections using immunohistochemistry (upper panel). Immunofluorescence staining of CD31 (red) and TUNEL (green) was performed to assess endothelial cell-specific apoptosis (lower panel). (B), Bar graph represents quantification of vessels in parental and resistant tumors treated with saline or bevacizumab. (C), Quantitative analysis of $CD31^+/TUNEL^+$ cells represented as percentage of apoptotic endothelial cells. Bevacizumab-resistant tumors showed significantly higher microvessel density ($P = 0.0428$) along with reduced endothelial cell apoptosis ($P = 0.0426$) compared to parental tumors treated with bevacizumab.

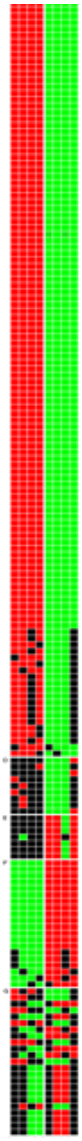

(A)

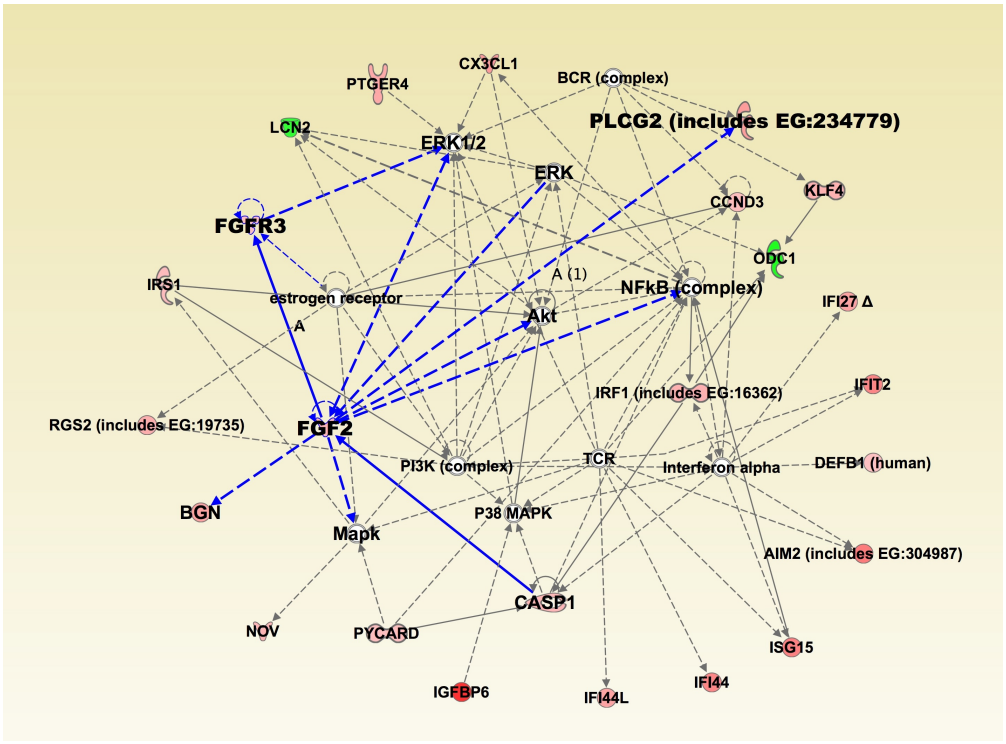

(B)

A. Over in A, Under in B
B. Over in A
C. Under in A
D. Under in B
E. Over in B
F. Under in A, Over in B
G. Others
Not Expressed

Figure 3.4: Bevacizumab-resistant tumors upregulate angiogenesis genes in response to chronic anti-VEGF therapy. (A), Gene expression grid displaying 181 differentially expressed genes between bevacizumab-sensitive (n=4) (Right column) and bevacizumab-resistant (n=4) (Left column) tumors. (B), Network analysis using IPA indicates a significant modulation in the predicted function FGF/FGFR signaling in bevacizumab-resistant tumors.

observed FGF2 as a highly connected nodal gene with upregulated proangiogenic genes FGFR3, PLCg2, CASP1 and BGN (Figure 3.4B). Interestingly, three of these genes FGF2, FGFR3 and PLCg2 belong to the FGF signaling pathway, which suggests that this axis might be involved in bevacizumab-associated acquired resistance in our HNSCC xenograft model.

3.3.4 Upregulation of FGF signaling in resistant xenografts

To test our hypothesis that FGF signaling contributes to bevacizumab resistance, we first validated the upregulation of FGF pathway genes in the resistant tumors by real-time RT-PCR and western blotting. We confirmed a 6-fold increase in the expression of FGF2 mRNA in bevacizumab-treated resistant tumors compared to bevacizumab-treated parental tumors (Figure 3.5A). Similarly, we observed a 4.5-fold increase in FGFR3 mRNA and a 8-fold increase in PLCg2 mRNA (Figure 3.5B-C). Plasma FGF2 protein levels were significantly higher in resistant/bevacizumab tumors compared to parental/bevacizumab tumors as shown by ELISA (Figure 3.6A). We also confirmed increased protein levels of these genes in tumor cells expanded from the bevacizumab-treated resistant xenografts compared to the parental Tu138 cell line (Figure 3.6C). Since, we observed an increased expression of the FGF2 ligand, FGFR3 receptor and PLCg2 downstream protein in the resistant cells, we assessed other members of the FGF pathway for increased signaling (Figure 3.6B). Between the two FGF ligands, we observed increased expression of FGF2 and not FGF1 in the resistant cells. Among the four FGFR receptors, FGFR1, 2 and 3 were upregulated and FGFR4 was down-regulated in the resistant cells. Among the downstream proteins, higher levels of phospho PLCg1, total PLCg1, phospho PLCg2, total PLCg2, phospho AKT and phospho ERK were seen in the resistant cells.

3.3.5 Increased ERK activation upregulates FGF2 expression in resistant cells

Studies have shown that activated ERK can positively regulate FGF levels [114]. We next examined if increased ERK activation in the resistant cells upregulated FGF2 expression. To test this, we treated parental and resistant cells with the MEK inhibitor U0126 to block ERK

Name	P-Value	# Molecules
Dermatological Diseases and Conditions	1.42×10^{-20} - 2.14×10^{-2}	56
Genetic Disorder	1.42×10^{-20} - 2.14×10^{-2}	72
Cancer	2.39×10^{-13} - 2.14×10^{-2}	85
Immunological Disease	2.44×10^{-12} - 1.18×10^{-2}	36
Inflammatory Disease	2.44×10^{-12} - 2.14×10^{-2}	34

Table 3.1: Differentially expressed genes enriched among specific diseases or disorders.

Name	P-Value	# Molecules
Cell Death	2.32×10^{-6} - 2.14×10^{-2}	45
Cellular Movement	1.38×10^{-5} - 2.14×10^{-2}	32
Cellular Growth and Proliferation	1.61×10^{-5} - 2.14×10^{-2}	50
Carbohdrate Metabolism	2.48×10^{-4} - 1.09×10^{-2}	10
Molecular Transport	2.48×10^{-4} - 1.82×10^{-2}	17

Table 3.2: Differentially expressed genes enriched among specific molecular or cellular functions.

Rank	Description	J5-score	Accession #
1	hemoglobin, beta (HBB)	27.473	NM_000518.4
2	insulin-like growth factor binding protein 6 (IGFBP6)	27.04	NM_002178.2
3	H19, imprinted maternally expressed transcript (non-protein coding) (H19), non-coding RNA.	25.785	NR_002196.1
4	alkaline phosphatase, liver/bone/kidney (ALPL), transcript variant 1	22.435	NM_000478.2
5	retinoic acid receptor responder (tazarotene induced) 3 (RARRES3)	21.255	NM_004585.2
6	hect domain and RLD 5 (HERC5)	19.807	NM_016323.1
7	keratin 10 (epidermolytic hyperkeratosis; keratosis palmaris et plantaris) (KRT10)	18.764	NM_000421.2
8	frizzled homolog 4 (Drosophila) (FZD4)	18.239	NM_012193.2
9	NADH dehydrogenase (ubiquinone) 1 alpha subcomplex, 4-like 2 (NDUFA4L2)	17.73	NM_020142.3
10	absent in melanoma 2 (AIM2)	17.325	NM_004833.1

Table 3.3: Top 10 upregulated genes in bevacizumab-resistant tumors.

Rank	Description	J5-score	Accession #
1	small proline-rich protein 2G (SPRR2G)	-24.715	NM_001014291.1
2	defensin, beta 103B (DEFB103B)	-22.442	XM_928791.1
3	late cornified envelope 3D (LCE3D)	-20.282	NM_032563.1
4	small proline-rich protein 2F (SPRR2F)	-16.568	NM_001014450.1
5	small proline-rich protein 2A (SPRR2A)	-16.539	NM_005988.2
6	PRED: hypothetical protein LOC647993 (LOC647993)	-15.078	XM_937048.1
7	ribonuclease, RNase A family, 7 (RNASE7)	-15.01	NM_032572.2
8	small proline-rich protein 2E (SPRR2E)	-14.686	NM_001024209.2
9	PRED: hypothetical LOC643161 (LOC643161)	-14.229	XM_926530.1
10	PRED: similar to Ribosome biogenesis protein BMS1 homolog (LOC647987)	-13.172	XM_937044.1

Table 3.4: Top 10 downregulated genes in bevacizumab-resistant tumors.

Rank	Description	J5-score	Accession #
1	insulin-like growth factor binding protein 6 (IGFBP6)	27.04	NM_002178.2
2	frizzled homolog 4 (Drosophila) (FZD4)	18.239	NM_012193.2
3	chemokine (C-X3-C motif) ligand 1 (CX3CL1)	13.329	NM_002996.3
4	chemokine (C-X-C motif) receptor 7 (CXCR7)	13.142	NM_020311.1
5	phospholipase C, gamma 2 (phosphatidylinositol-specific) (PLCG2)	12.871	NM_002661.1
6	biglycan (BGN)	12.165	NM_001711.3
7	XIAP associated factor 1 (XAF1), transcript variant 2	11.535	NM_199139.1
8	chemokine (C-C motif) ligand 5 (CCL5)	10.718	NM_002985.2
9	regulator of G-protein signalling 2, 24kDa (RGS2)	10.661	NM_002923.1
10	interferon regulatory factor 1 (IRF1)	10.254	NM_002198.1
11	Kruppel-like factor 4 (gut) (KLF4)	10.163	NM_004235.3
12	fibroblast growth factor 2 (basic) (FGF2)	9.741	NM_002006.3
13	caspase 1, apoptosis-related cysteine peptidase (interleukin 1, beta, convertase) (CASP1), transcript variant alpha	9.477	NM_033292.2
14	insulin receptor substrate 1 (IRS1)	8.817	NM_005544.1
15	fibroblast growth factor receptor 3 (achondroplasia, thanatophoric dwarfism) (FGFR3), transcript variant 2	8.424	NM_000142.2

Table 3.5: Angiogenesis-related genes upregulated in bevacizumab-resistant tumors.

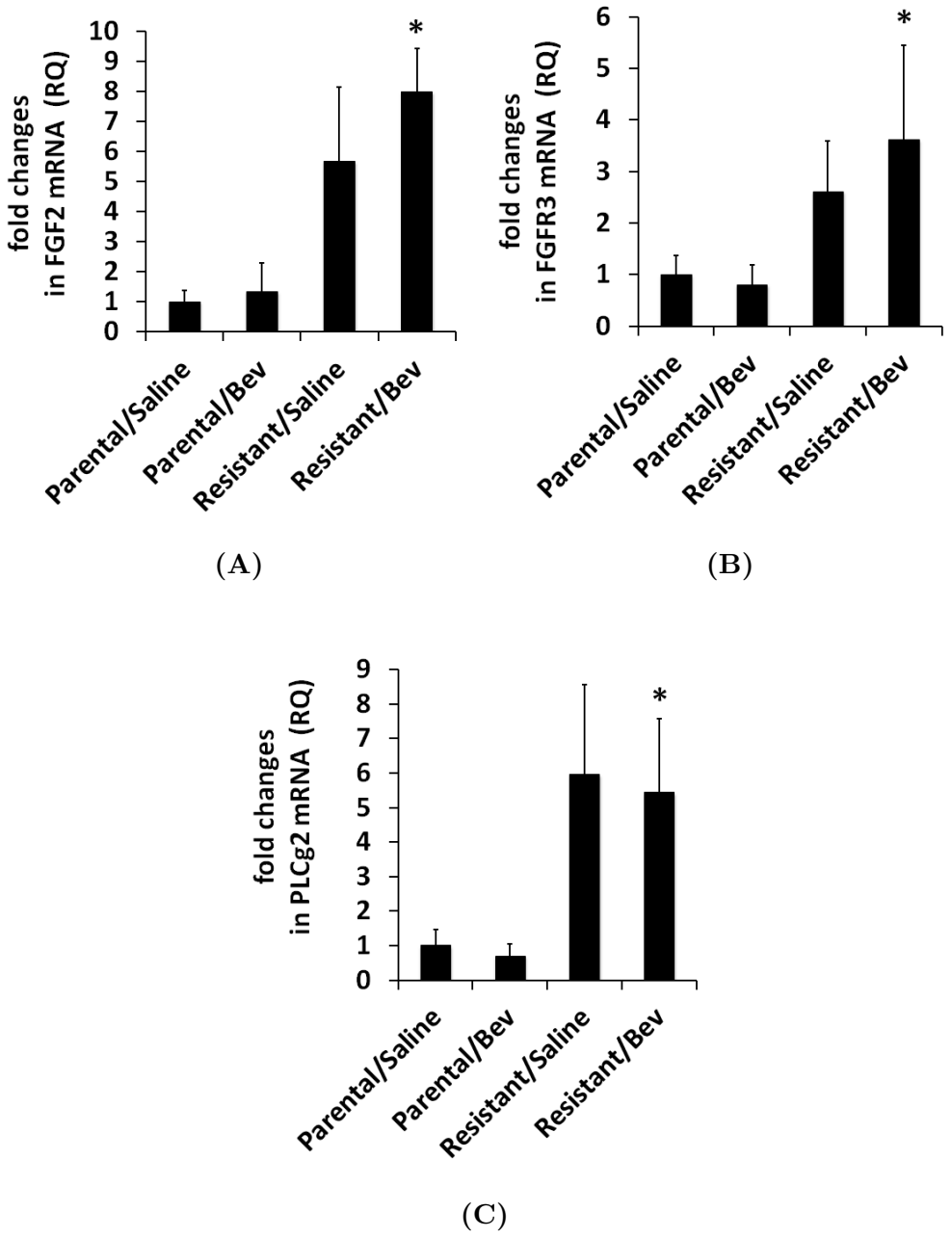

Figure 3.5: Increased expression of FGF2/ FGFR3/ PLCg2 mRNA in resistant xenografts. (A)-(C), qRT-PCR analysis of FGF2, FGFR3 and PLCg2 mRNA levels reveal 6-fold, 4.5-fold and 8-fold increase in expression in resistant/bevacizumab tumors compared to parental/bevacizumab tumors respectively (FGF2; P=0.0002, FGFR3; P=0.0439, PLCg2; P=0.0160).

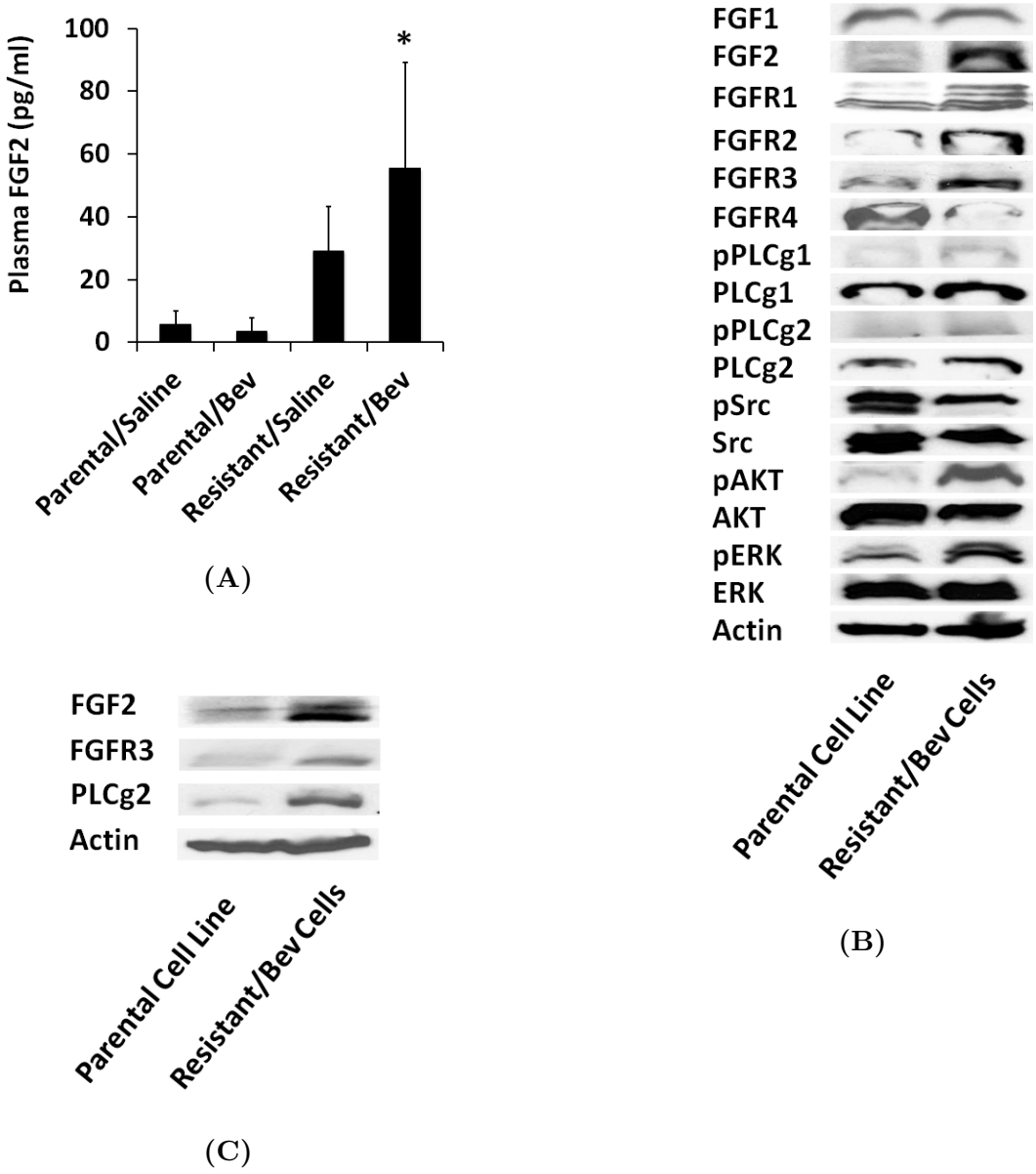

Figure 3.6: Upregulation of FGF signaling in resistant xenografts. (A), Plasma FGF2 protein levels were significantly higher in resistant/bevacizumab tumors compared to parental/bevacizumab tumors (P=0.0441) as shown by ELISA. (A), Western blot analysis confirmed increased protein levels of FGF2, FGFR3 and PLCg2 in tumor cells expanded from bevacizumab-treated resistant xenografts compared to the parental Tu138 cell line. (A), Increased expression of FGF2 ligand, FGFR1-3 receptors and downstream proteins, phospho PLCg1, total PLCg1, phospho PLCg2, total PLCg2, phospho AKT and phospho ERK were seen in resistant cells.

activation and examined FGF2 expression by western blotting and ELISA (Figure 3.7A-B). We observed complete abrogation of ERK activation in parental and resistant cells within 6hrs of inhibitor treatment and a significant decrease in FGF2 expression. These results suggest that increased activation of ERK in the resistant cells regulates increased expression of FGF2.

3.3.6 Upregulated angiogenesis genes regulate increased pERK and FGF2 in resistant tumors

Based on the above finding, we investigated other upregulated genes in the microarray that were known to activate ERK. Using the IPA tool, we generated a functional gene-interaction network, and found high J5 score-bearing differentially expressed genes FZD4, PLCg2, CX3CL1, CCL5, and FGFR3 as known activators of ERK (Figure 3.8). We hypothesized that in the resistant cells these upregulated genes lead to increased activation of ERK and subsequent increase in FGF2 expression. To test this, we first validated overexpression of these upstream genes in the resistant cells (Figure 3.9A-B). We then used siRNA approach to downregulate FZD4, PLCg2, CX3CL1, and CCL5 in both parental (Figure 3.10) and resistant (Figure 3.11) cells and examined the effect on pERK and FGF2 expression. We observed that downregulation of these genes resulted in a significant decrease in ERK activation and a corresponding decrease in FGF2 expression. Although this mechanism of FGF2 regulation is common to both parental and resistant cells, it appears to be amplified in the resistant cells due to overexpression of these upstream genes.

3.3.7 Co-targeting VEGF and FGFR sensitizes HNSCC tumors to bevacizumab

To test the contribution of FGF signaling in bevacizumab-associated acquired resistance, we inhibited FGFRs in the resistant xenografts using PD173074 small molecule inhibitor in combination with bevacizumab (Figure 3.12). Treatment with FGFR inhibitor alone resulted in a modest decrease in tumor growth. However, cotargeting VEGF and FGFR completely abrogated tumor growth in these resistant xenografts. Further, CD31 staining in the tumor sections revealed a significant decrease in MVD in the combination group

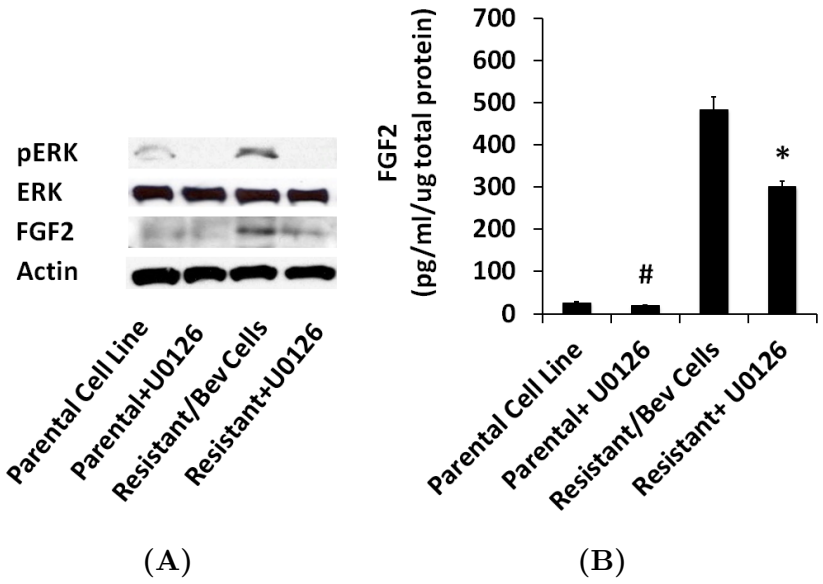

Figure 3.7: Increased ERK activation upregulates FGF2 expression in resistant cells. Parental and resistant cells were treated with the MEK inhibitor U0126 to block ERK activation and FGF2 expression was examined by western blotting (A) and ELISA (B). Complete abrogation of ERK activation was observed within 6hrs of inhibitor treatment and a significant decrease in FGF2 expression.

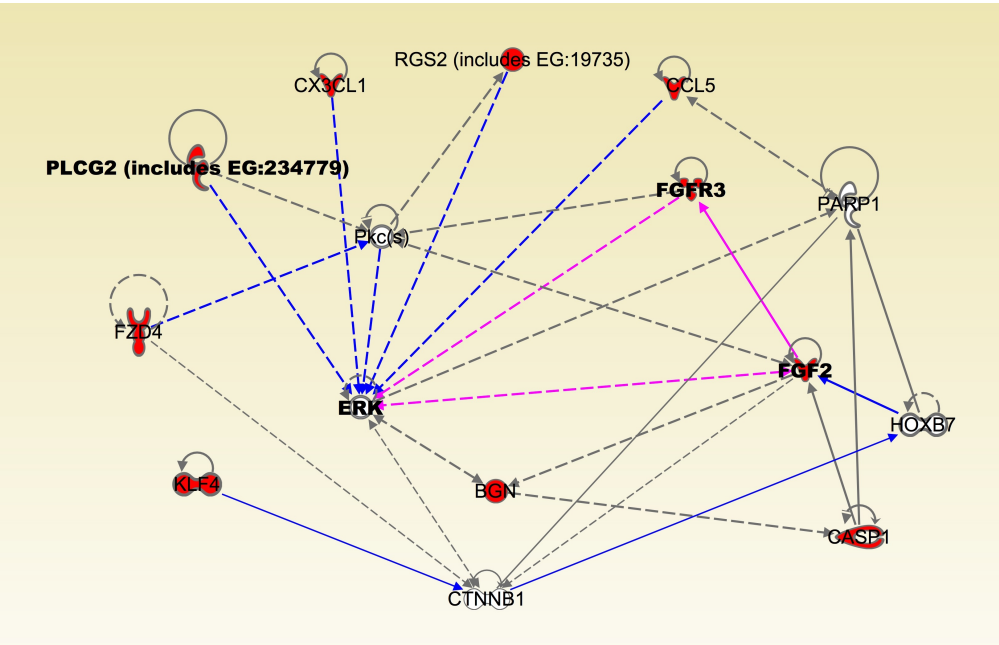

Figure 3.8: Upstream regulators of increased FGF2 expression in resistant tumors. Using IPA tool, we identified potential activators of FGF2 based on at least one literature reference. These included angiogenesis-related genes with high J5 scores such as FDZ4, PLC-g2, CX3CL1, CCL5, and FGFR3, which were found to be upregulated in the resistant tumors using microarray analysis. Majority of these proteins activate ERK, which is a known activator of FGF2.

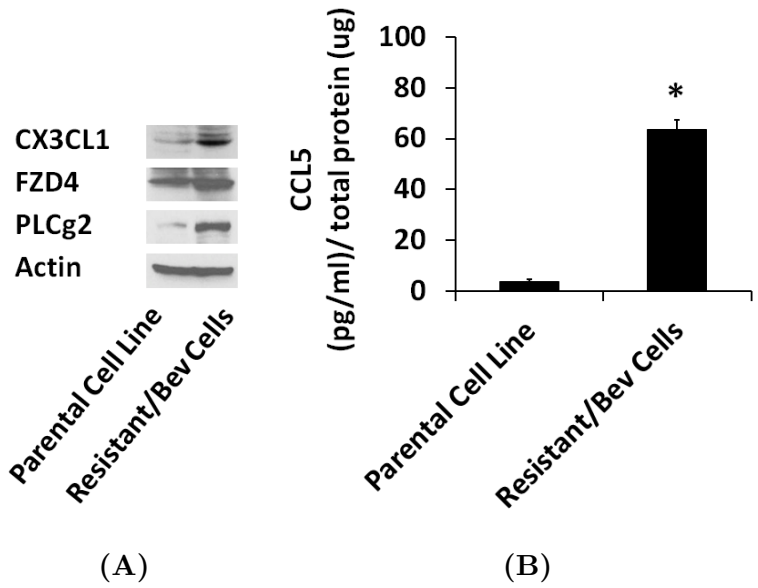

Figure 3.9: Increased expression of angiogenesis genes FZD4, PLCg2, CX3CL1 and CCL5 in resistant cells. (A), Western blot analysis confirmed increased protein levels of FZD4, PLCg2 and CX3CL1 in tumor cells expanded from bevacizumab-treated resistant xenografts compared to the parental Tu138 cell line. (B), Increased expression of CCL5 observed in resistant cells using ELISA.

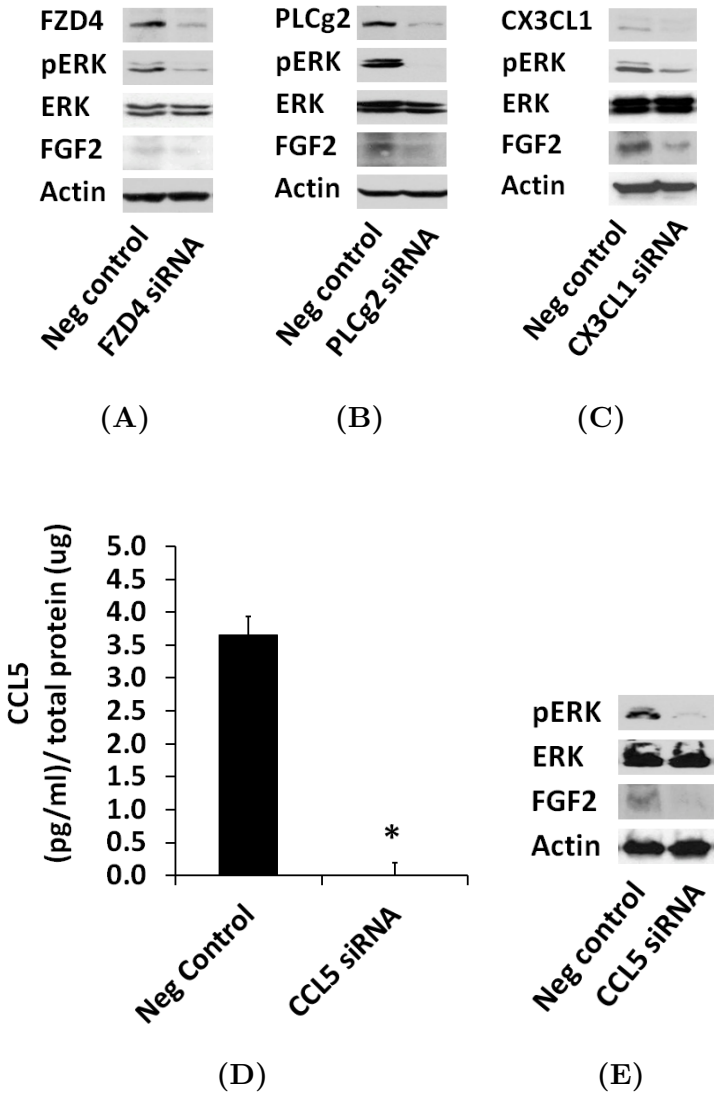

Figure 3.10: Angiogenesis genes induce pERK-mediated FGF2 expression in parental cells. We used siRNA approach to downregulate FZD4 (A), PLCg2 (B), CX3CL1 (C), and CCL5 (E) in parental cells and examined the effect on pERK and FGF2 expression. We observed that downregulation of these genes resulted in a significant decrease in ERK activation and a corresponding decrease in FGF2 expression. (D), siRNA-mediated knockdown of CCL5 protein in parental cells as measured by ELISA.

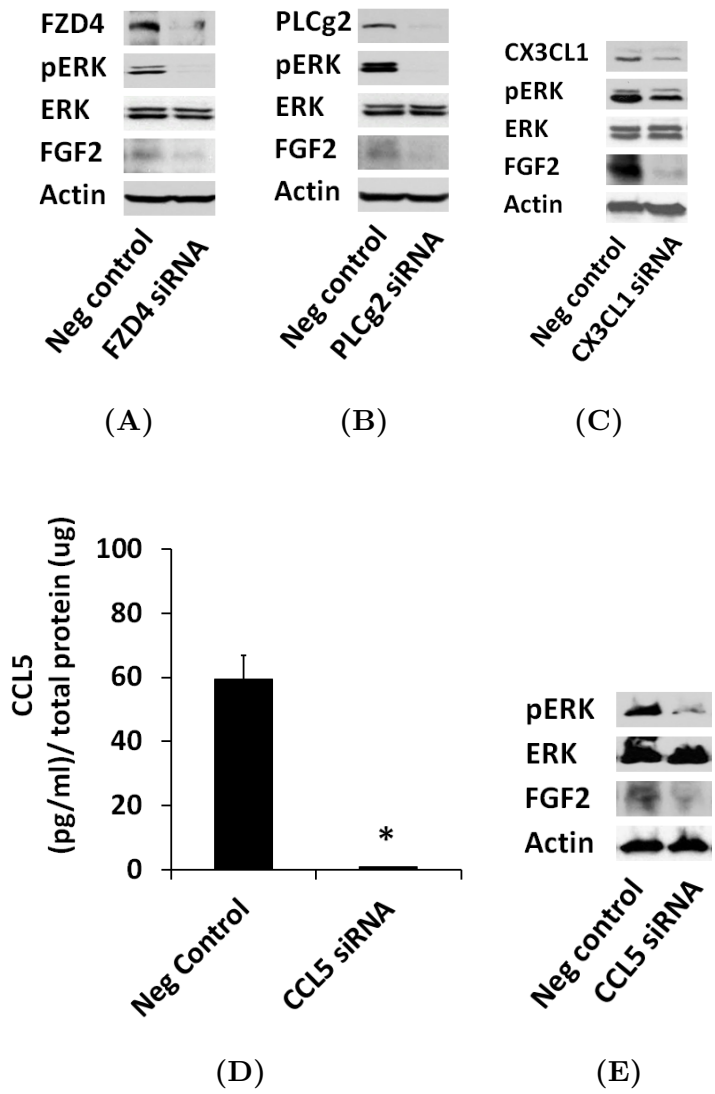

Figure 3.11: Increased expression of angiogenesis genes leads to increased pERK and FGF2 in resistant cells. We used siRNA approach to downregulate FZD4 (A), PLCg2 (B), CX3CL1 (C), and CCL5 (E) in resistant cells and examined the effect on pERK and FGF2 expression. We observed that downregulation of these genes resulted in a significant decrease in ERK activation and a corresponding decrease in FGF2 expression. (D), siRNA-mediated knockdown of CCL5 protein in resistant cells as measured by ELISA.

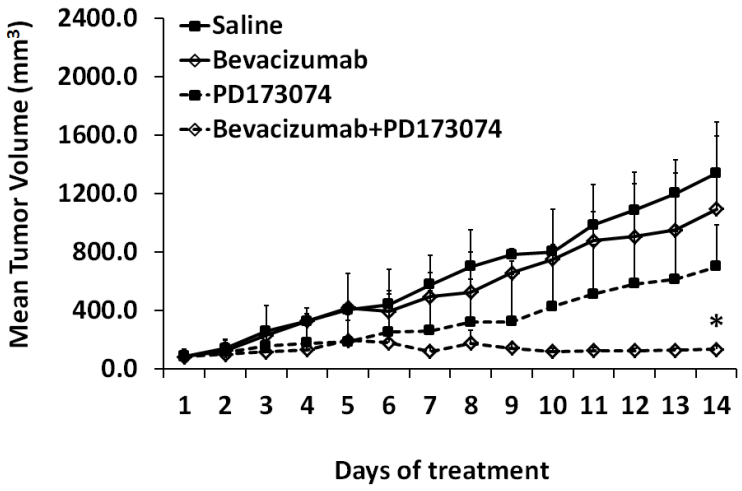

Figure 3.12: Co-targeting VEGF and FGFR sensitizes HNSCC tumors to bevacizumab. Resistant xenografts ($n = 12$) were randomized into four treatment groups receiving saline, single agent bevacizumab/ PD173074 or a combination. Bevacizumab and PD173074 were administered intraperitoneally at 8mg/kg and 25mg/kg respectively. Tumor growth was assessed for two weeks. ($\star$) $P = 0.0427$; combination vs. bevacizumab alone.

compared to bevacizumab alone (Figure 3.13A-B). These data suggest that co-targeting VEGF and FGFR sensitize resistant tumors to bevacizumab by disrupting angiogenesis.

3.4 CONCLUSIONS AND DISCUSSION

In recent years, there have been an increasing number of reports that described potential mechanisms of resistance to antiangiogenic therapy. These studies indicate that tumors can rely on multiple mechanisms of resistance using a variety of angiogenic proteins secreted by both tumor cells and stromal cells. Hence, selection of one critical mediator of resistance for cotargeting with VEGF remains a daunting task. To address this issue, preclinical models that test combinatorial therapies along with VEGF inhibitors are needed to assist selection of a suitable cotarget. Also, studies that elucidate the mechanisms of upregulation of these resistance-contributing proteins will enable identification of functional networks that integrate additional upstream genes as potential contributors of resistance.

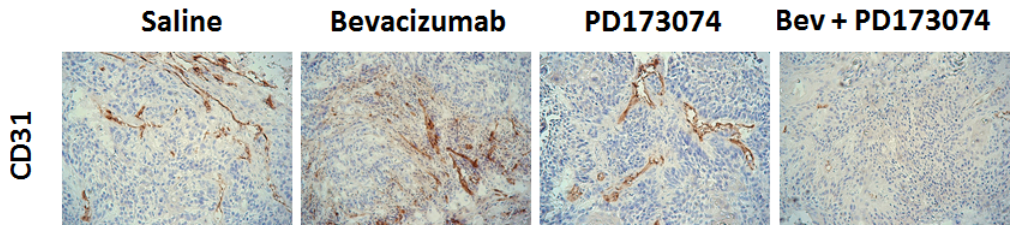

(A)

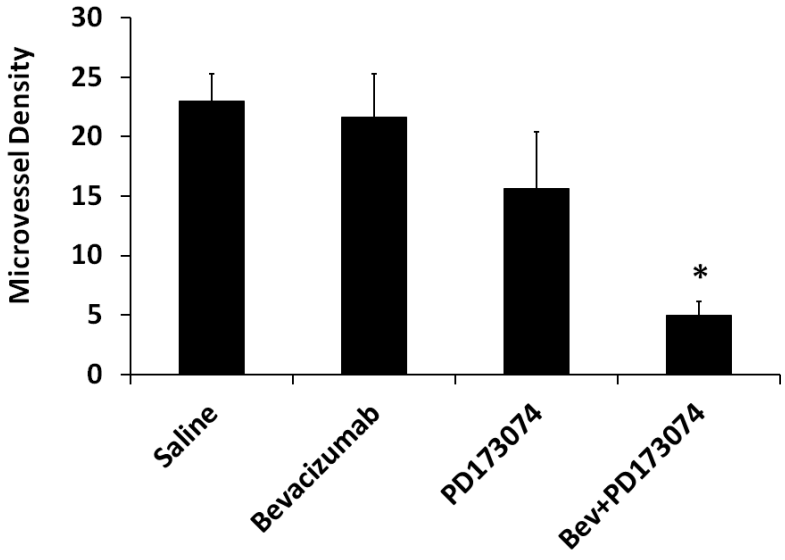

(B)

Figure 3.13: Co-targeting VEGF and FGFR disrupted vasculature in resistant xenografts. (A-B) CD31 staining in resistant xenografts showed significantly reduced microvessel density in the combination group (bevacizumab, PD173074) compared to bevacizumab alone.

In the present study, we established a novel HNSCC xenograft model of acquired resistance to bevacizumab and identified upregulation of FGF signaling in resistant tumors. Increased expression of FGF2 was regulated by upstream genes including PLCg2, FZD4, CX3CL1, and CCL5 via increased ERK signaling. We also showed that modulation of FGF signaling in the resistant xenografts regulated sensitivity to bevacizumab.

FGFs are known to play an important role in a variety of cellular processes including differentiation, cell proliferation, apoptosis, angiogenesis and inflammation [115–117]. These FGF signaling-mediated functions can greatly contribute to to the process of tumorigenesis. Accumulating evidence highlights the deregulation of FGF/FGFRs in cancer through different mechanisms, including aberrant expression, mutations, and gene amplifications [118]. There are 4 known FGFRs, FGFR1 through FGFR4. These receptors differ in the distribution patterns of specific isoforms on tumor cells and stromal cells, collectively mediating autocrine and paracrine signaling in tumors. Studies have shown that FGF2/FGFRs autocrine signaling contributes to EGFR TKI resistance in NSCLC lines [119, 120].

In our HNSCC xenograft model of acquired resistance to bevacizumab, we have shown upregulation of FGF signaling specifically in the tumors cells. Several members of the FGF pathway were found to be overexpressed including FGF2 ligand, FGFR1 through FGFR3 receptors, downstream proteins phospho PLCg1, PLCg1, phospho PCLg2, PLCg2, phospho AKT and phospho ERK. This suggests that upregulation FGF/FGFR autocrine signaling is one of the ways by which bevacizumab-resistant tumors cells bypass VEGF inhibition. However, along with the aggressive growth phenotype of these resistant xenografts, these tumors also display increased vasculature and reduced endothelial cell death. This clearly indicates the existence of paracrine signaling between tumor cell-secreted FGF ligands and endothelial cell-surface FGFRs. Although we have not analyzed the levels of FGFRs on the endothelial cells, a recent report by Cascone et. al. [76], described upregulation of stromal FGFR in a NSCLC xenograft model of acquired resistance to bevacizumab. FGF2 could also induce production of several other angiogenic factors downstream to FGF signaling in

both tumor cells and stromal cells, indirectly contributing to resistance.

We also demonstrated phospho ERK-mediated regulation of FGF expression in parental cells and bevacizumab-resistant cells. Since, there is increased expression of phospho ERK in the resistant cells, this can be one of the mechanisms by which the resistant cells increase FGF2 expression. Based on this finding, we investigated other upregulated genes in the microarray that were known to activate ERK. Using the IPA tool we selected high J5 score bearing differentially expressed genes including FZD4, PLCg2, CX3CL1 and CCL5 as known activators of ERK. Downregulation of these upstream genes, in both parental and resistant cells resulted in a decrease in activation of ERK and a corresponding decrease in FGF2 levels. Although this mechanism is common to both parental and resistant cells, the overexpression of upstream genes in resistant cells provides indirect evidence for increased FGF2 expression.

These results put forward an important concept in the phenomenon of acquired resistance. In response to anti-VEGF therapy, our HNSCC tumors showed an increased expression of a number of tumorigenesis and angiogenesis-related genes. From literature, we know that ERK is an integral growth-promoting protein, which is common to a wide variety of growth-factor signaling pathways. Hence, increased activation of ERK could serve as a default mechanism of resistance that the tumors acquire to sustain growth and survival. Also, FGF upregulation by the tumors will be a byproduct of increased ERK activation.

There is growing evidence that suggests upregulation of FGF/ FGFR axis in response to anti-VEGF therapy [72, 76, 77, 121, 122]. Recent studies in mouse models of pancreatic tumors and renal cell carcinoma have shown that dual inhibition of VEGFR and FGFR can overcome anti-VEGF therapy resistance [123, 124]. However, there are no reports that describe the mechanisms underlying FGF/ FGFR upregulation, in response to VEGF inhibitors.

Our results indicate that bevacizumab-refractory HNSCC tumors utilize FGF signaling as a path of least resistance using a battery of proangiogenic genes that converge on ERK

signaling to upregulate its expression and mediate resistance to anti-VEGF therapy. Knowledge of these regulatory networks provide a stronger mechanistic rationale for co-targeting VEGF and FGFR in future clinical trials.

4.0 DISCUSSION

HNSCC is the eighth most common malignancy worldwide [1]. Currently, the average five-year survival rate for this disease is 62%. This rate is highly dependent on the stage at diagnosis; with early stage diagnoses having an 82% five-year survival rate and advanced stages having only a 35% survival rate [2]. Despite advances in surgery and other treatment modalities that enhance quality of life, survival rates have not improved significantly in the past fifty years. This underscores the need for development of new therapeutic strategies in HNSCC.

Antiangiogenic therapy represents a new promising anticancer therapeutic strategy. However, clinical trials with VEGF-targeted agents (such as bevacizumab) in HNSCC [55,56,81] and several other cancers [109–111] indicate that the therapeutic efficacy of these drugs is limited to date. Majority of the patients treated with these drugs demonstrate an initial clinical response but eventually experience tumor re-growth. In addition, a subset of patients exhibit inherent resistance to angiogenesis inhibition. These incomplete drug responses suggest the presence of alternative signaling pathways that are active in the setting of VEGF blockade. Currently, there are no studies that elucidate these molecular mechanisms of resistance to anti-VEGF therapy in HNSCC. An understanding of these parallel pathways is needed for the design of more effective antiangiogenic therapies for treatment of HNSCC.

Several potential mechanisms have been proposed in other cancers to account for the resistance of tumors to antiangiogenic therapy [33,63–66]. These studies indicate that tumors can rely on multiple escape mechanisms using a variety of angiogenic proteins secreted by both tumor cells and stromal cells. In conjunction, there is a growing realization that each

patient's tumor carries a unique molecular profile, demanding a personalized cancer treatment plan. This demand is coupled with the need to identify which subsets of patients have the best chance of benefit. Clinical specimens including tumor tissue and patient sera can serve as valuable resources to investigate the expression of potential biomarkers. However, there are limitations to procuring high quality specimens in large numbers for a conclusive analysis. More importantly, such analyses can only show an association between altered proteins and resistance to anti-VEGF therapy, but not causation or an actual resistance mechanism. Therefore, relevant preclinical models are indispensable for characterizing these escape mechanisms. Animal models that test combinatorial therapies along with VEGF inhibitors are needed for selection of suitable cotargets.

In this dissertation, we established preclinical models of intrinsic and acquired resistance to anti-VEGF antibody bevacizumab and identified potential biomarkers of drug response.

4.1 MECHANISMS OF INTRINSIC RESISTANCE IN HNSCC

We initiated these studies by screening a panel of HNSCC cell lines in vivo to examine their differential response to bevacizumab treatment. The HNSCC cell lines that displayed low sensitivity to bevacizumab served as a model of intrinsic resistance and the cell lines that showed high sensitivity to bevacizumab were used as a non-isogenic model for comparison.

Clinical trials of the VEGF-pathway inhibitors indicate that a minority of patients fail to show even transitory clinical benefit [55, 56, 81]. One potential mechanism for this innate resistance might be the pre-existing multiplicity of redundant angiogenic factors. HNSCC cells are known to produce a plethora of angiogenic factors that might allow continued angiogenesis in the setting of bevacizumab therapy. Therefore, we assayed for differences in secreted angiogenic factors between the bevacizumab-sensitive and -resistant HNSCC cell lines using antibody array. We found higher expression of proangiogenic factors including IL-8, IL-1α, VEGF, FGF-a and TNF-α in the resistant cells compared to the sensitive cells.

Among these cytokines, IL-8 was the most differentially expressed protein in the resistant cells. Based on this *in vitro* data, we formulated the hypothesis that IL8 contributes to bevacizumab resistance in the HNSCC xenograft models. We then tested this hypothesis in vivo using shRNA-mediated knockdown of IL8 in resistant models and conversely overexpressing IL8 in sensitive models and showed that IL8 can modulate response to bevacizumab in these preclinical models.

In addition to identifying IL-8 as a mediator of bevacizumab resistance, we also examined signaling pathways upstream to IL-8 that regulated high expression levels of IL-8 in the resistant cells. It has been reported that SCC61 cells (bevacizumab-resistant) contain a PI3K activating mutation (E542K) in Exon 9 [87]. Our data suggests that constitutive activation of PI3K signaling in the bevacizumab-resistant SCC61 cells could serve as an escape mechanism to anti-VEGF therapy by regulating increased production of IL-8. PI3K signaling is one of the most commonly activated pathways in several cancer types including HNSCC. Our studies provide an added rationale for the use of PI3K inhibitors to overcome resistance to antiangiogenic agents such as bevacizumab. Also, PI3K inhibitors such as BYL719 and PX-866 are currently in phase I/ II clinical trials for recurrent/ metastatic HNSCC, NSCLC and CRC.

We also demonstrated IL-1α as a mechanism of IL-8 regulation in the resistant cells. Studies have shown that tumor cells upregulate IL-1α to promote angiogenesis, tumor growth and metastasis. Also, in our antibody array analysis, we have shown that the resistant cells express increased levels of IL-1α along with IL-8 and several other proangiogenic proteins. Our findings suggest that increased expression of IL-1α in the resistant cells contributes to increased IL-8 production, which mediates bevacizumab resistance. Hence, increased IL-1α signaling could be another potential mechanism of resistance to anti-VEGF therapy in HNSCC. Anti-IL1α monoclonal antibodies such as anakinra, which have shown clinical benefit in patients with rheumatoid arthritis, might also enhance antiangiogenic therapeutic efficacy.

As our data identified IL-8 as a mediator of bevacizumab resistance in preclinical HNSCC

xenograft models, we also assessed IL-8 levels in sera from HNSCC patients who received bevacizumab as a part of their treatment regimen. Serum analysis suggested an inverse correlation between IL-8 levels with clinical outcome. Future clinical trials with angioangiogenic agents that assess IL-8 levels in patients will further validate the use of IL-8 as a relevant biomarker of treatment response or resistance.

In the light of these preclinical and clinical findings, we foresee IL-8 to be an important player in governing sensitivity to antiangiogenic therapy. Several IL-8 targeting agents are currently in clinical development primarily for the treatment of inflammatory diseases and these agents have shown antitumor and antiangiogenic activity in preclinical models [105, 106].

Our data suggests that the concurrent use of anti-VEGF agents such as bevacizumab and IL-8 targeting agents may help overcome resistance and improve therapeutic efficacy of antiangiogenic therapy in HNSCC.

4.2 MECHANISMS OF ACQUIRED RESISTANCE IN HNSCC

In this body of work, we generated a novel HNSCC xenograft model of acquired resistance to bevacizumab and identified FGF as an escape mechanism to anti-VEGF therapy. In order to establish the xenograft model, we used an incremental drug dosing regime. Mice were treated with bevacizumab at an initial dose of 4mg/kg followed by increasing the dose by 4mg/kg with every subsequent increase in tumor volume. Although use of this incremental dosing regime is not representative of clinical therapy, we employed this approach to eliminate the sensitive tumor cells and sequentially selected for the resistant clones. After prolonged therapy, we observed a significant difference in the tumor growth between the chronically treated HNSCC xenografts (less sensitive) and the isogenic parental (more sensitive) xenografts. This isogenic nature of the sensitive and resistant tumors is a significant advantage of this model, as it enables ideal comparison within the isogenic pair overcoming

the genetic and phenotypic variation across different cell lines. We further characterized the preclinical model by assessing microvessel density and endothelial cell apoptosis and found that the bevacizumab-resistant phenotype is associated with revascularization of these tumors and reduced endothelial cell death.

After successful generation of the preclinical model, we next wanted to identify the molecular changes initiated by tumor cells to mediate bevacizumab resistance. In order to do so, we performed whole genome microarray analysis on the isogenic pair of becaizumab-sensitive and -resistant tumors. We found 150 genes that were upregulated and 31 genes that were downregulated in the resistant tumors. Among the angiogenesis-related genes, we found upregulation of FGF2, FGFR3, PLCg2, FZD4, CX3CL1, and CCL5 in the resistant tumors. Functional interaction network involving DE genes identified FGF2 as a highly connected nodal gene with upregulated proangiogenic genes FGFR3, PLCg2, CASP1 and BGN. Interestingly, three of these genes FGF2, FGFR3 and PLCg2 belong to the FGF signaling pathway. These results led us to hypothesize that the FGF axis may be involved in bevacizumab-associated acquired resistance in our HNSCC xenograft model.

FGFs are known to play an important role in a variety of cellular processes including differentiation, cell proliferation, apoptosis, angiogenesis and inflammation. These FGF signaling-mediated functions can greatly contribute to the process of tumorigenesis. Accumulating evidence highlights the deregulation of FGF/FGFRs in cancer through different mechanisms, including aberrant expression, mutations, and gene amplifications. There are 4 known FGFRs, FGFR1 through FGFR4. These receptors differ in the distribution patterns of specific isoforms on tumor cells and stromal cells, collectively mediating autocrine and paracrine signaling in tumors. Studies have shown that FGF2/FGFRs autocrine signaling contributes to EGFR-TKI resistance in NSCLC lines.

We also addressed the molecular basis for overexpression of FGF2 in the resistant tumors and observed that the resistant cells had higher levels of phospho ERK and that the expression of FGF2 was dependent in part to ERK activity in both parental and resistant cells.

Using the IPA tool we then found several high J5 score bearing DE genes including FZD4, PLCg2, CX3CL1 and CCL5 which are well-known activators of ERK. Downregulation of these upstream genes, in both parental and resistant cells resulted in a decrease in activation of ERK and a corresponding decrease in FGF2 levels. Although this mechanism of FGF2 regulation was common to both parental and resistant cells, it appears to be amplified in the resistant cells due to overexpression of these upstream genes.

In response to anti-VEGF therapy, our HNSCC tumors showed an increased expression of a number of tumorigenesis and angiogenesis-related genes. Despite the changes in the expression of many different cytokines, the cumulative effects of these changes appears to feed through a common protein or pathway to exert its effect. In our acquired model, the overexpression of FZD4, PLCg2, CX3CL1, and CCL5 has the common effect of ERK activation which eventually lead to the overexpression of FGF2. Based on this observation, we can put forth a hypothesis that although the treatment with antiangiogenic agents leads to pleiotrophic changes to the tumor, therapeutic attempts to reverse the resistance may not require the inhibition of all these differentially expressed cytokines but rather one or two pathways that these changes mainly feeds through. In our model, that common pathway appeared to be ERK and eventually FGF2. These data also provide an added rationale for use of ERK inhibitors in conjunction with bevacizumab as a means to overcome resistance to anti-VEGF therapy. A multicenter phase I trial of the ERK Inhibitor BAY 86-9766 in patients with advanced cancer indicated some evidence of clinical benefit across a range of tumor types [125], an encouraging trend for future clinical trials.

Since IL-8 was the primary mechanism of bevacizumab resistance in the intrinsic models, we also assessed IL-8 levels in our model of a acquired resistance. Interestingly, IL-8 was downregulated in the acquired resistant tumors, suggesting that the tumors excluded this mechanism to maintain angiogenesis and sustain tumor growth in presence of VEGF blockade. These findings indicate that there might be an inherent difference in the underlying mechanisms of intrinsic and acquired resistance to antiangiogenic therapies. These distinct mechanisms could correspond to different patient subpopulations. Identification of

these subsets can help improve pretreatment patient selection for personalized medicine and enhance the therapeutic efficacy of antiangiogenic therapies.

4.3 CONCLUDING REMARKS

Our work has generated preclinical HNSCC models of intrinsic and acquired resistance to anti-VEGF antibody bevacizumab. These models serve as a valuable resource to test novel combinatorial therapies with VEGF inhibitors. In these xenograft models, we identified two distinct molecular mechanisms of resistance to bevacizumab. IL-8 signaling mediated intrinsic resistance while upregulation of FGF signaling in response to anti-VEGF therapy contributed to acquired resistance. Although, IL-8 and FGF have been previously implicated in anti-VEGF therapy resistance in other cancers, our study is the first to validate these mechanisms in HNSCC.

The most novel finding of our work is the identification of regulatory mechanisms that result in upregulation of IL-8 and FGF in our resistant models. We believe that knowledge of these regulatory mechanisms is necessary to discover functional networks that integrate additional upstream genes as potential contributors of resistance. We identified PI3K and IL-1α signaling as positive regulators of IL-8 expression, indirectly contributing to intrinsic resistance. In the model of acquired resistance, we identified a proangiogenic signature including FZD4, PLCg2, CX3CL1, and CCL5 genes that mediated upregulation of FGF via increased ERK signaling. Above findings provide a mechanistic rationale for for co-targeting VEGF together with the elements of these evasive mechanisms such as IL-8 and FGF to enhance the therapeutic efficacy of antiangiogenic therapy.

APPENDIX

MICROARRAY DATA

Table A1: List of 181 differentially expressed genes in bevacizumab-resistant tumors.

Rank	Description	J5-score	Accession #
1	hemoglobin, beta (HBB)	27.473	NM_000518.4
2	insulin-like growth factor binding protein 6 (IGFBP6)	27.04	NM_002178.2
3	H19, imprinted maternally expressed transcript (non-protein coding) (H19), non-coding RNA.	25.785	NR_002196.1
4	alkaline phosphatase, liver/bone/kidney (ALPL), transcript variant 1	22.435	NM_000478.2
5	retinoic acid receptor responder (tazarotene induced) 3 (RARRES3)	21.255	NM_004585.2
6	hect domain and RLD 5 (HERC5)	19.807	NM_016323.1
7	keratin 10 (epidermolytic hyperkeratosis; keratosis palmaris et plantaris) (KRT10)	18.764	NM_000421.2
8	frizzled homolog 4 (Drosophila) (FZD4)	18.239	NM_012193.2
9	NADH dehydrogenase (ubiquinone) 1 alpha subcomplex, 4-like 2 (NDUFA4L2)	17.73	NM_020142.3
10	absent in melanoma 2 (AIM2)	17.325	NM_004833.1
11	lymphocyte antigen 6 complex, locus E (LY6E)	16.749	NM_002346.1
12	ISG15 ubiquitin-like modifier (ISG15)	16.646	NM_005101.1
13	Sp8 transcription factor (SP8), transcript variant 2	16.322	NM_198956.1

Continued on next page

Table A1 – *Continued from previous page*

Rank	Description	J5-score	Accession #
14	interferon-induced protein with tetratricopeptide repeats 2 (IFIT2)	16.015	NM_001547.3
15	DEAD (Asp-Glu-Ala-Asp) box polypeptide 60 (DDX60)	15.934	NM_017631.3
16	interferon-induced protein 44 (IFI44)	15.841	NM_006417.2
17	epithelial stromal interaction 1 (breast) (EPSTI1), transcript variant 2	14.501	NM_033255.2
18	interferon-induced protein with tetratricopeptide repeats 1 (IFIT1), transcript variant 2	14.27	NM_001548.2
19	mal, T-cell differentiation protein 2 (MAL2)	13.948	NM_052886.1
20	chemokine (C-X3-C motif) ligand 1 (CX3CL1)	13.329	NM_002996.3
21	PRED: similar to epiplakin 1 (LOC648526)	13.171	XM_937579.1
22	chemokine (C-X-C motif) receptor 7 (CXCR7)	13.142	NM_020311.1
23	MSTP131 (MST131) mRNA, complete cds	13.023	Hs.551128
24	phospholipase C, gamma 2 (phosphatidylinositol-specific) (PLCG2)	12.871	NM_002661.1
25	hect domain and RLD 6 (HERC6), transcript variant 1	12.702	NM_001013005.1
26	interferon, alpha-inducible protein 27 (IFI27), transcript variant 2	12.238	NM_005532.3
27	biglycan (BGN)	12.165	NM_001711.3
28	interferon-induced protein with tetratricopeptide repeats 3 (IFIT3)	12.135	NM_001031683.1
29	HLA complex P5 (HCP5)	12.074	NM_006674.2
30	interferon-induced protein 44-like (IFI44L)	12.059	NM_006820.1
31	major histocompatibility complex, class I, B (HLA-B)	11.901	NM_005514.5
32	major histocompatibility complex, class I, H (pseudogene) (HLA-H), non-coding RNA.	11.736	NR_001434.1
33	interleukin 20 receptor beta (IL20RB)	11.685	NM_144717.2
34	interferon stimulated exonuclease gene 20kDa (ISG20)	11.617	NM_002201.4
35	sterile alpha motif domain containing 9 (SAMD9)	11.609	NM_017654.2
36	phosducin-like 3 (PDCL3)	11.58	XM_929879.1
37	XIAP associated factor 1 (XAF1), transcript variant 2	11.535	NM_199139.1

Continued on next page

Table A1 – *Continued from previous page*

Rank	Description	J5-score	Accession #
38	growth factor receptor-bound protein 10 (GRB10), transcript variant 1	11.518	NM_005311.3
39	neuromedin U (NMU)	11.506	NM_006681.1
40	prostaglandin E receptor 4 (subtype EP4) (PTGER4)	11.382	NM_000958.2
41	cellular retinoic acid binding protein 2 (CRABP2)	11.227	NM_001878.2
42	histone cluster 1, H2bk (HIST1H2BK)	11.207	NM_080593.1
43	prostaglandin E synthase (PTGES)	11.144	NM_004878.3
44	protease, serine, 23 (PRSS23)	11.034	NM_007173.3
45	KH homology domain containing 1-like (KHDC1L)	11.014	NM_001126063.2
46	PRED: hypothetical gene supported by BC013438 (LOC375295)	10.953	XM_944366.1
47	transcobalamin I (vitamin B12 binding protein, R binder family) (TCN1)	10.862	NM_001062.2
48	chemokine (C-C motif) ligand 5 (CCL5)	10.718	NM_002985.2
49	regulator of G-protein signalling 2, 24kDa (RGS2)	10.661	NM_002923.1
50	chromosome 5 open reading frame 15 (C5orf15)	10.617	NM_020199.1
51	carbonyl reductase 3 (CBR3)	10.615	NM_001236.3
52	2'-5'-oligoadenylate synthetase-like (OASL), transcript variant 1	10.599	NM_003733.2
53	interferon induced transmembrane protein 3 (1-8U) (IFITM3)	10.587	NM_021034.1
54	receptor (chemosensory) transporter protein 4 (RTP4)	10.558	NM_022147.2
55	Rho GDP dissociation inhibitor (GDI) beta (ARHGDIB)	10.533	NM_001175.4
56	zinc finger CCCH-type, antiviral 1 (ZC3HAV1), transcript variant 2	10.333	NM_024625.3
57	sperm associated antigen 9 (SPAG9), transcript variant 2	10.261	NM_172345.1
58	interferon regulatory factor 1 (IRF1)	10.254	NM_002198.1
59	calmodulin-like 3 (CALML3)	10.191	NM_005185.2
60	STAM binding protein-like 1 (STAMBPL1)	10.182	NM_020799.2
61	Kruppel-like factor 4 (gut) (KLF4)	10.163	NM_004235.3

Continued on next page

Table A1 – *Continued from previous page*

Rank	Description	J5-score	Accession #
62	myxovirus (influenza virus) resistance 1, interferon-inducible protein p78 (mouse) (MX1)	10.12	NM_002462.2
63	cysteine and glycine-rich protein 2 (CSRP2)	10.062	NM_001321.1
64	PRED: similar to creatine kinase, mitochondrial 1B precursor (LOC649970)	9.97	XM_939056.1
65	transporter 1, ATP-binding cassette, sub-family B (MDR/TAP) (TAP1)	9.969	NM_000593.5
66	desmocollin 1 (DSC1), transcript variant Dsc1b	9.939	NM_004948.2
67	transcription elongation factor A (SII)-like 8 (TCEAL8), transcript variant 1	9.883	NM_153333.2
68	Rho guanine exchange factor (GEF) 16 (ARHGEF16)	9.851	NM_014448.2
69	transmembrane protein 66 (TMEM66)	9.822	NM_016127.4
70	microtubule-associated protein, RP/EB family, memb 2 (MAPRE2)	9.817	NM_014268.1
71	interferon induced with helicase C domain 1 (IFIH1)	9.8	NM_022168.2
72	SAR1 gene homolog A (S. cerevisiae) (SAR1A)	9.779	NM_020150.3
73	fibroblast growth factor 2 (basic) (FGF2)	9.741	NM_002006.3
74	nephroblastoma overexpressed gene (NOV)	9.724	NM_002514.2
75	interferon induced transmembrane protein 2 (1-8D) (IFITM2)	9.676	NM_006435.1
76	HD domain containing 2 (HDDC2)	9.647	NM_016063.1
77	UDP-Gal:betaGlcNAc beta 1,4- galactosyltransferase, polypeptide 5 (B4GALT5)	9.642	NM_004776.2
78	beta-2-microglobulin (B2M)	9.626	NM_004048.2
79	chloride channel, calcium activated, family memb 2 (CLCA2)	9.512	NM_006536.4
80	caspase 1, apoptosis-related cysteine peptidase (interleukin 1, beta, convertase) (CASP1), transcript variant alpha	9.477	NM_033292.2
81	prominin 2 (PROM2)	9.456	NM_144707.1
82	thioredoxin interacting protein (TXNIP)	9.372	NM_006472.1

Continued on next page

Table A1 – *Continued from previous page*

Rank	Description	J5-score	Accession #
83	small nucleolar RNA, C/D box 13 (SNORD13), small nucleolar RNA.	9.329	Hs.583806
84	peptidase D (PEPD)	9.311	NM_000285.1
85	amyotrophic lateral sclerosis 2 (juvenile) chromosome region, candidate 4 (ALS2CR4), transcript variant 1	9.26	NM_152388.1
86	2'-5'-oligoadenylate synthetase 2, 69/71kDa (OAS2), transcript variant 2	9.257	NM_002535.2
87	histone cluster 1, H1c (HIST1H1C)	9.221	NM_005319.3
88	CDC42 effector protein (Rho GTPase binding) 4 (CDC42EP4)	9.207	NM_012121.4
89	hyaluronan-mediated motility receptor (RHAMM) (HMMR), transcript variant 2	9.178	NM_012485.1
90	pyridoxamine 5'-phosphate oxidase (PNPO)	9.147	NM_018129.1
91	solute carrier family 9 (sodium/hydrogen exchanger), memb 3 regulator 1 (SLC9A3R1)	9.117	NM_004252.1
92	vav 3 guanine nucleotide exchange factor (VAV3), transcript variant 1	9.094	NM_006113.4
93	leprecan-like 1 (LEPREL1)	9.091	NM_018192.2
94	major histocompatibility complex class I HLA-A29.1	9.044	NM_001080840.1
95	transmembrane protein 106C (TMEM106C)	9.029	NM_024056.2
96	LSM1 homolog, U6 small nuclear RNA associated (S. cerevisiae) (LSM1)	8.899	NM_014462.1
97	coiled-coil domain containing 6 (CCDC6)	8.843	NM_005436.2
98	insulin receptor substrate 1 (IRS1)	8.817	NM_005544.1
99	ash2 (absent, small, or homeotic)-like (Drosophila) (ASH2L)	8.767	NM_004674.1
100	tumor necrosis factor (ligand) superfamily, memb 10 (TNFSF10)	8.742	NM_003810.2
101	PRED: misc_RNA (LOC729816), miscRNA.	8.74	XR_042352.1
102	cyclin D3 (CCND3)	8.728	NM_001760.2
103	major histocompatibility complex, class I, F (HLA-F), transcript variant 1	8.705	NM_018950.1

Continued on next page

Table A1 – *Continued from previous page*

Rank	Description	J5-score	Accession #
104	major histocompatibility complex, class I, A (HLA-A)	8.68	NM_002116.5
105	NAD(P)H dehydrogenase, quinone 1 (NQO1), transcript variant 1	8.631	NM_000903.2
106	PDZ binding kinase (PBK)	8.594	NM_018492.2
107	PRED: similar to hCG1983233 (LOC100134304)	8.56	XM_001720739.1
108	Cbp/p300-interacting transactivator, with Glu/Asp-rich carboxy-terminal domain, 2 (CITED2), transcript variant 1	8.501	NM_006079.3
109	anillin, actin binding protein (ANLN)	8.5	NM_018685.2
110	heterogeneous nuclear ribonucleoprotein A1 pseudogene (LOC728643), non-coding RNA.	8.472	NR_003277.1
111	PYD and CARD domain containing (PYCARD), transcript variant 1	8.469	NM_145183.1
112	proline synthetase co-transcribed homolog (bacterial) (PROSC)	8.454	NM_007198.2
113	PRED: hypothetical protein LOC100130919 (LOC100130919)	8.448	XM_001722872.1
114	poly (ADP-ribose) polymerase family, memb 9 (PARP9)	8.448	NM_031458.1
115	enhancer of rudimentary homolog (Drosophila) (ERH)	8.447	NM_004450.1
116	neuregulin 4 (NRG4)	8.433	NM_138573.1
117	NADH dehydrogenase (ubiquinone) 1 beta subcomplex, 10, 22kDa (NDUFB10)	8.433	NM_004548.1
118	fibroblast growth factor receptor 3 (achondroplasia, thanatophoric dwarfism) (FGFR3), transcript variant 2	8.424	NM_000142.2
119	chromosome 10 open reading frame 99 (C10orf99)	8.405	NM_207373.1
120	minichromosome maintenance complex component 6 (MCM6)	8.352	NM_005915.4
121	calpain 1, (mu/I) large subunit (CAPN1)	8.316	NM_005186.2
122	tumor protein p73-like (TP73L)	8.262	NM_003722.3
123	carboxymethylenebutenolidase homolog (Pseudomonas) (CMBL)	8.202	NM_138809.2

Continued on next page

Table A1 – *Continued from previous page*

Rank	Description	J5-score	Accession #
124	asp (abnormal spindle) homolog, microcephaly associated (Drosophila) (ASPM)	8.189	NM_018136.2
125	tumor protein p63 (TP63), transcript variant 5	8.182	NM_001114981.1
126	PRED: similar to Nonhistone chromosomal protein HMG-17 (High-mobility group nucleosome binding domain 2) (LOC148915)	8.181	XM_937758.1
127	leptin receptor overlapping transcript-like 1 (LEPROTL1)	8.154	NM_015344.1
128	chromosome X open reading frame 26 (CXorf26)	8.143	NM_016500.3
129	exportin 1 (CRM1 homolog, yeast) (XPO1)	8.135	NM_003400.3
130	microsomal glutathione S-transferase 2 (MGST2)	8.128	NM_002413.3
131	general transcription factor IIE, polypeptide 2, beta 34kDa (GTF2E2)	8.122	NM_002095.3
132	defensin, beta 1 (DEFB1)	8.109	NM_005218.3
133	chromosome 6 open reading frame 173 (C6orf173)	8.103	NM_001012507.1
134	cyclin B2 (CCNB2)	8.092	NM_004701.2
135	complement factor D (adipsin) (CFD)	8.065	NM_001928.2
136	COBL-like 1 (COBLL1)	8.064	NM_014900.3
137	metallothionein 1E (functional) (MT1E)	8.057	NM_175617.2
138	glutathione reductase (GSR)	8.038	NM_000637.2
139	RNA, U1A3 small nuclear (RNU1A3), small nuclear RNA.	-8.131	NR_004430.1
140	collagen, type V, alpha 2 (COL5A2)	-8.2	NM_000393.2
141	late cornified envelope 3E (LCE3E)	-8.245	NM_178435.2
142	small proline-rich protein 2C (pseudogene) (SPRR2C), non-coding RNA.	-8.265	NR_003062.1
143	immediate early response 3 (IER3)	-8.484	NM_052815.1
144	tribbles homolog 3 (Drosophila) (TRIB3)	-8.591	NM_021158.3
145	serpin peptidase inhibitor, clade E (nexin, plasminogen activator inhibitor type 1), memb 2 (SERPINE2)	-8.669	NM_006216.2
146	small proline-rich protein 2B (SPRR2B)	-9.017	NM_001017418.1
147	cathepsin L2 (CTSL2)	-9.25	NM_001333.2

Continued on next page

Table A1 – *Continued from previous page*

Rank	Description	J5-score	Accession #
148	fatty acid binding protein 4, adipocyte (FABP4)	-9.319	NM_001442.1
149	cornifelin (CNFN)	-9.335	NM_032488.2
150	keratin 80 (KRT80), transcript variant 1	-9.359	NM_182507.2
151	RNA, U1 small nuclear 3 (RNU1-3), small nuclear RNA.	-9.392	NR_004408.1
152	RNA, U1G2 small nuclear (RNU1G2), small nuclear RNA.	-9.445	NR_004426.1
153	tripartite motif family-like 2 (TRIML2)	-9.485	NM_173553.1
154	RNA, U1 small nuclear 5 (RNU1-5), small nuclear RNA.	-9.488	NR_004400.1
155	protein phosphatase 1, regulatory (inhibitor) subunit 15A (PPP1R15A)	-9.518	NM_014330.2
156	secretory leukocyte peptidase inhibitor (SLPI)	-9.607	NM_003064.2
157	colony stimulating factor 2 (granulocyte-macrophage) (CSF2)	-9.845	NM_000758.2
158	heparin-binding EGF-like growth factor (HBEGF)	-10.066	NM_001945.1
159	uridine phosphorylase 1 (UPP1), transcript variant 1	-10.249	NM_003364.2
160	PRED: family with sequence similarity 25, memb A (FAM25A)	-10.852	XM_001723781.1
161	lipocalin 2 (LCN2)	-10.964	NM_005564.2
162	PRED: similar to Ribosome biogenesis protein BMS1 homolog (LOC643150)	-11.046	XM_926523.1
163	PRED: hypothetical LOC643479 (LOC643479)	-11.134	XM_926802.1
164	cysteine-rich C-terminal 1 (CRCT1)	-11.457	NM_019060.1
165	ornithine decarboxylase 1 (ODC1)	-11.953	NM_002539.1
166	hemoglobin, alpha 2 (HBA2)	-12.011	NM_000517.3
167	interleukin 1 family, memb 9 (IL1F9)	-12.163	NM_019618.2
168	cyclin A1 (CCNA1)	-12.222	NM_003914.2
169	interleukin 8 (IL8)	-12.319	NM_000584.2
170	matrix metallopeptidase 9 (gelatinase B, 92kDa gelatinase, 92kDa type IV collagenase) (MMP9)	-12.672	NM_004994.2
171	small proline-rich protein 2D (SPRR2D)	-12.987	NM_006945.3

Continued on next page

Table A1 – *Continued from previous page*

Rank	Description	J5-score	Accession #
172	PRED: similar to Ribosome biogenesis protein BMS1 homolog (LOC647987)	-13.172	XM_937044.1
173	PRED: hypothetical LOC643161 (LOC643161)	-14.229	XM_926530.1
174	small proline-rich protein 2E (SPRR2E)	-14.686	NM_001024209.2
175	ribonuclease, RNase A family, 7 (RNASE7)	-15.01	NM_032572.2
176	PRED: hypothetical protein LOC647993 (LOC647993)	-15.078	XM_937048.1
177	small proline-rich protein 2A (SPRR2A)	-16.539	NM_005988.2
178	small proline-rich protein 2F (SPRR2F)	-16.568	NM_001014450.1
179	late cornified envelope 3D (LCE3D)	-20.282	NM_032563.1
180	defensin, beta 103B (DEFB103B)	-22.442	XM_928791.1
181	small proline-rich protein 2G (SPRR2G)	-24.715	NM_001014291.1

BIBLIOGRAPHY

[1] R. Siegel, D. Naishadham, and A. Jemal, "Cancer statistics, 2013," *CA: A Cancer Journal for Clinicians*, vol. 63, no. 1, pp. 11–30, 2013.

[2] S. Altekruse, C. Kosary, M. Krapcho, N. Neyman, R. Aminou, W. Waldron, J. Ruhl, N. Howlader, Z. Tatalovich, H. Cho, A. Mariotto, M. Eisner, D. Lewis, K. Cronin, H. Chen, E. Feuer, D. Stinchcomb, and B. e. Edwards, "Seer cancer statistics review, 1975-2007, national cancer institute. bethesda, md," 2009.

[3] D. Goldenberg, J. Lee, W. M. Koch, M. M. Kim, B. Trink, D. Sidransky, and C. S. Moon, "Habitual risk factors for head and neck cancer," *Otolaryngol Head Neck Surg.*, vol. 131, no. 6, pp. 986–93., 2004.

[4] Z. F. Zhang, H. Morgenstern, M. R. Spitz, D. P. Tashkin, G. P. Yu, T. C. Hsu, and S. P. Schantz, "Environmental tobacco smoking, mutagen sensitivity, and head and neck squamous cell carcinoma," *Cancer Epidemiol Biomarkers Prev.*, vol. 9, no. 10, pp. 1043–9., 2000.

[5] C. H. Lee, Y. C. Ko, H. L. Huang, Y. Y. Chao, C. C. Tsai, T. Y. Shieh, and L. M. Lin, "The precancer risk of betel quid chewing, tobacco use and alcohol consumption in oral leukoplakia and oral submucous fibrosis in southern taiwan," *Br J Cancer.*, vol. 88, no. 3, pp. 366–72., 2003.

[6] D. Goldenberg, N. E. Benoit, S. Begum, W. H. Westra, Y. Cohen, W. M. Koch, D. Sidransky, and J. A. Califano, "Epstein-barr virus in head and neck cancer assessed by quantitative polymerase chain reaction," *Laryngoscope.*, vol. 114, no. 6, pp. 1027–31., 2004.

[7] W. Shi, I. Pataki, C. MacMillan, M. Pintilie, D. Payne, B. O'Sullivan, B. J. Cummings, P. Warde, and F. F. Liu, "Molecular pathology parameters in human nasopharyngeal carcinoma," *Cancer.*, vol. 94, no. 7, pp. 1997–2006., 2002.

[8] M. L. Gillison, "Human papillomavirus-associated head and neck cancer is a distinct epidemiologic, clinical, and molecular entity," *Semin Oncol.*, vol. 31, no. 6, pp. 744–54., 2004.

[9] C. H. Shiboski, B. L. Schmidt, and R. C. Jordan, "Tongue and tonsil carcinoma: increasing trends in the u.s. population ages 20-44 years," *Cancer.*, vol. 103, no. 9, pp. 1843–9., 2005.

[10] D. Hardisson, "Molecular pathogenesis of head and neck squamous cell carcinoma," *Eur Arch Otorhinolaryngol.*, vol. 260, no. 9, pp. 502–8. Epub 2003 May 8., 2003.

[11] J. D. Klein and J. R. Grandis, "The molecular pathogenesis of head and neck cancer," *Cancer Biol Ther.*, vol. 9, no. 1, pp. 1–7. Epub 2010 Jan 9., 2010.

[12] W. Risau, H. Drexler, V. Mironov, A. Smits, A. Siegbahn, K. Funa, and C. H. Heldin, "Platelet-derived growth factor is angiogenic in vivo," *Growth Factors.*, vol. 7, no. 4, pp. 261–6., 1992.

[13] F. Arnold and D. C. West, "Angiogenesis in wound healing," *Pharmacol Ther.*, vol. 52, no. 3, pp. 407–22., 1991.

[14] A. O. Welsh and A. C. Enders, "Chorioallantoic placenta formation in the rat: Ii. angiogenesis and maternal blood circulation in the mesometrial region of the implantation chamber prior to placenta formation," *Am J Anat.*, vol. 192, no. 4, pp. 347–65., 1991.

[15] J. Folkman, "Tumor angiogenesis: therapeutic implications," *N Engl J Med.*, vol. 285, no. 21, pp. 1182–6., 1971.

[16] N. Bouck, V. Stellmach, and S. C. Hsu, "How tumors become angiogenic," *Adv Cancer Res.*, vol. 69, pp. 135–74., 1996.

[17] J. Folkman and D. Hanahan, "Switch to the angiogenic phenotype during tumorigenesis," *Princess Takamatsu Symp.*, vol. 22, pp. 339–47., 1991.

[18] G. Gasparini, N. Weidner, S. Maluta, F. Pozza, P. Boracchi, M. Mezzetti, A. Testolin, and P. Bevilacqua, "Intratumoral microvessel density and p53 protein: correlation with metastasis in head-and-neck squamous-cell carcinoma," *Int J Cancer.*, vol. 55, no. 5, pp. 739–44., 1993.

[19] G. J. Petruzzelli, C. H. Snyderman, J. T. Johnson, and E. N. Myers, "Angiogenesis induced by head and neck squamous cell carcinoma xenografts in the chick embryo chorioallantoic membrane model," *Ann Otol Rhinol Laryngol.*, vol. 102, no. 3 Pt 1, pp. 215–21., 1993.

[20] R. F. Cohen, J. Contrino, J. D. Spiro, E. A. Mann, L. L. Chen, and D. L. Kreutzer, "Interleukin-8 expression by head and neck squamous cell carcinoma," *Arch Otolaryngol Head Neck Surg.*, vol. 121, no. 2, pp. 202–9., 1995.

[21] D. R. Smith, P. J. Polverini, S. L. Kunkel, M. B. Orringer, R. I. Whyte, M. D. Burdick, C. A. Wilke, and R. M. Strieter, "Inhibition of interleukin 8 attenuates angiogenesis in bronchogenic carcinoma," *J Exp Med.*, vol. 179, no. 5, pp. 1409–15., 1994.

[22] D. T. Connolly, D. M. Heuvelman, R. Nelson, J. V. Olander, B. L. Eppley, J. J. Delfino, N. R. Siegel, R. M. Leimgruber, and J. Feder, "Tumor vascular permeability factor stimulates endothelial cell growth and angiogenesis.," *The Journal of Clinical Investigation*, vol. 84, pp. 1470–1478, 11 1989.

[23] C. Liss, M. J. Fekete, R. Hasina, C. D. Lam, and M. W. Lingen, "Paracrine angiogenic loop between head-and-neck squamous-cell carcinomas and macrophages," *Int J Cancer.*, vol. 93, no. 6, pp. 781–5., 2001.

[24] H.-P. Gerber, J. Kowalski, D. Sherman, D. A. Eberhard, and N. Ferrara, "Complete inhibition of rhabdomyosarcoma xenograft growth and neovascularization requires blockade of both tumor and host vascular endothelial growth factor," *Cancer Research*, vol. 60, no. 22, pp. 6253–6258, 2000.

[25] L. L. Gleich, N. Zimmerman, Y. O. Wang, and J. L. Gluckman, "Angiogenic inhibition for the treatment of head and neck cancer," *Anticancer Res.*, vol. 18, no. 4A, pp. 2607–9., 1998.

[26] K. J. Kim, B. Li, J. Winer, M. Armanini, N. Gillett, H. S. Phillips, and N. Ferrara, "Inhibition of vascular endothelial growth factor-induced angiogenesis suppresses tumour growth in vivo," *Nature.*, vol. 362, no. 6423, pp. 841–4., 1993.

[27] F. Riedel, K. Gotte, M. Li, K. Hormann, and J. R. Grandis, "Abrogation of vegf expression in human head and neck squamous cell carcinoma decreases angiogenic activity in vitro and in vivo," *Int J Oncol.*, vol. 23, no. 3, pp. 577–83., 2003.

[28] C. G. Willett, Y. Boucher, E. di Tomaso, D. G. Duda, L. L. Munn, R. T. Tong, D. C. Chung, D. V. Sahani, S. P. Kalva, S. V. Kozin, M. Mino, K. S. Cohen, D. T. Scadden, A. C. Hartford, A. J. Fischman, J. W. Clark, D. P. Ryan, A. X. Zhu, L. S. Blaszkowsky, H. X. Chen, P. C. Shellito, G. Y. Lauwers, and R. K. Jain, "Direct evidence that the vegf-specific antibody bevacizumab has antivascular effects in human rectal cancer," *Nat Med.*, vol. 10, no. 2, pp. 145–7. Epub 2004 Jan 25., 2004.

[29] D. J. Hicklin and L. M. Ellis, "Role of the vascular endothelial growth factor pathway in tumor growth and angiogenesis," *J Clin Oncol.*, vol. 23, no. 5, pp. 1011–27. Epub 2004 Dec 7., 2005.

[30] E. Tischer, R. Mitchell, T. Hartman, M. Silva, D. Gospodarowicz, J. C. Fiddes, and J. A. Abraham, "The human gene for vascular endothelial growth factor. multiple protein forms are encoded through alternative exon splicing," *Journal of Biological Chemistry*, vol. 266, no. 18, pp. 11947–11954, 1991.

[31] N. Ferrara, H. P. Gerber, and J. LeCouter, "The biology of vegf and its receptors," *Nat Med.*, vol. 9, no. 6, pp. 669–76., 2003.

[32] H. Takahashi and M. Shibuya, "The vascular endothelial growth factor (vegf)/vegf receptor system and its role under physiological and pathological conditions.," *Clin. Sci.*, vol. 109, no. 3, pp. 227–241, 2005.

[33] L. M. Ellis and D. J. Hicklin, "Pathways mediating resistance to vascular endothelial growth factortargeted therapy," *Clinical Cancer Research*, vol. 14, no. 20, pp. 6371–6375, 2008.

[34] Y. Takahashi, Y. Kitadai, C. D. Bucana, K. R. Cleary, and L. M. Ellis, "Expression of vascular endothelial growth factor and its receptor, kdr, correlates with vascularity, metastasis, and proliferation of human colon cancer," *Cancer Res*, vol. 55, no. 18, pp. 3964–3968, 1995.

[35] M. Volm, R. Koomagi, J. Mattern, and G. Stammler, "Angiogenic growth factors and their receptors in non-small cell lung carcinomas and their relationships to drug response in vitro," *Anticancer Res*, vol. 17, no. 1A, pp. 99–103, 1997. Using Smart Source Parsing Jan-Feb.

[36] J. Jacobsen, K. Grankvist, T. Rasmuson, A. Bergh, G. Landberg, and B. Ljungberg, "Expression of vascular endothelial growth factor protein in human renal cell carcinoma," *BJU International*, vol. 93, no. 3, pp. 297–302, 2004.

[37] E. R. Sauter, M. Nesbit, J. C. Watson, A. Klein-Szanto, S. Litwin, and M. Herlyn, "Vascular endothelial growth factor is a marker of tumor invasion and metastasis in squamous cell carcinomas of the head and neck," *Clinical Cancer Research*, vol. 5, no. 4, pp. 775–782, 1999.

[38] N. Wakisaka, Q. H. Wen, T. Yoshizaki, T. Nishimura, M. Furukawa, E. Kawahara, and I. Nakanishi, "Association of vascular endothelial growth factor expression with angiogenesis and lymph node metastasis in nasopharyngeal carcinoma," *Laryngoscope.*, vol. 109, no. 5, pp. 810–4., 1999.

[39] H. Mineta, K. Miura, T. Ogino, S. Takebayashi, K. Misawa, Y. Ueda, I. Suzuki, M. Dictor, A. Borg, and J. Wennerberg, "Prognostic value of vascular endothelial growth factor (vegf) in head and neck squamous cell carcinomas," *Br J Cancer.*, vol. 83, no. 6, pp. 775–81., 2000.

[40] M. Ivan, K. Kondo, H. Yang, W. Kim, J. Valiando, M. Ohh, A. Salic, J. M. Asara, W. S. Lane, and J. Kaelin, W. G., "Hifalpha targeted for vhl-mediated destruction by proline hydroxylation: implications for o2 sensing," *Science.*, vol. 292, no. 5516, pp. 464–8. Epub 2001 Apr 5., 2001.

[41] P. Jaakkola, D. R. Mole, Y. M. Tian, M. I. Wilson, J. Gielbert, S. J. Gaskell, A. Kriegsheim, H. F. Hebestreit, M. Mukherji, C. J. Schofield, P. H. Maxwell, C. W. Pugh, and P. J. Ratcliffe, "Targeting of hif-alpha to the von hippel-lindau ubiquitylation complex by o2-regulated prolyl hydroxylation," *Science.*, vol. 292, no. 5516, pp. 468–72. Epub 2001 Apr 5., 2001.

[42] N. Ferrara and T. Davis-Smyth, "The biology of vascular endothelial growth factor," *Endocr Rev*, vol. 18, no. 1, pp. 4–25, 1997.

[43] M. Bouvet, L. M. Ellis, M. Nishizaki, T. Fujiwara, W. Liu, C. D. Bucana, B. Fang, J. J. Lee, and J. A. Roth, "Adenovirus-mediated wild-type p53 gene transfer down-regulates vascular endothelial growth factor expression and inhibits angiogenesis in human colon cancer," *Cancer Res.*, vol. 58, no. 11, pp. 2288–92., 1998.

[44] F. Riedel, K. Gotte, J. Schwalb, C. Schafer, and K. Hormann, "Vascular endothelial growth factor expression correlates with p53 mutation and angiogenesis in squamous cell carcinoma of the head and neck," *Acta Otolaryngol.*, vol. 120, no. 1, pp. 105–11., 2000.

[45] R. Gyanchandani and S. Kim, "Predictive biomarkers to anti-vegf therapy: Progress toward an elusive goal," *Clinical Cancer Research*, vol. 19, no. 4, pp. 755–757, 2013.

[46] N. Ferrara, K. J. Hillan, H. P. Gerber, and W. Novotny, "Discovery and development of bevacizumab, an anti-vegf antibody for treating cancer," *Nat Rev Drug Discov.*, vol. 3, no. 5, pp. 391–400., 2004.

[47] N. Ferrara, K. J. Hillan, and W. Novotny, "Bevacizumab (avastin), a humanized anti-vegf monoclonal antibody for cancer therapy," *Biochemical and Biophysical Research Communications*, vol. 333, no. 2, pp. 328–335, 2005.

[48] E. Cabebe and H. Wakelee, "Sunitinib: a newly approved small-molecule inhibitor of angiogenesis," *Drugs Today (Barc).*, vol. 42, no. 6, pp. 387–98., 2006.

[49] J. T. Lee and J. A. McCubrey, "Bay-43-9006 bayer/onyx," *Curr Opin Investig Drugs.*, vol. 4, no. 6, pp. 757–63., 2003.

[50] N. Denaro, E. G. Russi, I. Colantonio, V. Adamo, and M. C. Merlano, "The role of antiangiogenic agents in the treatment of head and neck cancer," *Oncology*, vol. 83, no. 2, pp. 108–116, 2012.

[51] V. L. Heath and R. Bicknell, "Anticancer strategies involving the vasculature," *Nature Reviews Clinical Oncology*, vol. 6, no. 7, pp. 395–404, 2009.

[52] S. Cao, F. A. Durrani, K. Toth, Y. M. Rustum, and M. Seshadri, "Bevacizumab enhances the therapeutic efficacy of irinotecan against human head and neck squamous cell carcinoma xenografts," *Oral oncology*, vol. 47, no. 6, pp. 459–466, 2011.

[53] A. Bozec, A. Sudaka, J. L. Fischel, M. C. Brunstein, M. C. Etienne-Grimaldi, and G. Milano, "Combined effects of bevacizumab with erlotinib and irradiation: a preclinical study on a head and neck cancer orthotopic model," *Br J Cancer*, vol. 99, no. 1, pp. 93–99, 2008.

[54] C. N. Prichard, S. Kim, Y. D. Yazici, D. D. Doan, S. A. Jasser, M. Mandal, and J. N. Myers, "Concurrent cetuximab and bevacizumab therapy in a murine orthotopic model of anaplastic thyroid carcinoma," *The Laryngoscope*, vol. 117, no. 4, pp. 674–679, 2007.

[55] E. E. Vokes, E. E. W. Cohen, A. M. Mauer, T. G. Karrison, S. J. Wong, L. J. Skoog-Sluman, M. F. Kozloff, J. Dancey, and A. Dekker, "A phase i study of erlotinib and bevacizumab for recurrent or metastatic squamous cell carcinoma of the head and neck (hnc)," *J of Clin Oncol MeetingAbstracts*, vol. 23, no. 16_suppl, pp. 5504–, 2005.

[56] M. V. Karamouzis, D. Friedland, R. Johnson, K. Rajasenan, B. Branstetter, and A. Argiris, "Phase ii trial of pemetrexed (p) and bevacizumab (b) in patients (pts) with recurrent or metastatic head and neck squamous cell carcinoma (hnscc): An interim analysis," *J of Clin Oncol MeetingAbstracts*, vol. 25, no. 18_suppl, pp. 6049–, 2007.

[57] O. c. P, P. Rhys-Evans, H. Modjtahedi, and S. A. Eccles, "Vascular endothelial growth factor family members are differentially regulated by c-erbb signaling in head and neck squamous carcinoma cells," *Clin Exp Metastasis.*, vol. 18, no. 2, pp. 155–61., 2000.

[58] N. W. Choong, M. Kozloff, D. Taber, H. S. Hu, r. Wade, J., P. Ivy, T. G. Karrison, A. Dekker, E. E. Vokes, and E. E. Cohen, "Phase ii study of sunitinib malate in head and neck squamous cell carcinoma," *Invest New Drugs.*, vol. 28, no. 5, pp. 677–83. Epub 2009 Aug 4., 2010.

[59] S. Kim, Y. D. Yazici, G. Calzada, Z. Y. Wang, M. N. Younes, S. A. Jasser, A. K. El-Naggar, and J. N. Myers, "Sorafenib inhibits the angiogenesis and growth of orthotopic

anaplastic thyroid carcinoma xenografts in nude mice," *Mol Cancer Ther.*, vol. 6, no. 6, pp. 1785–92., 2007.

[60] C. Elser, L. L. Siu, E. Winquist, M. Agulnik, G. R. Pond, S. F. Chin, P. Francis, R. Cheiken, J. Elting, A. McNabola, D. Wilkie, O. Petrenciuc, and E. X. Chen, "Phase ii trial of sorafenib in patients with recurrent or metastatic squamous cell carcinoma of the head and neck or nasopharyngeal carcinoma," *Journal of Clinical Oncology*, vol. 25, no. 24, pp. 3766–3773, 2007.

[61] A. Christopoulos, S. M. Ahn, J. D. Klein, and S. Kim, "Biology of vascular endothelial growth factor and its receptors in head and neck cancer: Beyond angiogenesis," *Head and Neck*, vol. 33, no. 8, pp. 1220–1229, 2011.

[62] J. G. Bender, E. M. Cooney, J. J. Kandel, and D. J. Yamashiro, "Vascular remodeling and clinical resistance to antiangiogenic cancer therapy," *Drug Resistance Updates*, vol. 7, no. 45, pp. 289 – 300, 2004.

[63] G. Bergers and D. Hanahan, "Modes of resistance to anti-angiogenic therapy," *Nat Rev Cancer*, vol. 8, no. 8, pp. 592–603, 2008. 10.1038/nrc2442.

[64] P. Carmeliet and R. K. Jain, "Molecular mechanisms and clinical applications of angiogenesis," *Nature*, vol. 473, no. 7347, pp. 298–307, 2011. 10.1038/nature10144.

[65] Y. Crawford and N. Ferrara, "Tumor and stromal pathways mediating refractoriness/resistance to anti-angiogenic therapies," *Trends in Pharmacological Sciences*, vol. 30, no. 12, pp. 624–630, 2009.

[66] H. P. Eikesdal and R. Kalluri, "Drug resistance associated with antiangiogenesis therapy," *Seminars in Cancer Biology*, vol. 19, no. 5, pp. 310–317, 2009.

[67] D. Huang, Y. Ding, M. Zhou, B. I. Rini, D. Petillo, C. N. Qian, R. Kahnoski, P. A. Futreal, K. A. Furge, and B. T. Teh, "Interleukin-8 mediates resistance to antiangiogenic agent sunitinib in renal cell carcinoma," *Cancer Res.*, vol. 70, no. 3, pp. 1063–71. Epub 2010 Jan 26., 2010.

[68] F. Shojaei, X. Wu, A. K. Malik, C. Zhong, M. E. Baldwin, S. Schanz, G. Fuh, H.-P. Gerber, and N. Ferrara, "Tumor refractoriness to anti-vegf treatment is mediated by cd11b+gr1+ myeloid cells," *Nat Biotech*, vol. 25, no. 8, pp. 911–920, 2007. 10.1038/nbt1323.

[69] F. Shojaei, J. H. Lee, B. H. Simmons, A. Wong, C. O. Esparza, P. A. Plumlee, J. Feng, A. E. Stewart, D. D. Hu-Lowe, and J. G. Christensen, "Hgf/c-met acts as an alternative angiogenic pathway in sunitinib-resistant tumors," *Cancer Res.*, vol. 70, no. 24, pp. 10090–100. doi: 10.1158/0008–5472.CAN–10–0489. Epub 2010 Oct 15., 2010.

[70] R. K. Jain, "Normalization of tumor vasculature: an emerging concept in antiangiogenic therapy," *Science.*, vol. 307, no. 5706, pp. 58–62., 2005.

[71] J. Huang, S. Z. Soffer, E. S. Kim, K. W. McCrudden, J. Huang, T. New, C. A. Manley, W. Middlesworth, K. O'Toole, D. J. Yamashiro, and J. J. Kandel, "Vascular remodeling marks tumors that recur during chronic suppression of angiogenesis11nih u10 ca13539-27, subcontract 6641 (j. k.), nih 1 r01 ca08895101-a1 (d. y.), pediatric cancer foundation, and sorkin gift fund.note: J. huang and s. z. soffer contributed equally to this work.," *Molecular Cancer Research*, vol. 2, no. 1, pp. 36–42, 2004.

[72] O. Casanovas, D. J. Hicklin, G. Bergers, and D. Hanahan, "Drug resistance by evasion of antiangiogenic targeting of vegf signaling in late-stage pancreatic islet tumors," *Cancer Cell.*, vol. 8, no. 4, pp. 299–309., 2005.

[73] M. Paez-Ribes, E. Allen, J. Hudock, T. Takeda, H. Okuyama, F. Viaals, M. Inoue, G. Bergers, D. Hanahan, and O. Casanovas, "Antiangiogenic therapy elicits malignant progression of tumors to increased local invasion and distant metastasis.," *Cancer Cell*, vol. 15, no. 3, pp. 220–31, 2009.

[74] J. M. Ebos, C. R. Lee, J. G. Christensen, A. J. Mutsaers, and R. S. Kerbel, "Multiple circulating proangiogenic factors induced by sunitinib malate are tumor-independent and correlate with antitumor efficacy," *Proc Natl Acad Sci U S A.*, vol. 104, no. 43, pp. 17069–74. Epub 2007 Oct 17., 2007.

[75] C. Fischer, B. Jonckx, M. Mazzone, S. Zacchigna, S. Loges, L. Pattarini, E. Chorianopoulos, L. Liesenborghs, M. Koch, M. De Mol, M. Autiero, S. Wyns, S. Plaisance, L. Moons, N. van Rooijen, M. Giacca, J. M. Stassen, M. Dewerchin, D. Collen, and P. Carmeliet, "Anti-plgf inhibits growth of vegf(r)-inhibitor-resistant tumors without affecting healthy vessels," *Cell.*, vol. 131, no. 3, pp. 463–75., 2007.

[76] T. Cascone, M. H. Herynk, L. Xu, Z. Du, H. Kadara, M. B. Nilsson, C. J. Oborn, Y. Y. Park, B. Erez, J. J. Jacoby, J. S. Lee, H. Y. Lin, F. Ciardiello, R. S. Herbst, R. R. Langley, and J. V. Heymach, "Upregulated stromal egfr and vascular remodeling in mouse xenograft models of angiogenesis inhibitor-resistant human lung adenocarcinoma," *J Clin Invest.*, vol. 121, no. 4, pp. 1313–28. doi: 10.1172/JCI42405. Epub 2011 Mar 23., 2011.

[77] C. Carbone, T. Moccia, C. Zhu, G. Paradiso, A. Budillon, P. J. Chiao, J. L. Abbruzzese, and D. Melisi, "Anti-vegf treatmentresistant pancreatic cancers secrete proinflammatory factors that contribute to malignant progression by inducing an emt cell phenotype," *Clinical Cancer Research*, vol. 17, no. 17, pp. 5822–5832, 2011.

[78] S. Davies, D. Dai, G. Pickett, K. Thiel, V. Korovkina, and K. Leslie, "Effects of bevacizumab in mouse model of endometrial cancer: Defining the molecular basis for resistance.," *Oncol Rep*, vol. 25, no. 3, pp. 855–62, 2011.

[79] Q. Zhou, H. Lv, A. R. Mazloom, H. Xu, A. Ma'ayan, and J. M. Gallo, "Activation of alternate prosurvival pathways accounts for acquired sunitinib resistance in u87mg glioma xenografts," *Journal of Pharmacology and Experimental Therapeutics*, vol. 343, no. 2, pp. 509–519, 2012.

[80] A. Argiris, A. P. Kotsakis, T. Hoang, F. P. Worden, P. Savvides, M. K. Gibson, R. Gyanchandani, G. R. Blumenschein, H. X. Chen, J. R. Grandis, P. M. Harari, M. S. Kies, and S. Kim, "Cetuximab and bevacizumab: preclinical data and phase ii trial in recurrent or metastatic squamous cell carcinoma of the head and neck," *Annals of Oncology*, 2012.

[81] E. E. W. Cohen, D. W. Davis, T. G. Karrison, T. Y. Seiwert, S. J. Wong, S. Nattam, M. F. Kozloff, J. I. Clark, D.-H. Yan, W. Liu, C. Pierce, J. E. Dancey, K. Stenson, E. Blair, A. Dekker, and E. E. Vokes, "Erlotinib and bevacizumab in patients with recurrent or metastatic squamous-cell carcinoma of the head and neck: a phase i/ii study," *The Lancet Oncology*, vol. 10, no. 3, pp. 247–257, 2009.

[82] J. D. Hainsworth, D. R. Spigel, F. A. Greco, D. L. Shipley, J. Peyton, M. Rubin, M. Stipanov, and A. Meluch, "Combined modality treatment with chemotherapy, radiation therapy, bevacizumab, and erlotinib in patients with locally advanced squamous carcinoma of the head and neck: A phase ii trial of the sarah cannon oncology research consortium," *The Cancer Journal*, vol. 17, no. 5, pp. 267–272 10.1097/PPO.0b013e3182329791, 2011.

[83] M. Zhao, D. Sano, C. R. Pickering, S. A. Jasser, Y. C. Henderson, G. L. Clayman, E. M. Sturgis, T. J. Ow, R. Lotan, T. E. Carey, P. G. Sacks, J. R. Grandis, D. Sidransky, N. E. Heldin, and J. N. Myers, "Assembly and initial characterization of a panel of 85 genomically validated cell lines from diverse head and neck tumor sites," *Clinical Cancer Research*, vol. 17, no. 23, pp. 7248–7264, 2011.

[84] A. Cromer, A. Carles, R. Millon, G. Ganguli, F. Chalmel, F. Lemaire, J. Young, D. Dembele, C. Thibault, D. Muller, O. Poch, J. Abecassis, and B. Wasylyk, "Identification of genes associated with tumorigenesis and metastatic potential of hypopharyngeal cancer by microarray analysis," *Oncogene.*, vol. 23, no. 14, pp. 2484–98., 2004.

[85] M. A. Ginos, G. P. Page, B. S. Michalowicz, K. J. Patel, S. E. Volker, S. E. Pambuccian, F. G. Ondrey, G. L. Adams, and P. M. Gaffney, "Identification of a gene expression signature associated with recurrent disease in squamous cell carcinoma of the head and neck," *Cancer Research*, vol. 64, no. 1, pp. 55–63, 2004.

[86] H. Ye, T. Yu, S. Temam, B. Ziober, J. Wang, J. Schwartz, L. Mao, D. Wong, and X. Zhou, "Transcriptomic dissection of tongue squamous cell carcinoma," *BMC Genomics*, vol. 9, no. 1, p. 69, 2008.

[87] W. Yarbrough, A. Whigham, B. Brown, M. Roach, and R. Slebos, "Phosphoinositide kinase-3 status associated with presence or absence of human papillomavirus in head and neck squamous cell carcinomas.," *Int J Radiat Oncol Biol Phys*, vol. 69, no. 2 Suppl, pp. S98–101, 2007.

[88] J. S. Wolf, Z. Chen, G. Dong, J. B. Sunwoo, C. C. Bancroft, D. E. Capo, N. T. Yeh, N. Mukaida, and C. V. Waes, "Il (interleukin)-1 promotes nuclear factor-b and ap-1-induced il-8 expression, cell survival, and proliferation in head and neck squamous cell carcinomas," *Clinical Cancer Research*, vol. 7, no. 6, pp. 1812–1820, 2001.

[89] E. P. Christofakis, H. Miyazaki, D. S. Rubink, and W. A. Yeudall, "Roles of cxcl8 in squamous cell carcinoma proliferation and migration," *Oral Oncol.*, vol. 44, no. 10, pp. 920–6. doi: 10.1016/j.oraloncology.2007.12.002. Epub 2008 Feb 20., 2008.

[90] J. Y. Yoo, J. H. Kim, J. Kim, J. H. Huang, S. N. Zhang, Y. A. Kang, H. Kim, and C. O. Yun, "Short hairpin rna-expressing oncolytic adenovirus-mediated inhibition of il-8: effects on antiangiogenesis and tumor growth inhibition," *Gene Ther.*, vol. 15, no. 9, pp. 635–51. doi: 10.1038/gt.2008.3. Epub 2008 Feb 14., 2008.

[91] A. Li, S. Dubey, M. L. Varney, B. J. Dave, and R. K. Singh, "Il-8 directly enhanced endothelial cell survival, proliferation, and matrix metalloproteinases production and regulated angiogenesis," *The Journal of Immunology*, vol. 170, no. 6, pp. 3369–3376, 2003.

[92] R. Salcedo, J. H. Resau, D. Halverson, E. A. Hudson, M. Dambach, D. Powell, K. Wasserman, and J. J. Oppenheim, "Differential expression and responsiveness of chemokine receptors (cxcr1-3) by human microvascular endothelial cells and umbilical vein endothelial cells," *Faseb J.*, vol. 14, no. 13, pp. 2055–64., 2000.

[93] S. Singh, K. C. Nannuru, A. Sadanandam, M. L. Varney, and R. K. Singh, "Cxcr1 and cxcr2 enhances human melanoma tumourigenesis, growth and invasion," *Br J Cancer.*, vol. 100, no. 10, pp. 1638–46. doi: 10.1038/sj.bjc.6605055. Epub 2009 Apr 28., 2009.

[94] S. Singh, A. Sadanandam, K. C. Nannuru, M. L. Varney, R. Mayer-Ezell, R. Bond, and R. K. Singh, "Small-molecule antagonists for cxcr2 and cxcr1 inhibit human melanoma growth by decreasing tumor cell proliferation, survival, and angiogenesis," *Clin Cancer Res.*, vol. 15, no. 7, pp. 2380–6. doi: 10.1158/1078–0432.CCR–08–2387. Epub 2009 Mar 17., 2009.

[95] M. L. Petreaca, M. Yao, Y. Liu, K. Defea, and M. Martins-Green, "Transactivation of vascular endothelial growth factor receptor-2 by interleukin-8 (il-8/cxcl8) is required for il-8/cxcl8-induced endothelial permeability," *Mol Biol Cell.*, vol. 18, no. 12, pp. 5014–23. Epub 2007 Oct 10., 2007.

[96] J. R. Dunlevy and J. R. Couchman, "Interleukin-8 induces motile behavior and loss of focal adhesions in primary fibroblasts," *J Cell Sci.*, vol. 108, no. Pt 1, pp. 311–21., 1995.

[97] F. Shojaei, X. Wu, X. Qu, M. Kowanetz, L. Yu, M. Tan, Y. G. Meng, and N. Ferrara, "G-csf-initiated myeloid cell mobilization and angiogenesis mediate tumor refractoriness to anti-vegf therapy in mouse models," *Proc Natl Acad Sci U S A.*, vol. 106, no. 16, pp. 6742–7. doi: 10.1073/pnas.0902280106. Epub 2009 Apr 3., 2009.

[98] J. LeCouter, R. Lin, M. Tejada, G. Frantz, F. Peale, K. J. Hillan, and N. Ferrara, "The endocrine-gland-derived vegf homologue bv8 promotes angiogenesis in the testis: Localization of bv8 receptors to endothelial cells," *Proceedings of the National Academy of Sciences*, vol. 100, no. 5, pp. 2685–2690, 2003.

[99] J. LeCouter, C. Zlot, M. Tejada, F. Peale, and N. Ferrara, "Bv8 and endocrine gland-derived vascular endothelial growth factor stimulate hematopoiesis and hematopoietic cell mobilization," *Proceedings of the National Academy of Sciences of the United States of America*, vol. 101, no. 48, pp. 16813–16818, 2004.

[100] E. O. Hanrahan, H. Y. Lin, E. S. Kim, S. Yan, D. Z. Du, K. S. McKee, H. T. Tran, J. J. Lee, A. J. Ryan, P. Langmuir, B. E. Johnson, and J. V. Heymach, "Distinct patterns of cytokine and angiogenic factor modulation and markers of benefit for vandetanib and/or chemotherapy in patients with nonsmall-cell lung cancer," *Journal of Clinical Oncology*, vol. 28, no. 2, pp. 193–201, 2010.

[101] S. Kopetz, P. M. Hoff, J. S. Morris, R. A. Wolff, C. Eng, K. Y. Glover, R. Adinin, M. J. Overman, V. Valero, S. Wen, C. Lieu, S. Yan, H. T. Tran, L. M. Ellis, J. L. Abbruzzese, and J. V. Heymach, "Phase ii trial of infusional fluorouracil, irinotecan, and bevacizumab for metastatic colorectal cancer: Efficacy and circulating angiogenic biomarkers associated with therapeutic resistance," *Journal of Clinical Oncology*, vol. 28, no. 3, pp. 453–459, 2010.

[102] L. Yu, X. Wu, Z. Cheng, C. V. Lee, J. LeCouter, C. Campa, G. Fuh, H. Lowman, and N. Ferrara, "Interaction between bevacizumab and murine vegf-a: a reassessment," *Invest Ophthalmol Vis Sci.*, vol. 49, no. 2, pp. 522–7. doi: 10.1167/iovs.07–1175., 2008.

[103] D. Vallbohmer, W. Zhang, M. Gordon, D. Y. Yang, J. Yun, O. A. Press, K. E. Rhodes, A. E. Sherrod, S. Iqbal, K. D. Danenberg, S. Groshen, and H. J. Lenz, "Molecular determinants of cetuximab efficacy," *J Clin Oncol.*, vol. 23, no. 15, pp. 3536–44., 2005.

[104] A. Abajo, V. Boni, I. Lopez, M. Gonzalez-Huarriz, N. Bitarte, J. Rodriguez, R. Zarate, E. Bandres, and J. Garcia-Foncillas, "Identification of predictive circulating biomarkers of bevacizumab-containing regimen efficacy in pre-treated metastatic colorectal cancer patients.," *Br J Cancer*, vol. 107, no. 2, pp. 287–90, 2012.

[105] R. Bertini, L. S. Barcelos, A. R. Beccari, B. Cavalieri, A. Moriconi, C. Bizzarri, P. Di Benedetto, C. Di Giacinto, I. Gloaguen, E. Galliera, M. M. Corsi, R. C. Russo, S. P. Andrade, M. C. Cesta, G. Nano, A. Aramini, J. C. Cutrin, M. Locati, M. Allegretti, and M. M. Teixeira, "Receptor binding mode and pharmacological characterization of a potent and selective dual cxcr1/cxcr2 non-competitive allosteric inhibitor," *Br J Pharmacol.*, vol. 165, no. 2, pp. 436–54. doi: 10.1111/j.1476–5381.2011.01566.x., 2012.

[106] R. W. Chapman, J. E. Phillips, R. W. Hipkin, A. K. Curran, D. Lundell, and J. S. Fine, "Cxcr2 antagonists for the treatment of pulmonary disease," *Pharmacol Ther.*, vol. 121, no. 1, pp. 55–68. doi: 10.1016/j.pharmthera.2008.10.005. Epub 2008 Oct 31., 2009.

[107] H. Hurwitz, L. Fehrenbacher, W. Novotny, T. Cartwright, J. Hainsworth, W. Heim, J. Berlin, A. Baron, S. Griffing, E. Holmgren, N. Ferrara, G. Fyfe, B. Rogers, R. Ross, and F. Kabbinavar, "Bevacizumab plus irinotecan, fluorouracil, and leucovorin for metastatic colorectal cancer," *N Engl J Med*, vol. 350, no. 23, pp. 2335–2342, 2004.

[108] F. Kabbinavar, H. I. Hurwitz, L. Fehrenbacher, N. J. Meropol, W. F. Novotny, G. Lieberman, S. Griffing, and E. Bergsland, "Phase ii, randomized trial comparing bevacizumab plus fluorouracil (fu) leucovorin (lv) with fu/lv alone in patients with metastatic colorectal cancer," *Journal of Clinical Oncology*, vol. 21, no. 1, pp. 60–65, 2003. 685UF Times Cited:698 Cited References Count:31.

[109] B. J. Giantonio, P. J. Catalano, N. J. Meropol, P. J. O'Dwyer, E. P. Mitchell, S. R. Alberts, M. A. Schwartz, and r. Benson, A. B., "Bevacizumab in combination with oxaliplatin, fluorouracil, and leucovorin (folfox4) for previously treated metastatic colorectal cancer: results from the eastern cooperative oncology group study e3200," *J Clin Oncol*, vol. 25, no. 12, pp. 1539–44, 2007.

[110] A. Sandler, R. Gray, M. C. Perry, J. Brahmer, J. H. Schiller, A. Dowlati, R. Lilenbaum, and D. H. Johnson, "Paclitaxel-carboplatin alone or with bevacizumab for non-small-cell lung cancer," *N Engl J Med*, vol. 355, no. 24, pp. 2542–2550, 2006.

[111] J. C. Yang, L. Haworth, R. M. Sherry, P. Hwu, D. J. Schwartzentruber, S. L. Topalian, S. M. Steinberg, H. X. Chen, and S. A. Rosenberg, "A randomized trial of bevacizumab, an anti-vascular endothelial growth factor antibody, for metastatic renal cancer," *N Engl J Med*, vol. 349, no. 5, pp. 427–434, 2003.

[112] S. Patel and J. Lyons-Weiler, "cageda: a web application for the integrated analysis of global gene expression patterns in cancer," *Appl Bioinformatics.*, vol. 3, no. 1, pp. 49–62., 2004.

[113] S. Draghici, P. Khatri, A. L. Tarca, K. Amin, A. Done, C. Voichita, C. Georgescu, and R. Romero, "A systems biology approach for pathway level analysis," *Genome Res.*, vol. 17, no. 10, pp. 1537–45. Epub 2007 Sep 4., 2007.

[114] K. J. Sales, S. C. Boddy, A. R. W. Williams, R. A. Anderson, and H. N. Jabbour, "F-prostanoid receptor regulation of fibroblast growth factor 2 signaling in endometrial adenocarcinoma cells," *Endocrinology*, vol. 148, no. 8, pp. 3635–3644, 2007.

[115] N. Turner and R. Grose, "Fibroblast growth factor signalling: from development to cancer," *Nature Reviews Cancer*, vol. 10, pp. 116–129, February 2010.

[116] E. M. Haugsten, A. Wiedlocha, S. Olsnes, and J. Wesche, "Roles of fibroblast growth factor receptors in carcinogenesis," *Molecular Cancer Research*, vol. 8, no. 11, pp. 1439–1452, 2010.

[117] G. Andres, D. Leali, S. Mitola, D. Coltrini, M. Camozzi, M. Corsini, M. Belleri, E. Hirsch, R. Schwendener, G. Christofori, A. Alcam, and M. Presta, "A pro-inflammatory signature mediates fgf2-induced angiogenesis.," *J Cell Mol Med*, 2008.

[118] P. d'Avis, S. Robertson, A. Meyer, W. Bardwell, M. Webster, and D. Donoghue, "Constitutive activation of fibroblast growth factor receptor 3 by mutations responsible for the lethal skeletal dysplasia thanatophoric dysplasia type i," *Cell Growth Differ*, vol. 9, no. 1, pp. 71–78, 1998.

[119] L. Marek, K. E. Ware, A. Fritzsche, P. Hercule, W. R. Helton, J. E. Smith, L. A. McDermott, C. D. Coldren, R. A. Nemenoff, D. T. Merrick, B. A. Helfrich, P. A. Bunn, and L. E. Heasley, "Fibroblast growth factor (fgf) and fgf receptor-mediated autocrine signaling in non-small-cell lung cancer cells," *Molecular Pharmacology*, vol. 75, no. 1, pp. 196–207, 2009.

[120] K. E. Ware, M. E. Marshall, L. R. Heasley, L. Marek, T. K. Hinz, P. Hercule, B. A. Helfrich, R. C. Doebele, and L. E. Heasley, "Rapidly acquired resistance to egfr tyrosine kinase inhibitors in nsclc cell lines through de-repression of fgfr2 and fgfr3 expression," *PLoS One*, vol. 5, p. e14117, 11 2010.

[121] N. T. Fernando, M. Koch, C. Rothrock, L. K. Gollogly, P. A. D'Amore, S. Ryeom, and S. S. Yoon, "Tumor escape from endogenous, extracellular matrix-associated angiogenesis inhibitors by up-regulation of multiple proangiogenic factors," *Clin Cancer Res.*, vol. 14, no. 5, pp. 1529–39. doi: 10.1158/1078–0432.CCR–07–4126., 2008.

[122] H. Huynh, V. C. Ngo, J. Fargnoli, M. Ayers, K. C. Soo, H. N. Koong, C. H. Thng, H. S. Ong, A. Chung, P. Chow, P. Pollock, S. Byron, and E. Tran, "Brivanib alaninate, a dual inhibitor of vascular endothelial growth factor receptor and fibroblast growth factor receptor tyrosine kinases, induces growth inhibition in mouse models of human hepatocellular carcinoma," *Clin Cancer Res.*, vol. 14, no. 19, pp. 6146–53. doi: 10.1158/1078–0432.CCR–08–0509., 2008.

[123] E. Allen, I. B. Walters, and D. Hanahan, "Brivanib, a dual fgf/vegf inhibitor, is active both first and second line against mouse pancreatic neuroendocrine tumors developing adaptive/evasive resistance to vegf inhibition," *Clin Cancer Res.*, vol. 17, no. 16, pp. 5299–310. doi: 10.1158/1078–0432.CCR–10–2847. Epub 2011 May 27., 2011.

[124] E. Bello, G. Colella, V. Scarlato, P. Oliva, A. Berndt, G. Valbusa, S. C. Serra, M. D'Incalci, E. Cavalletti, R. Giavazzi, G. Damia, and G. Camboni, "E-3810 is a potent dual inhibitor of vegfr and fgfr that exerts antitumor activity in multiple preclinical models," *Cancer Res.*, vol. 71, no. 4, pp. 1396–405. doi: 10.1158/0008–5472.CAN–10–2700. Epub 2011 Jan 6., 2011.

[125] C. D. Weekes, D. D. Von Hoff, A. A. Adjei, D. P. Leffingwell, S. G. Eckhardt, L. Gore, K. D. Lewis, G. J. Weiss, R. K. Ramanathan, G. K. Dy, W. W. Ma, B. Sheedy, C. Iverson, J. N. Miner, Z. Shen, L.-T. Yeh, R. L. Dubowy, M. Jeffers, P. Rajagopalan, and N. J. Clendeninn, "Multicenter phase i trial of the mitogen-activated protein kinase 1/2 inhibitor bay 86-9766 in patients with advanced cancer," *Clinical Cancer Research*, vol. 19, no. 5, pp. 1232–1243, 2013.